Karlsruhe Institute of Technology

A catalogue of gravimetric factor and phase variations for twelve wave groups

by Eva Schroth[1], Thomas Forbriger[2], Malte Westerhaus[1]

KIT SCIENTIFIC WORKING PAPERS 101

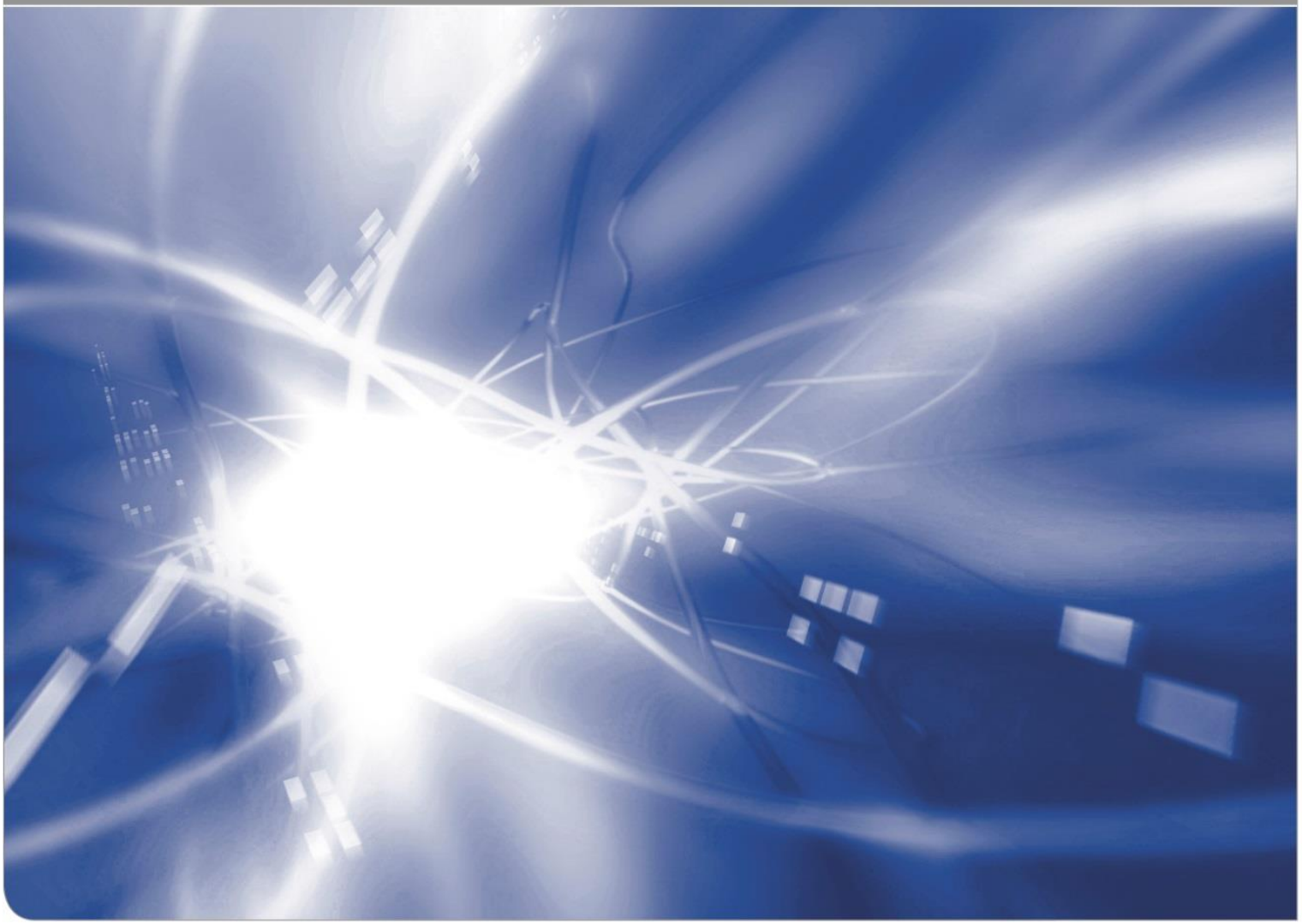

[1] Geodetic Institute
[2] Geophysical Institute, Black Forest Observatory

Impressum

Karlsruher Institut für Technologie (KIT)
www.kit.edu

2018

ISSN: 2194-1629

1. Introduction

Moving window tidal analyses of gravity recordings show temporal variations of tidal parameters. Modern superconducting gravimeters (SG) produce data of unprecedented accuracy and precision such that observed variations are significant with respect to standard deviation of tidal parameters as obtained from data residuals (Meurers, 2004, Meurers et al., 2016; Jahr, 2015; Schroth, 2013). Since the admittance of Earth's body to tidal forces is not expected to vary rapidly (within a few months), the causes of this phenomenon must be searched in temporal variations in the oceans and possibly the atmosphere, deficiencies in the method of analysis, or neglected influence of non-tidal gravity signals.

This report compares time-dependent tidal parameters for 19 European and global SG stations. We point out similarities and differences, identify probably involved tidal harmonics and discuss possible causes for the observed variations. Evidence for these causes is not shown here and is the subject of ongoing research.

2. Moving window tidal analysis

During tidal analysis, gravimetric factor and phase, the tidal parameters, are adjusted by linear regression. A synthetic signal, hereafter called analysis model (meaning described below), is fit to the measured data by minimizing the residual in a least-squares sense. We use a modified version of the software Eterna 3.4 (program analyze) (Wenzel, 1996), where the period of the free core nutation (FCN) was set to the value of 431.37 sidereal days (Dehant et al., 1999), which is close to recent estimations with very long baseline interferometry (VLBI) (Krásná et al., 2013), replacing the outdated resonance model with a period of about 460.53 sidereal days.

The gravimetric factor is an amplitude factor, defined as ratio of measured to exciting acceleration and scales the model signal used in the regression. The phase accounts for the phase shift between analysis model and measured signal. Leads are defined positive, which means that the response leads the forcing.

The model signal, in the following called analysis model, describes in principle the exciting tidal acceleration. The forcing field is available through tidal catalogues after harmonic development, which represent the tidal potential by a sum of cosine functions (=harmonics) with known amplitude, phase and frequency. The here used catalogue (Hartmann and Wenzel, 1995a,b) contains 12935 harmonics. Because of the limited frequency resolution and the signal-to-noise ratio (Munk and Hasselmann, 1964) we are not able to determine tidal parameters for each single harmonic. Therefore the tidal parameters are estimated for wave groups. The amplitudes and phases of the harmonics within the frequency band of the

wave group are kept in fixed ratios as expected for a reference Earth model. In order to describe the measured signal as well as possible the approximately known response of the Earth is taken into account. The analysis model, thus, is not the pure forcing. The ratios within a wave group are predicted by the body tide model, which is a model for an elliptical, uniformly rotating Earth with liquid inner core and viscous mantle (Wahr-Dehant-Zschau model, Dehant, 1987). As this model does describe the solid Earth only and does not include oceans or atmosphere, we refer to it as body tide model. Respectively we use 'Earth body' or 'solid Earth' when the solid earth without oceans and atmosphere is meant, while 'earth' is the system of solid Earth, atmosphere and oceans.

The moving window analysis uses tidal analysis for adjusting tidal parameters for time windows taken from a longer time series. The results are plotted over the centroid time of the window and show how the tidal parameters change with time. We use data segments of 90 days length, successively shifted by 2 days. A band-pass from 1 cpd to 5 cpd was applied to data and analysis model. The analysis uses a Hanning taper and applies local air-pressure as an additional regressor. Wave groups are assembled as recommended by Wenzel (1997b, section 17.2) for time series of less than six months and are given in Tab. 5 in the appendix. Wave groups Q1 and higher (frequency > approx. 0.5 cpd) are used.

The computation of the standard deviations for the estimated parameters is based on the residuals. The standard deviation changes if filters are applied. The tidal analysis with filtered data, which is used in this study, produces standard deviations up to eight times smaller than the standard deviations estimated from unfiltered data.

3. Observations

3.1 Data

Except for BFO and Onsala, where the data was provided by the station operators, we use hourly gravity data that was obtained from the data center of the International Geodynamics and Earth Tide Service (IGETS, https://isdc.gfz-potsdam.de/igets-data-base/). Tab. 1 gives the names and symbols of the stations and the length of the analysed data set. The used data set does not necessarily contain all available data. The results shown here where produced for a study, in which we investigated the influence of non-stationary ocean-loading by using sea surface height from time-dependent hydrodynamic models. The lengths of the data sets were chosen due to the requirements of that study. In case of Syowa we skipped data after 2001, because of significant disturbances.

Data from all European stations were analysed, except for Borowa Gora, Poland, where no hourly data is available up to now. They are located relatively close to each other, therefore global or regional effects should affect them all in the same way. Not from all global stations data was used. They were chosen due to their location on different continents and at different latitudes as well as the data quality. The distribution of stations is shown in Fig. 1.

Table 1: Names and symbols of stations and lengths of the used datasets. In Wettzell two different gravimeters were operated. The length is given idividually for each instrument. *In case of dual-sphere gravimeters we used the data from the lower sensor.

Symbol: station	length of used data set
BF: Black Forest Observatory, Germany*	27.11.2009 – 31.12.2013
BH: Bad Homburg, Germany*	13.02.2007 – 27.02.2015
CA: Cantley, Canada	02.07.1997 – 30.07.2013
CB: Canberra, Australia	02.07.1997 – 30.03.2015
CO: Conrad, Austria	16.11.2007 – 01.11.2014
KA: Kamioka, Japan	23.10.2004 – 30.07.2013
MB: Membach, Begium	01.01.1998 – 30.12.2011
MC: Medicina, Italy	01.01.2004 – 27.02.2015
ME: Metsähovi, Finland	11.05.2005 – 29.04.2015
MO: Moxa, Germany*	02.01.2000 – 27.02.2014
NY: Ny-Ålesund, Svalbard	01.01.2002 – 31.12.2011
OS: Onsala, Sweden	15.06.2009 – 15.03.2018
PE: Pecny, Czech Republic	02.05.2007 – 30.12.2014
ST: Strasbourg, France	02.03.1997 – 30.01.2015
SU: Sutherland, South Africa*	28.03.2000 – 30.12.2014
SY: Syowa, Antarctica	01.07.1997 – 03.10.2001
TC: TIGO Concepcion; Chile	16.02.2003 – 30.12.2014
WE: Wettzell, Germany D029* CD030*	05.11.1998 – 06.10.2010 26.10.2010 – 27.02.2015
YS: Yebes, Spain	01.01.2015 – 03.06.2017

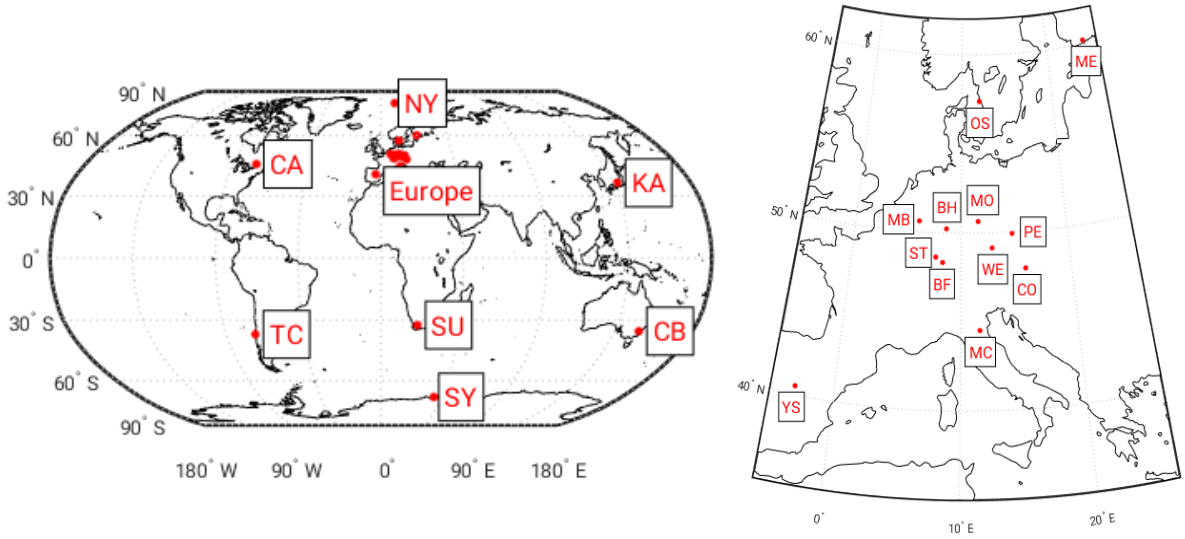

Figure 1: left: location of global stations: CA, Cantley, Canada; CB, Canberra, Australia; KA, Kamioka, Japan; NY, Ny-Ålesund, Svalbard; SU, Sutherland, South Africa; SY, Syowa, Antarctica; TC, TIGO Concepcion, Chile.
right: location of European stations: BF, Black Forest Observatory, Schiltach, Germany; BH, Bad Homburg, Germany; CO, Conrad, Austria; MB, Membach, Belgium; MC, Medicina, Italy; ME, Metsähovi, Finland; MO, Moxa, Germany; OS, Onsala, Sweden; PE, Pecny, Czech Republic; ST, Strasbourg, France; WE: Wettzell, Germany; YS: Yebes, Spain

Table 2: Mean value of the gravimetric factors for the tidal parameters shown in Fig. 4 –11.

Station	δ(Q1)	δ(O1)	δ(M1)	δ(K1)	δ(J1)	δ(OO1)
Cantley	1.1648	1.1654	1.1649	1.1475	1.1692	1.1678
Canberra	1.1843	1.1674	1.1581	1.1299	1.1382	1.1257
Concepcion	1.1552	1.1659	1.1730	1.1584	1.1732	1.1602
Kamioka	1.2034	1.2009	1.1988	1.1805	1.1939	1.1784
Medicina	1.1475	1.1486	1.1512	1.1347	1.1566	1.1557
Metsähovi	1.1467	1.1524	1.1553	1.1395	1.1575	1.1583
Onsala	1.1430	1.1462	1.1563	1.1388	1.1582	1.1520
Sutherland	1.1606	1.1629	1.1612	1.1348	1.1468	1.1333
Ny-Ålesund	1.0572	1.1463	1.1729	1.1450	1.1511	1.1214
Syowa	1.3059	1.2720	1.2339	1.2022	1.1982	1.2054
Yebes	1.1510	1.1467	1.1602	1.1342	1.1614	1.1568
Station	δ(2N2)	δ(N2)	δ(M2)	δ(L2)	δ(S2)	δ(M3M6)
Cantley	1.2024	1.2103	1.2032	1.1872	1.1839	1.0804
Canberra	1.2154	1.1968	1.1787	1.1647	1.1553	1.0670
Concepcion	1.2009	1.1600	1.1248	1.1258	1.1013	1.0520
Onsala	1.1299	1.1764	1.1858	1.1791	1.1775	1.0716
Kamioka	1.1929	1.1860	1.1906	1.2016	1.2001	1.0879
Medicina	1.1586	1.1737	1.1807	1.1811	1.1794	1.0686
Metsähovi	1.1703	1.1778	1.1805	1.1802	1.1743	1.0805
Sutherland	1.1073	1.1392	1.1570	1.1767	1.1992	1.0434
Ny-Ålesund	0.9287	0.7083	0.7757	1.0666	1.3864	1.5944
Syowa	1.2615	1.4285	1.4027	1.3774	1.5011	1.0744
Yebes	1.0818	1.1235	1.1503	1.2072	1.1804	1.0653

3.2 Observed variations of tidal parameters

The gravimetric factors and phases for the European stations are shown in Figs. 2-7 and for all other stations in Figs. 8-11. For all stations or groups of stations, there are separate plots for the gravimeteric factor (e.g. Fig. 2 for the gravimetric factors of the central European stations) and phases (Fig. 3 respectivly). Each wave group is plotted in its own panel with the diurnal wave goups on the left hand side of the figure and the semi-diurnal and higher frequency wave groups on the right hand side. The thickness of the line represents the standard deviation. Outliers were removed from the results. Usually they are related to large gaps (several weeks to months) in the data sets.

The offsets of the tidal parameters of stations far away from each other scatter more than those of the nearby located stations in central Europe. This is presumably, to some extent, caused by stationary ocean loading. To allow a comparison of the variations, for all stations not located in central Europe, the mean value of each time-dependent tidal parameter is calculated and removed. The mean values are given in Tab. 2 for the gravimetric factors and in Tab. 3 for the phases. All results are plotted for each station individually in Fig. 12-49 in the appendix.

The offsets are in general close to the tidal parameters from the tidal analysis of the complete times. Differences may occur if the length of the data set is not an integer multiple of the variation period of a parameter. In a few cases the difference is larger than the standard deviation plus the variation, for example the gravimetric factors of O1 and K1 from Ny-Ålesund compared to the results of Sato et al. (2001, 2006) and the phase of O1 and M2 from Syowa compared to results from Iwano et al. (2005). This could be caused by the usage of different data sets and different wave grouping in the analysis.

From the body tide model, the gravimetric factor is assumed to be approx. 1.154 for diurnal wave groups (except for K1, $\delta(K1) \approx 1.13$) and about 1.16 for semi-diurnal wave groups (1.07 for degree 3). The phase is expected to be close to 0° in all cases. The offset values in Fig. 2 and 3 and Tab. 3 and 4 show that the estimated tidal parameters differ from that expectation. In most cases, especially for the semi-diurnal wave groups the gravimetric factor and/or the phases are larger. For the central European stations $\delta(M2)$ is about 1.18 and between 1° and 2.5°.

We observe temporal variations for practically all wave groups, which are significantly larger than the standard deviation as estimated by Eterna from the gravity residuals.

Table 3: Mean value of the phase lead for the variations shown in Fig. 4 – 11.

Station	ϕ(Q1) in °	ϕ(O1) in °	ϕ(M1) in °	ϕ(K1) in °	ϕ(J1) in °	ϕ(OO1) in °
Cantley	0.5614	0.5613	0.6362	0.5876	0.5781	0.5750
Canberra	-0.6093	-0.7447	-0.7840	-0.8359	-0.7575	-0.0540
Concepcion	2.3589	1.8365	0.8570	0.8318	-0.0482	-1.3805
Kamioka	1.0055	0.5689	0.0959	-0.1396	-0.8310	-1.3301
Medicina	-0.1416	0.1455	0.2803	0.3567	0.2623	0.4070
Metsähovi	0.0837	0.2561	0.1225	0.0735	0.0079	0.1533
Onsala	-0.2917	0.1740	0.1752	0.1720	-0.0870	0.1856
Sutherland	0.6542	0.1130	-0.4378	-0.4960	-0.4527	-0.0111
Ny-Ålesund	0.6070	1.0862	-1.1503	-1.9114	-1.1654	-0.0990
Syowa	2.1503	0.8623	0.1901	0.8652	0.8652	1.8590
Yebes	-0.8226	-0.2119	0.2860	0.4161	0.1828	0.0593
Station	ϕ(2N2) in °	ϕ(N2) in °	ϕ(M2) in °	ϕ(L2) in °	ϕ(S2) in °	ϕ(M3M6) in °
Cantley	0.5971	0.0735	-0.4979	-0.7394	-1.1152	-0.1797
Canberra	-2.5130	-2.6790	-2.5201	-2.1863	-1.3188	0.0121
Concepcion	-1.9545	-2.5247	-2.3043	-1.4049	-1.8316	0.8397
Kamioka	0.0959	0.0959	0.5164	0.3891	-0.2905	0.7828
Medicina	1.8459	1.7447	1.2577	0.7140	0.1733	0.2624
Metsähovi	1.0754	1.0331	0.7088	0.2562	0,0678	0.3111
Onsala	1.6286	2.1663	1.3587	-0.0858	0.4008	1.5000
Sutherland	5.4508	5.4955	5.2476	5.4008	4.3121	0.0401
Ny-Ålesund	-121.9362	170.3551	107.7439	42.7601	58.0473	-17.6571
Syowa	6.8083	1.9701	0.8332	-0.1684	-1.0668	-20.4977
Yebes	3.6517	4.8296	4.5109	3.0145	2.7561	-0.5441

The variation of the tidal parameters for many of the wave groups show some kind of periodicity. The observed periods are about 8.8 years, 1.0 years, 0.56 years and 0.5 years. Tab. 4 lists the periods for the different wave groups. These are typical astronomical periods. 8.8 years correspond to the mean longitude of the lunar perigee and 1 year and half a year corresponds to time the Earth needs for one cycle around the Sun. 0.56 years probably corresponds to the half of the 411.8 days period, which comes from an interference of variational and evectional with the elliptical terms (Bartels, 1957).

Periodical behaviour is mainly present in the parameters of the semi-diurnal wave groups 2N2 to S2, but also for Q1, M1 and K1. The variations observed for the European SG stations are quite similar throughout the network. There are larger differences in the variations of the other stations but in general they also show similar periodicity and character of the temporal behaviour of the tidal parameters. Therefore it seems likely that the same causes produce variations of the tidal parameters at all stations.

The estimation for the tidal parameters of O1, K1, M2 and S2 should be the most accurate of all the wave groups because these harmonics have the largest amplitudes which is reflected by their small standard deviations. Disturbances therefore should not affect their tidal parameters as strongly as for the groups with smaller amplitudes.

The tidal parameters of O1 (in the second panel on the left side of each Figure) as well as J1, OO1 and M3M6, show no clear periodicity. The variations are of the order of 10^{-4} for the gravimetric factor and 10^{-2}° for the phase, at most stations. In the O1 tidal parameters single features are present, which are similar for central European SG stations, e.g. the minimum in the gravimetric factor of the European stations (Fig. 2) at the beginning of 2008. For J1 an example is the maximum in the gravimetric factor in 2003 and for OO1 the variations of the phase in 2006. This maybe points to transient phenomena which influence gravity records at several stations on a regional scale in a similar way. The variation of the M2 tidal parameters, third panel on the right side, is of the same order of magnitude for most stations, but has a clear annual periodicity.

For K1 and S2 the tidal parameters (forth panel on the left and fifth panel on the right) vary with annual and semi-annual period. The gravimetric factor shows a variation in the order of 10^{-3} or larger and the phase of 0.1° or larger. This means that the effect causing the variation has to occur with a relatively large amplitude.

With the data from Ny-Ålesund, see Figs. 10 and 11 as well as Figs. 32 and 33 in the appendix, we get the largest variations and the largest offset compared to the other stations. The phase of the N2 wave group is close to 180° which causes the jumps of 360° in Fig. 11. Also in the phases of 2N2 and M3M6 360° jumps are observed. In order to make the variation visible, 360° were added or subtracted, respectively (phase unwrapping). That way we get the smooth curves in Fig. 33 in the appendix.

Furthermore, the phases of 2N2 and M3M6 have large standard deviations, larger than 360°, in short time spans within the whole data set. This occurs when the tidal signal (estimated with the analysis model) of the wave group is smaller than 0.7 nm/s² and the noise level (estimated from the residuals) is increased at the same time. This probably happens in Ny-Ålesund in particular, because the diurnal and semi-diurnal tides have small amplitudes at high latitudes, while the ocean causes a high noise level at stations close to the coast.

The time-dependent tidal parameters at Wettzell contain several steps which can be seen in Figs. 2 and 3 for example in the tidal parameters of O1, K1 and N2, M2 in 2008. They most likely also exist in the parameters of the other wave groups but the temporal variations are larger there and probably hide the steps. These steps correspond to changes in the sensitivities (calibration factor) and time lag in the IGETS data files. This was also observed by Meurers et al. (2016). The time lag of the instrument CD030 could be corrected (H. Wziontek, pers. comm.), but the time lags and sensitivities of CD029 remained uncertain, so we tried to use values that produce as few and small steps as possible. This is done because these values only influence the offset of the curve but not the temporal variations which are of interest for us and are better visible without steps. It does, of course, not mean that the changed values are correct. The smoother curves are shown in Figs. 46 and 47 in the appendix. Tab. 6 in the appendix gives the original and replaced values

The variations can be regarded in two different ways. On one hand the variations of the tidal parameters can be understood as a variation of the measured tidal amplitude compared to the analysis model. The variation is then not assumed to be perfectly periodic and can even be aperiodic. This concept is often used for ocean tides. On the other hand, if we assume that the variation is periodic, it can be understood as the fit of two beating signals (measured data and analysis models) with slightly different beat amplitudes, which results in a variation of the tidal parameters with the beat frequency. The tidal acceleration of a wave group has a beat character because in the wave group harmonics with similar frequencies interfere.

The variation frequency (i.e. beat frequency) is the frequency distance between die harmonics causing the variation. If we assume that the harmonics with large amplitudes are involved, we can identify the harmonics potentially causing the variation.

Tab. 4 lists the dominant periodicity of the variations observed for the different wave groups. They are related to the harmonics within the wave group by the corresponding frequency distance. The names of the harmonics and their origin are given. Please note that the wave groups are named after the largest harmonic within their frequency band, in the fourth column of the Table the name of the individual harmonic is given.

The 8.8-years-variation which corresponds to the mean longitude of the lunar perigee seems to be caused by degree 3 harmonics in all cases and occur in the diurnal and semi-diurnal band. The shorter periods appear mainly in the semi diurnal band, except for K1.

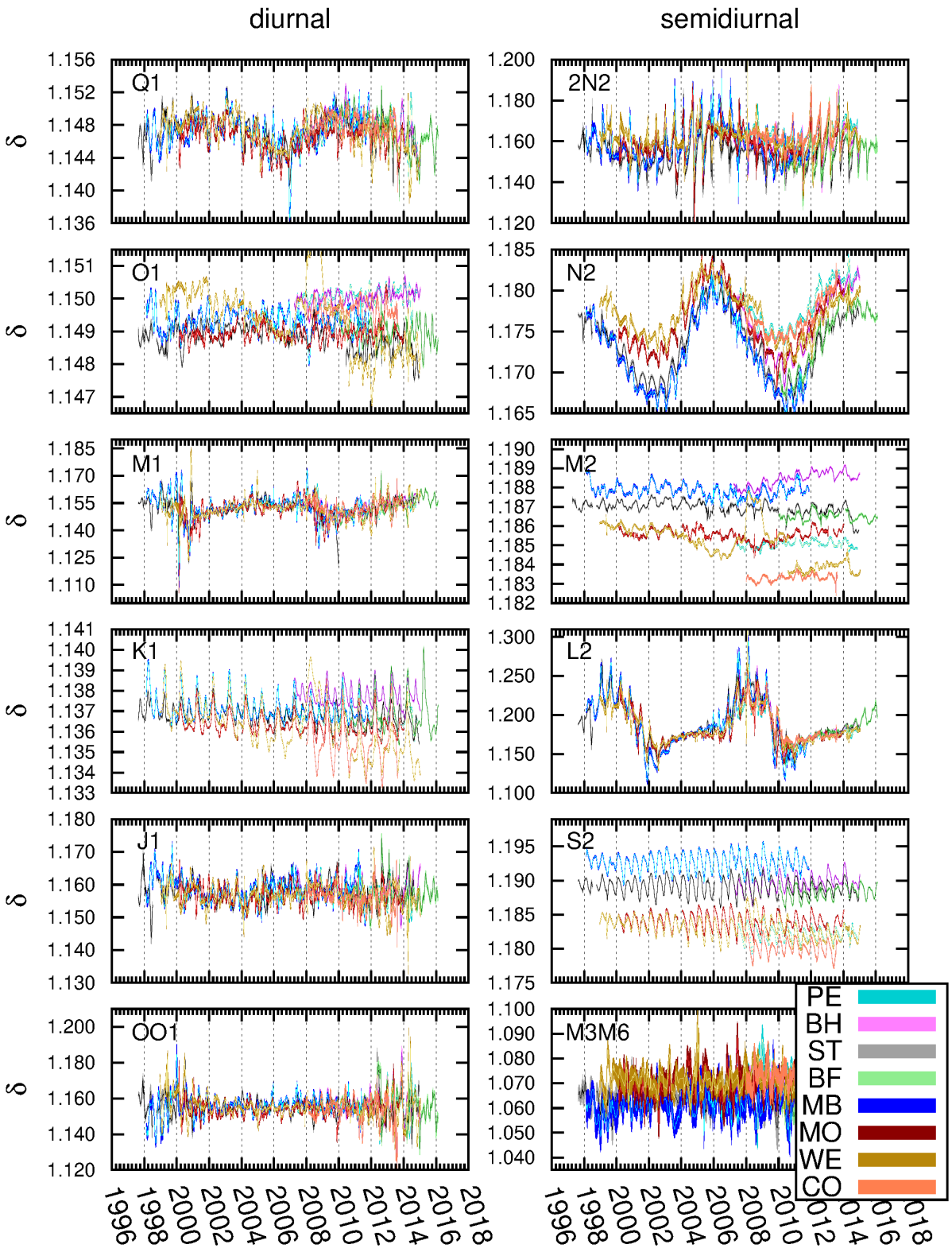

Figure 2: Gravimetric factors for the central European stations shown in Fig. 1

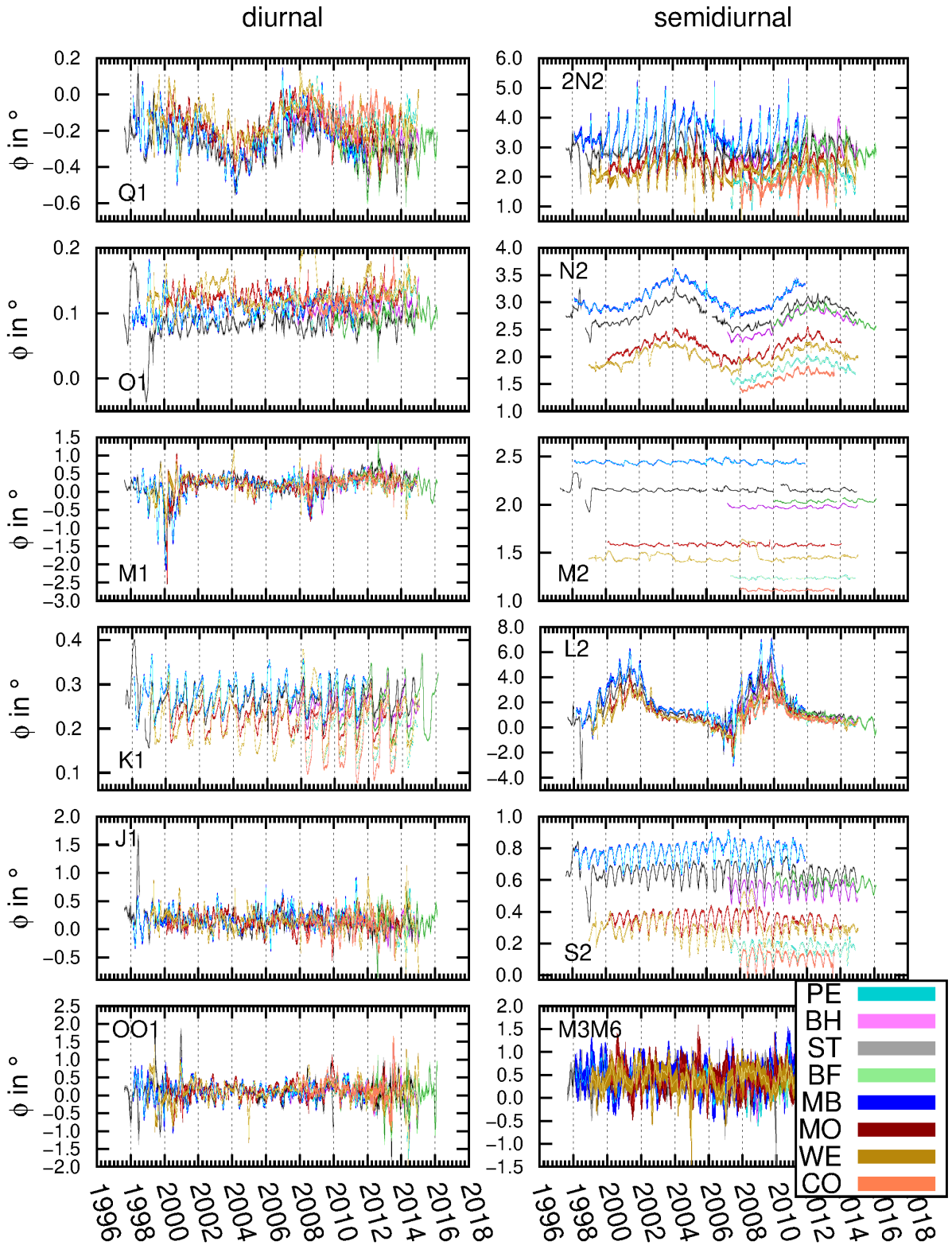

Figure 3: Phases lead for the central European stations shown in Fig. 1

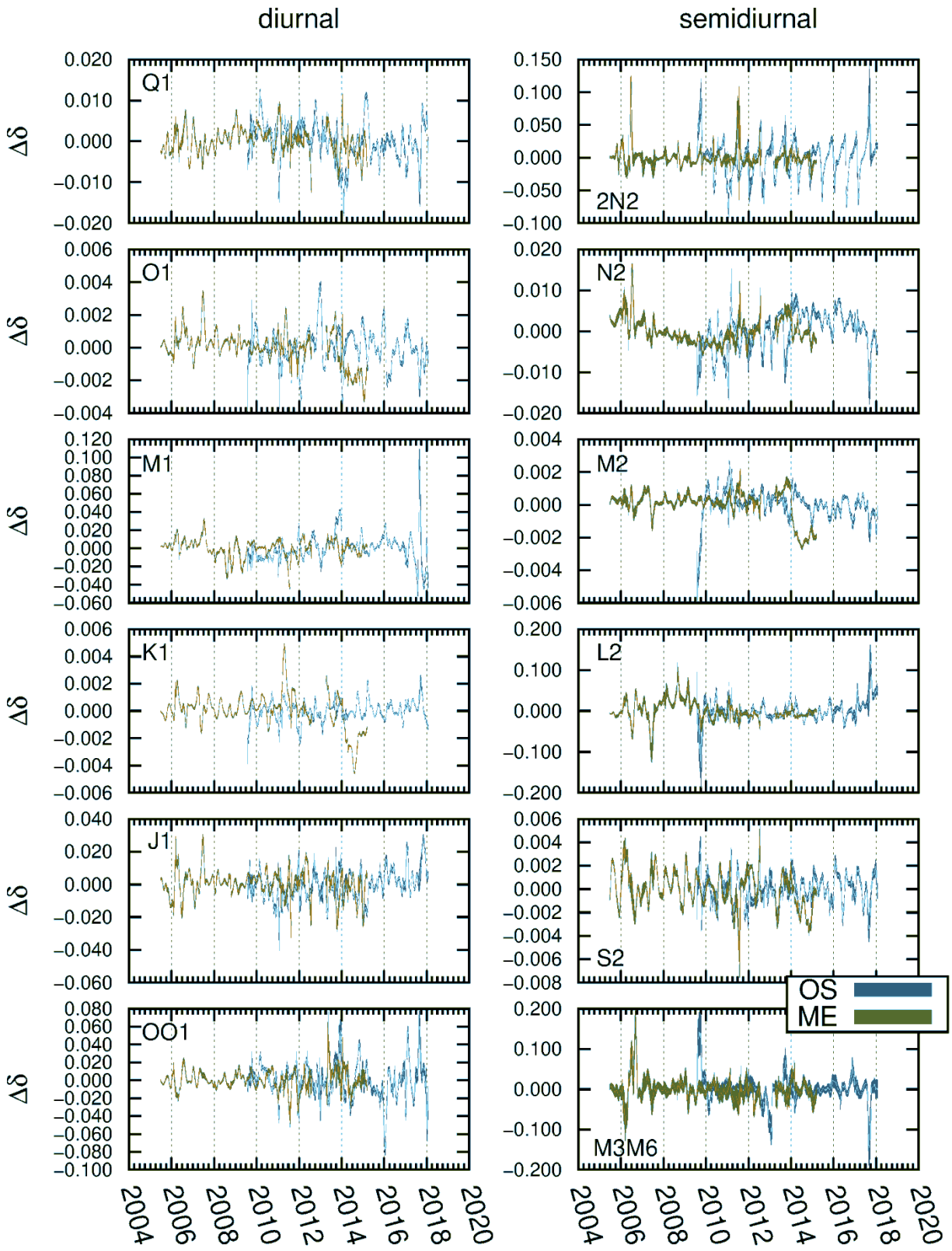

Figure 4: Variation of the gravimetric factors for the Scandinavian stations, shown in Fig. 1. Mean values are given in Tab.2.

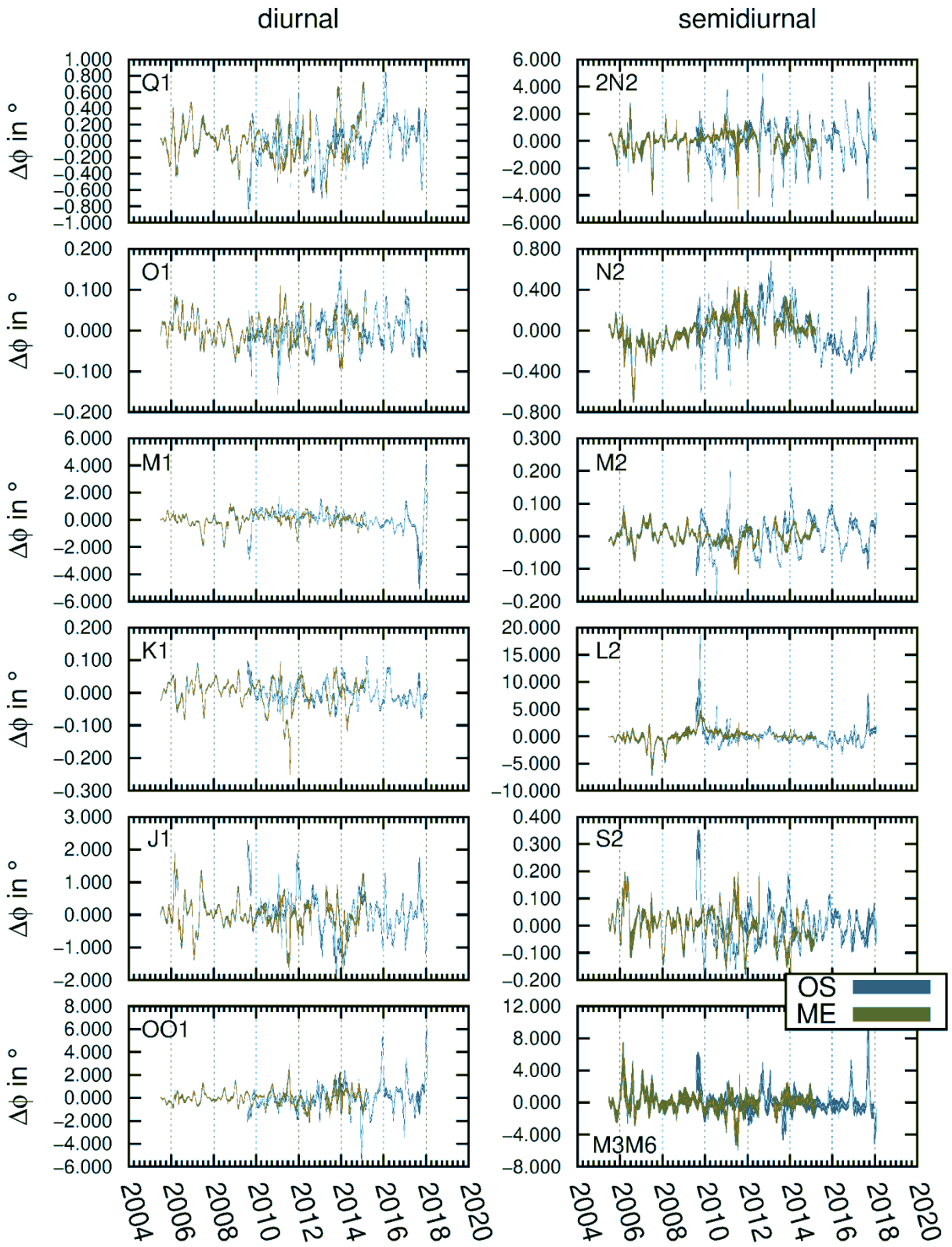

Figure 5: Variation of the phase lead for Scandinavian stations, shown in Fig. 1. Mean values are given in Tab. 4.

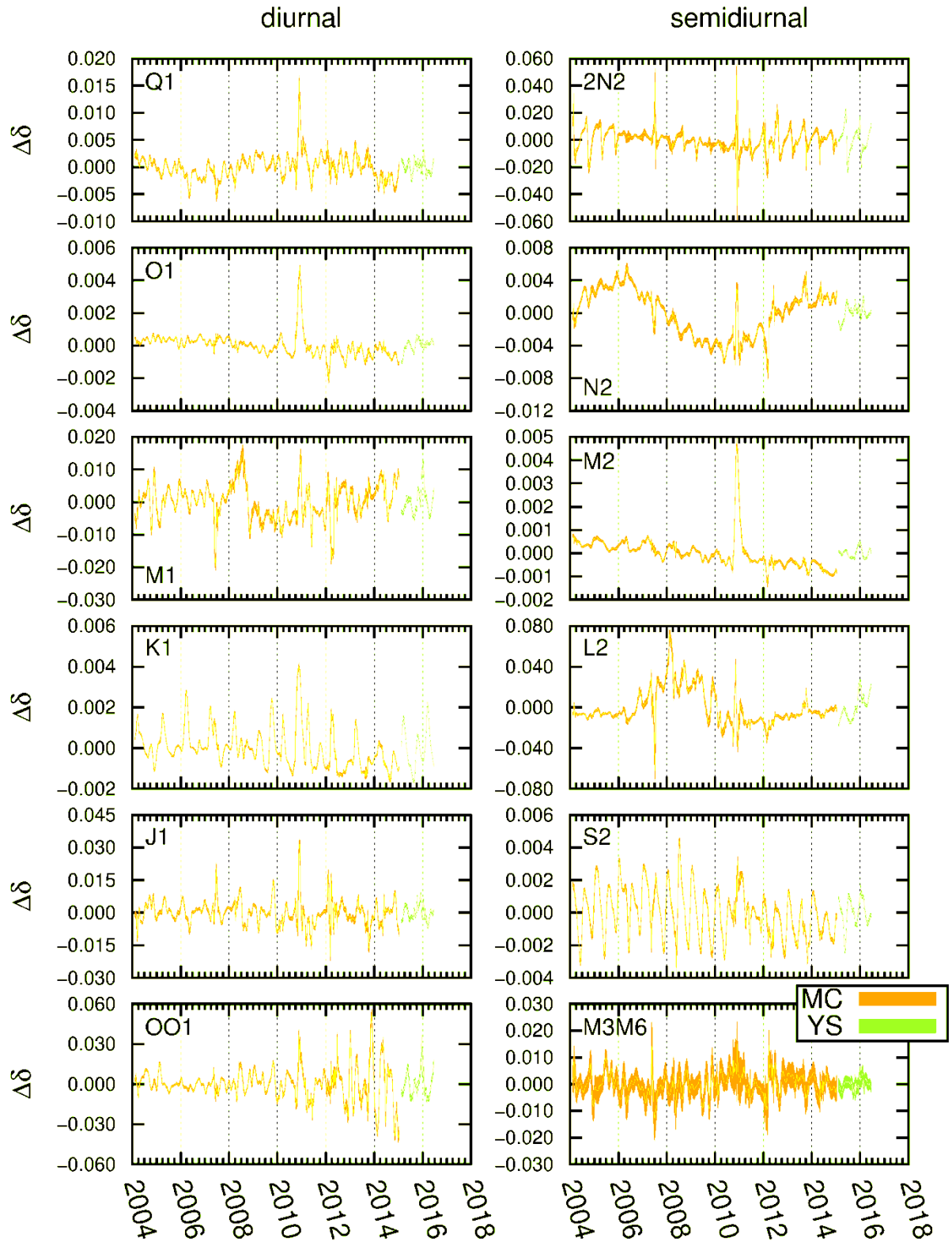

Figure 6: Variation of the gravimetric factors for southern European stations shown in Fig. 1. Mean values are given in Tab. 2. The curve for YS appears like a continuation of the curve for MC. Please note that this is just by chance.

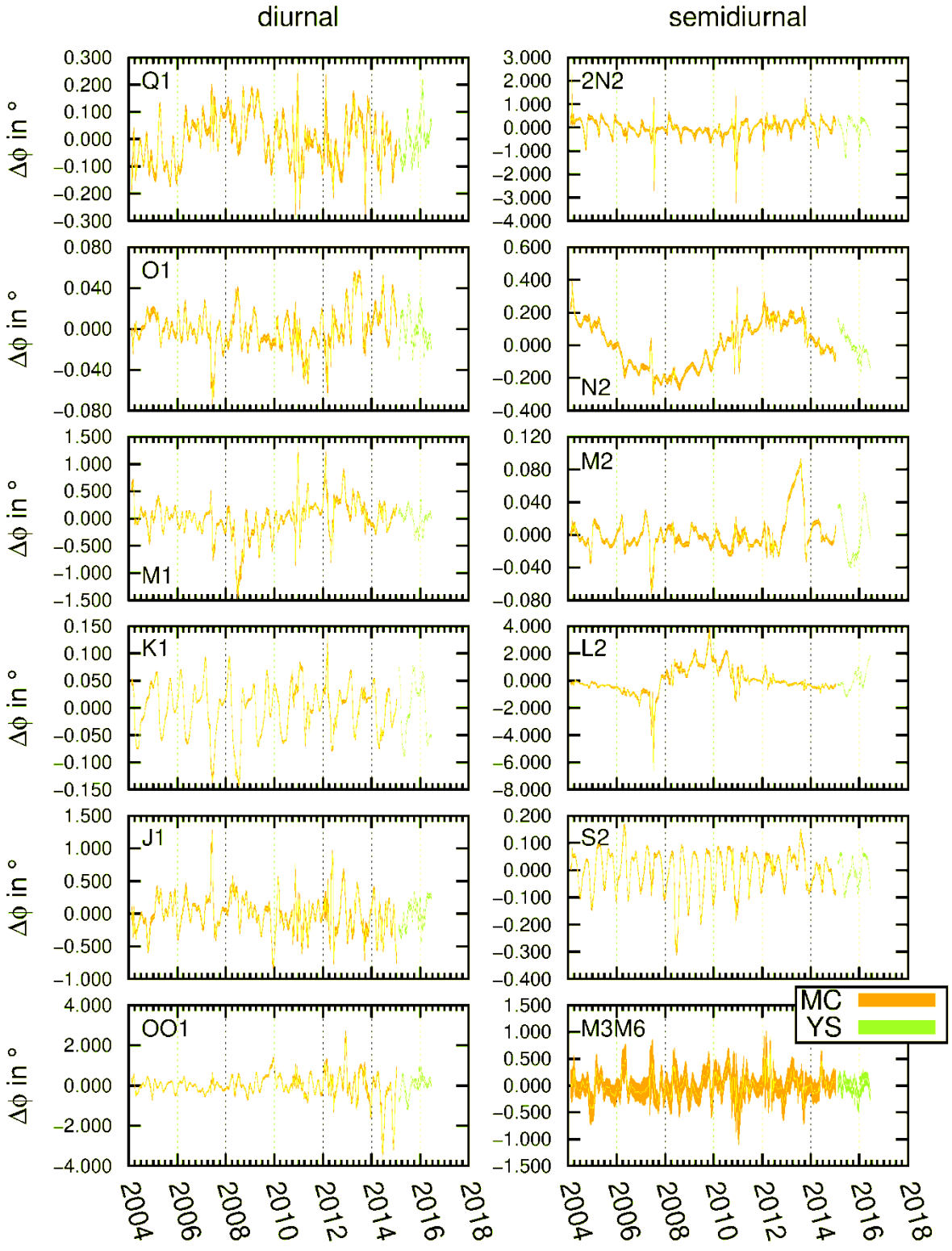

Figure 7: Variation of the phase lead for southern European stations shown in Fig. 1. Mean values are given in Tab. 3. The curve for YS appears like a continuation of the curve for MC. Please note that this is just by chance.

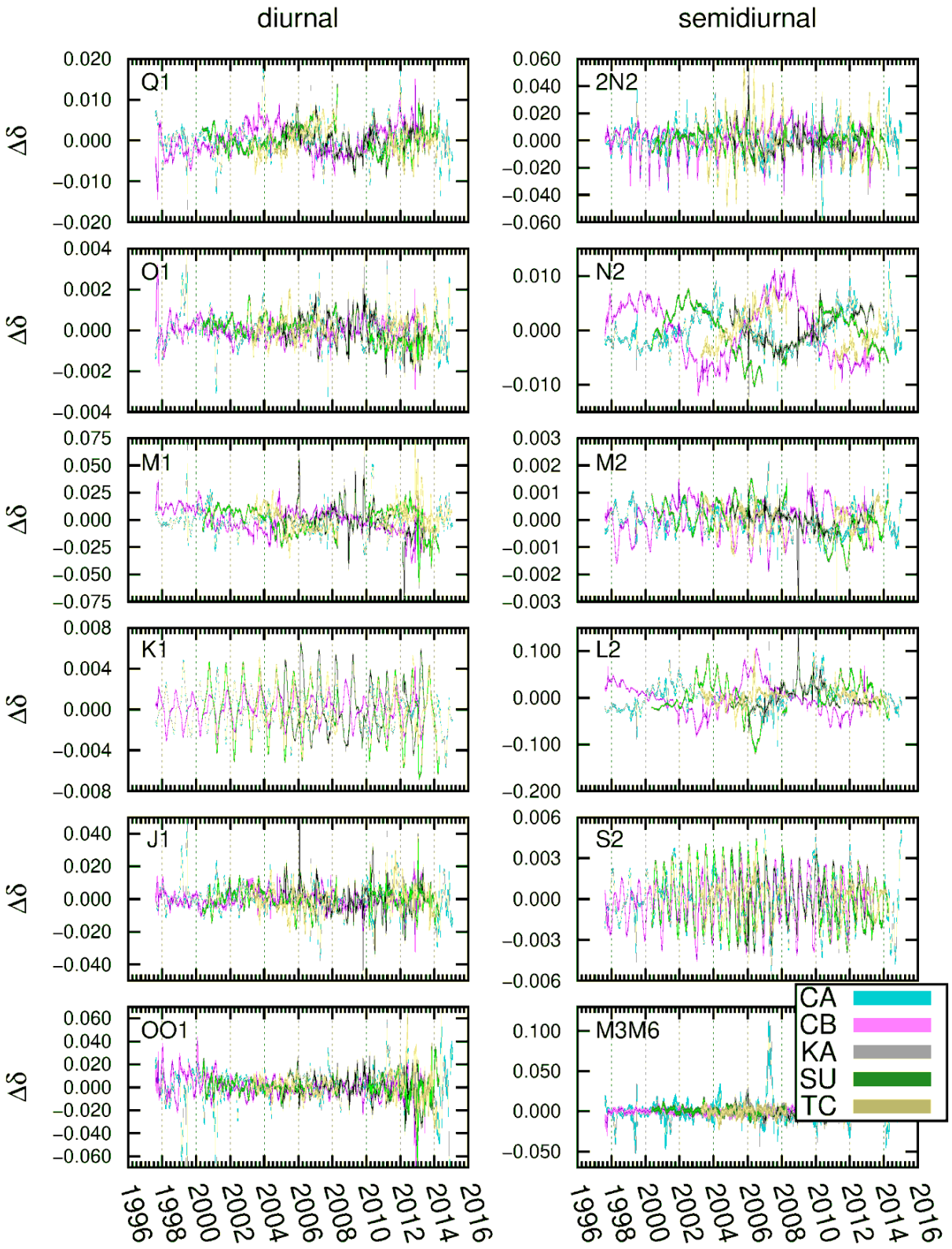

Figure 8: Variation of the gravimetric factors for the global stations shown in Fig. 1. Mean values are given in Tab. 2.

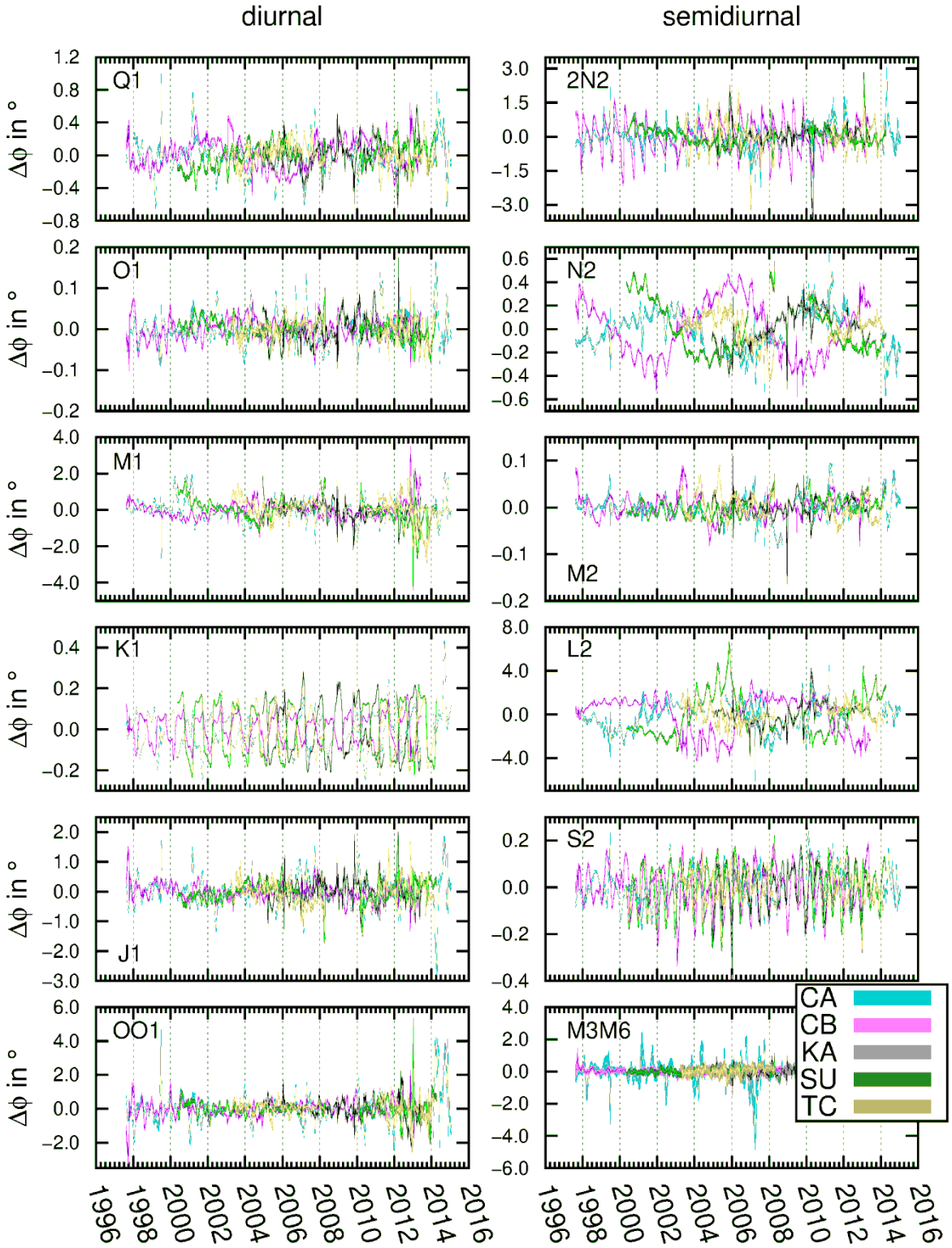

Figure 9: Variation of the phase lead for the global stations shown in Fig. 1. Mean values are given in Tab. 3.

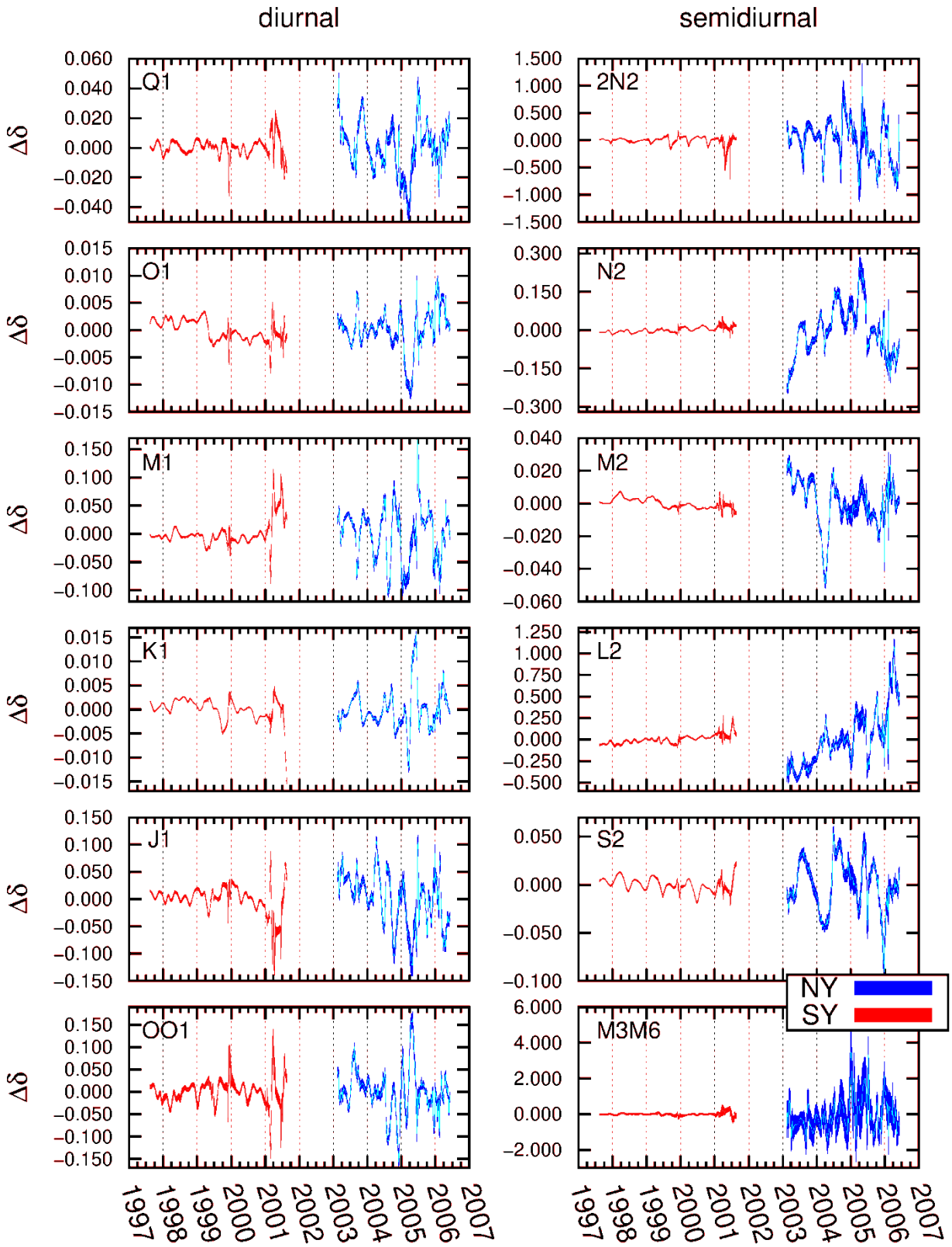

Figure 10: Variation of gravimetric factors for the Ny-Alesund and Syowa stations shown in Fig. 1. Mean values are given in Tab. 2.

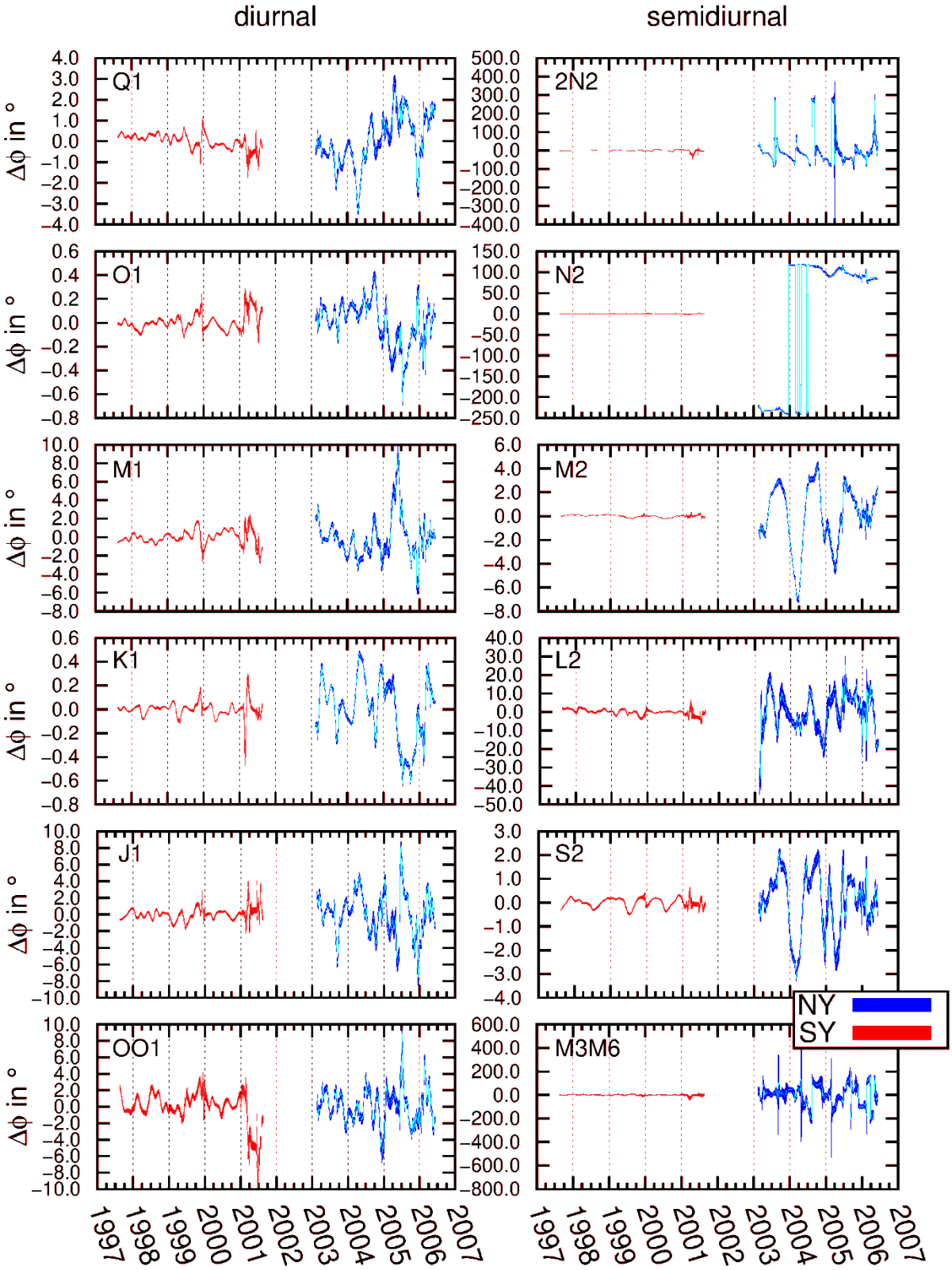

Figure 11: Variation of phase lead of the Ny-Alesund and Syowa stations shown in Fig. 1. Mean values are given in Tab. 3.

Table 4: Harmonics whose amplitude ratios within the wave group probably differ from expected ratios from the body tide model. Name of wave group/main wave, period of observed variation in years, name/number in Hartmann Wenzel tidal catalogue (Hartmann & Wenzel, 1995 a,b) of the tide as well as its origin if known, after Bartels (1957) (when nothing is mentioned, the harmonic is a 2. degree lunar tide).

wave group	variation period in yr	frequency in cpd	name/no. (HW95)	origin
Q1	8.8	0.89293	4235&4326	deg. 3 & quadrupole momentum
		0.89324	Q1	1. order elliptical tide of O1
	8.8	0.89355	4286&4287	deg. 3 & quadrupole mom.
M1	8.8	0.96614	5081-5083	deg. 3 & quadrupole momentum & deg. 5
		0.96645	M1	1. order elliptical tide of K1m
	8.8	0.96676	5128-5130	deg. 3 & quadrupole momentum & deg. 5
K1	0.5	0.99726	P1	main solar tide
	1.0	1.00000	S1	1. order elliptical tide of K1s
		1.00274	K1	diurnal main declination tide
	1.0	1.00548	ψ1	K1m&K1s
	0.5	1.00821	φ1	1. order elliptical tide of K1s
				diurnal 2. order declination tide
2N2	0.56	1.85483	8548	
		1.85969	2N2	2. order elliptical tide of M2
	0.56	1.86455	μ1	larger variational tide of M2
N2	0.56	1.89112	8874&8875	deg. 2 & 4
	8.8	1.89597	8949&8950	deg. 3 & 5
		1.89598	N2	larger 1. order elliptical tide of M2
	8.8	1.89629	8999&9000	deg. 3 & 5
	0.56	1.90084	ν1&9084	larger evectional tide & deg. 4
M2	1.0	1.92954	α2	smaller tide of annual inequality
		1.93227	M2	semidiurnal main tide
	1.0	1.93501	β2	larger tide of annual inequality
L2	0.56	1.96371	λ2	smaller evectional tide of M2
	8.8	1.96825	9612	deg. 3
		1.96857	L2	smaller 1. order elliptical tide of M2
	8.8	1.96887	9642&9643	deg. 3 & 5
	0.56	1.97342	9711	
S2	0.5	1.99452	2T2&9873	2. order elliptical tide of S2
	1.0	1.99726	T2&9945	larger 1. order elliptical tide of S2
		2.00000	S2	main solar tide & S2m smaller variational tide of M2
	1.0	2.00274	R2	
	0.5	2.00548	K2m&K2s& 10305-10311	smaller 1. order elliptical tide of S2 2. semidiurnal declination tide of M2 and S2 & Mercury & Venus & Mars & Saturn & Moon deg. 4 & 6

4. Hypothesis for the causes of the temporal variations of tidal parameters

A short-term variation (month to several years) of the admittance of Earth's body to tidal gravity appears physically unreasonable and the observed tidal parameters are not a proper measure for global properties of Earth's body alone.

We rule out instrumental causes. A variation of instrumental gain would affect the tidal parameters of all groups in the same way. This is not observed in our analysis for any SG station. A drift-like variation of δ(M2) at Bad Homburg, which was discussed by Meurers et al. (2016) is also present in our results (see Figs. 14 and 38 in the appendix). Since other parameters, like δ(O1), do not show long-term trends , a changing gain of the SG a this station cannot be the reason for the apparent trend in the M2 gravimetric factor.

Further, non-linearity of the gravimeters response could appear like an amplitude-dependent gain factor. Non-linear distortion of the rich tidal signal would result in a multitude of spectral components in the residuals of tidal analysis. The majority of these components is not present in the residuals of analysed recordings. The response to strong earthquakes as well shows no non-linearity of the instruments at a level required to explain the observed variations.

Similar variations of the tidal parameters are obtained not only with Eterna but also with Baytap (Tamura et al., 1991). Meurers (2004), Meurers et al. (2016) and Jahr (2015) as well report temporal variations of gravimetric factors similar to our results. Further, Merriam (1995) applies the response method to gravity data and resolves satellite harmonics of M2, which are consistent with our observations of temporal variation. The phenomenon obviously is not caused by a simple software problem.

Tidal parameters of groups with smaller amplitude might simply suffer from spectral leakage from large-amplitude tides which are improperly handled in the analysis.

The following causes may contribute to the observed variations:

1) shortcomings of the body tide model used in the analysis (improper ratio of tides of degree two and three, improper description of the FCN),

2) time-dependent response of the Earth (means the system of solid Earth, oceans and atmosphere) to tidal forcing,

3) trade-off between parameters for different wave groups in the inversion, such that noise signals of small amplitude can strongly affect model parameters.

4.1 Body tide model

The model of Earth's admittance (body tide model) as used by Eterna in the analysis might not be appropriate. The ratio between the admittance to tidal potentials of degree two and

three are set to a fixed a priori value (Dehant, 1987), as well as the updated version of FCN, as mentioned in section 2.1. If the ratio is taken at a wrong value, the beat amplitude of the regressor for the respective wave group does not match the actual one. Meurers et al. (2016) discuss components of degree three in the M2 group. The oceans might have a different admittance to degree two and degree three potentials, which could cause a long-period variation (18.6 years nodal modulation, 8.85 years lunar perigee modulation) of tidal parameters. Tidal potentials of degree three for the moon contribute about 1/60 to the total amplitude, while potentials of degree four contribute only 1/3600. We therefore disregard the contributions of degree four in the present discussion.

4.2 Earth

Earth itself may present a time-varying admittance. As mentioned before we believe it to be unlikely that the admittance of the solid Earth varies within month or several years. In contrast, oceans and atmosphere are subject to strong internal variations.

4.2.1 Ocean loading

Like Merriam (1995), Meurers (2004), and Jahr (2015) we suppose a significant contribution of varying ocean loading to the gravity signal. Ocean tides, in particular in shallow water, are well known to show an annual modulation in their M2-admittance. Huess and Andersen (2001) show an annual modulation of the M2 amplitude of 20 cm (15%) at Cuxhaven, Germany and 7 cm (10%) at Esbjerg, Denmark.

Leeuwenburgh et al. (1999) show similar results for further North Sea levels. Baker and Alcock (1983) discuss an annual modulation of M2, S2, and K1 in data from several tide gauges on the N.W. European shelf and the North Atlantic. Kang et. al. (1995) discuss an annual modulation of M2 in tide gauge data from the Korean Strait. Several authors (Merriam, 1995; Meurers, 2004; Jahr, 2015; Sato, 2006; Meurers et al., 2016) investigate this modulation, which would result in temporally varying ocean loading and hence could be source of temporal variations of the tidal parameters.

However, only Merriam (1995) attempts to quantitatively estimate the order of magnitude of ocean loading by comparison with sea-level observations. He shows that amplitude and phase of satellite harmonics MA2 (α2) and MB2 (β2) in gravity data from Cantley are consistent with sea level observations at the Bay of Fundy taken from a study by Godin and Gutiérrez (1986).

4.2.2 Radiation tides

The so-called radiation tides are not driven by the tidal gravity field. Masses e.g. in the atmosphere are driven thermally and produce variations of gravity with the frequency of one cycle per solar day and overtones. These signals appear exactly at the frequencies of S1 and S2 (and higher harmonics) but are not included in the model used for the analysis. If the S1 signal is separated in the setup of wave groups, this produces a noticeable bias. δ(S1) is about 1.2 instead of the approx. expected 1.16 and several degrees in phase instead of 0° for the central European stations.

In moving window analysis this will show up as a temporal variation of the tidal parameters of the K1 group. The S1 harmonic is only a minor contribution to the total signal of the group. However, the deviation in amplitude of this signal from what would be expected due to Earth's body admittance is large enough to produce the required modification of the annual beat amplitude.

The contribution of radiation tides may even be time variable. Spectrogram analysis of the air-pressure recording from BFO shows clear signals at the frequencies of S1 and S2 with amplitudes varying with an annual cycle.

4.3 Technical Causes

Trade-off between model parameters increases the vulnerability to cross-talk. Eterna lacks means of regularization or some sort of damping with respect to a priori constraints in the linear regression. As a consequence, if regressors become linearly dependent, i.e. the condition number of the system of linear equations becomes large, this can result in significant trade-off between model parameters, in particular in the presence of noise.

Large modifications then are applied to tidal parameters in order to produce insignificant reductions in the signal energy of the residual, simulating an otherwise unexplained component of the recorded signal. This, together with the fact that wave groups can only be defined by choosing a frequency band, restricts the options to separate potential causes of bias (harmonics of degree three, harmonics at frequencies of radiation tides, etc). The consequences of the regression becoming increasingly singular are potentially boosted by non-tidal noise in the recording.

The time window, in the simplest case a boxcar window, can influence the estimation of tidal parameters (Schüller, 1976), due to spectral leakage caused by the window function.

Some of these effects can be identified by the usage of time windows of different length. We applied 60 days and 90 days time windows. The variations, discussed below, did not change due to the time window. The variations caused by the time window itself can be reduced by using a Hann taper (Schüller, 2015). A Hann taper was used in this study.

5. Results and discussion

In this section, we discuss probable causes for the temporal variations of tidal parameters, but show no verification. If no possible cause for the variation of the tidal parameters of one wave group is mentioned, there is, in our opinion, no evidence that one cause is more likely than another.

Wave group M3M6 is only shown for the sake of completeness. It covers a very large frequency range, which results in interaction of many variations with different periods and makes an identification of harmonics unreliable.

5.1 Body tide model

As mentioned in section 4.1 there are several possibilities how inappropriate assumptions in the body tide model can cause temporal variations of the tidal parameters.

The ratio of the admittance for degree 2 and 3 harmonics could be responsible for the 8.8 year variation of the parameters of Q1, M1, N2 and L2 (see Tab. 4). Dehant et al. (1999) calculate theoretical tidal parameters based on a more recent Earth model. The gravimetric factors for degree 2 and 3 are slightly different from the values used in Eterna. The difference of about 0.1% is of the order of magnitude of the variation of the tidal parameters of Q1 and M1, but too small to explain the observed variations for N2 and L2, because the latter are an order of magnitude larger (see for example Fig. 2 & 3). Especially the semidiurnal wave groups are influenced by ocean loading therefore the variation is probably, at least partly, caused by the oceans.

5.2 Earth

5.2.1 Ocean loading

Ocean loading probably causes the annual variation of the M2 tidal parameters. An annual variation of the M2 amplitudes in the oceans that is larger than we would expect it to be from tidal potential is well known.

A rigorous estimation of non-stationary ocean loading must take account of signal amplitude and phase and therefore requires a full time-dependent calculation of ocean loading with an appropriate model of spatial and temporal variations of sea surface height. This will be the scope of future studies. Here we put a simple consideration to provide a test for order of magnitude. We approximate the water of the North Sea by a parallelogram with a total area of $1.6 \cdot 10^{11} m^2$. The distance of the center of mass of this area to Black Forest Observatory (BFO) is about 6° and the loading Green's function for this distance is $0.23 \cdot 10^{-22}$ $(m/s^2)/kg$ (Na and Beak, 2011). Gravity at BFO would thus respond with 0.04 $(nm/s^2)/cm$ to coherent changes in sea surface height in the given area. The observed variation of δ(M2) could be caused by an annual modulation of 2.5 cm in sea surface height. This of in the order of magnitude of observed and predicted variations of sea surface height for M2 in the North Sea (Huess and Andersen, 2001; Müller et al., 2014). The oceans certainly play an important role at Syowa and Ny-Ålesund, where the coast lines are very close. Additionally the amplitudes of diurnal and semidiurnal tides become smaller with high latitudes. Ocean loading therefore has a larger influence on the tidal parameters at these stations.

As mentioned in section 3.2, the offsets of the tidal parameters deviate from what is predicted by the body tide model. This is usually associated to ocean loading. Baker and Bos (2003) calculate the loading for several ocean models at Conrad, Medicina, Strasbourg, Wettzell, Membach, Metsähovi, Cantley, Canberra, and Syowa. Their results would approximately fit to the deviation of our results from the expected values of the body tide model.

For the stationary contribution of ocean loading to tidal parameters obtained by analysis of gravity records, we observe a clear dependence on location in the European network of superconducting gravimeters. The amplitude of the temporal variation of gravimetric factors, however is very similar for all stations (see Fig. 2 and 3). Like the cause of stationary ocean loading the causes for temporal variations therefore cannot be effects local to the station or the SG itself. It apparently does not depend on the distance of the station to the coast. This is different to what Meurers et al. (2016) report. In any case, if the ocean is the source of the temporal variation, the spatial pattern of the amplitude of temporal variations should correspond to the spatial distribution of the modulation of M2 in the oceans on the one hand. On the other hand the pattern of stationary ocean loading must correspond to the distribution of the mean amplitude of M2.

5.2.2 Radiation tides

The atmosphere has a strong influence at solar frequencies S1 and S2. As shown in Tab. 4 S1 is part of the K1 group and will therefore influence the variation of K1 factors. The radiation tide at S1 is a well known phenomenon and will for sure contribute to the difference of tidal parameters of S1 to the expected values for the body tide model. However we can not rule out that there is also a contribution caused by ocean loading. Schindelegger et al. (2016) show with hydrodynamical ocean modeling that the amplitude of S1 in the oceans could be much larger, up to 2 cm, instead of a few millimeters, as we would expect due to tidal forcing and comparison with the tidal parameters of K1 and P1. The loading of this effect would contribute as well to the deviation of the S1 tidal parameters and therefore to the variation of the parameters of the K1 group.

A similar case is the contribution of the radiation tide at S2 frequency. It seems likely that the radiation tides change the ratio of the S2 harmonic relative to the other harmonics in the group which results in variations of the tidal parameters. An amplitude and phase ratio of S2 relative to K2,2T2, R2 and T2 (see Tab. 4), deviating from the expectations due to the body tide model, would explain the occurrence of the annual and semi-annual variation.

For the variations given in Tab. 4 and not mentioned here, several causes related to oceans or atmosphere are imaginable but we have no evidence that one is more likely than another.

For the parameters of O1, J1 and OO1 single features are observed that are similar at several stations, as described in section 3.2. They maybe could also be caused by oceans or atmosphere but we have no conception of the responsible mechanisms, yet.

5.2 Technical causes

As mentioned in section 4.3 we ruled out some technical causes by using time windows of different length. The influence of the taper could also be identified with this test. We observed short period (few month) variations, which depended on the window length when a boxcar window is used and almost vanish when the Hann taper is applied. They are still visible for example in the maxima of M2 gravimetric factors.

6. Summary

Systematic variations of tidal parameters larger than the standard deviation are observed all over the globe. The apparent admittance of the Earth to tidal forcing is not stationary. For the semi-diurnal wave groups as well as Q1, M1, and K1 a clear periodicity is observed. The long periodic variation of 8.8 year is probably due to third degree harmonics, while shorter periods between one year and a half year could be caused by atmosphere and oceans.

Especially for the central European SG stations, with their small interstation distances, the variations show clear similarities. Although their variations show larger differences, the characteristics of the variations are also found for the globally distributed stations. That indicates that on regional and global scale the same causes or same phenomena influence gravity measurements. We name probably responsible harmonics and discussed probable causes for every wave group. As they are often related to oceans and atmosphere, the temporal variations of the gravimetric factor and the phase thus can provide observational data of changes in the oceans as well as atmosphere. They can be useful to study changes in the ocean's behaviour due to a changing ocean climate or for validation of non-stationary ocean models. On the other hand effects like non-stationary ocean loading limits the inferences that could be drawn from a moving window analysis with respect to the properties of the solid Earth. The resulting bias should be mitigated by taking non-stationary loading into account in tidal analysis. For the O1, J1, OO1 and M3M6 no periodicity in the variations of the tidal parameters is observed, but similar transient signals for some stations.

Acknowledgements

We are grateful to Walter Zürn for fruitful discussions and for helpful comments on the manuscript as well as to Ann-Kathrin Edrich and Clara Bützler who completed the catalogue with results for Conrad and Medicina. The data used for this study was provided by the International Geodynamics and Earth Tide Service (IGETS) and Hans-Georg Scherneck, Onsala Space Observatory, Chalmers, Sweden. P. Wolf and H. Wziontek from the Federal Acgency for Cartography and Geodesy (Bundesamt für Kartographie und Geodäsie, BKG) provided information about their data from the SG in Wettzell. The project is funded by the German Research Foundation (Deutsche Forschungsgmeinschaft, WE-2628/4-1).

References

Baker, T. F. and G. A. Alcock (1983): Time variation of ocean tides. In: *Proceedings of the Ninth International Symposium on Earth Tides*. Ed. by T. Kuo. Stuttgart: E. Schweizerbart'sche Verlagsbuchhandlung, pp. 341-350.

Baker, T. F. and M. S. Bos (2003): Validating Earth and ocean tide models using tidal gravity measurements. *Geophys. J. Int.* 152, pp. 468-485. DOI:10.1046./j.1345-246X.2003.01863.x.

Bartels, J. (1957): Gezeitenkräfte. In: *Handbuch der Physik 48, Geophysik 2*. Ed. by S. Flügge. Berlin: Springer.

Calvo, M., J. Hinderer, S. Rosat, H. Legros, J.-P. Boy, B. Ducarme and W. Zürn (2014): Time stability of spring and superconducting gravimeters through the analysis of very long gravity records. *Journal of Geodynamics* 80, pp. 20-33. DOI: 10.1016/j.jog.2014.04.009.

Dehant, V. (1987): Tidal parameters for an inelastic Earth. *Physics of the Earth and Planetary Interiors* 49, pp. 97-116. DOI: 10.1016.0031-9201(87)90134-8

Dehant, V., P. Defraingne and J. M. Wahr (1999): Tides for a convective Earth. *J. Geophys. Res.* 104, pp. 1035-1058. DOI:10.1029/1998JB900051

Godin, G. and G. Gutiérrez (1986): Non-linear effects in the tide of the Bay of Fundy. *Continental Shelf Research* 5.3, pp. 379-402.

Hartmann, T. and H.-G. Wenzel (1995a): Catalogue HW95 of the tide generating potential. *Bulletin d'Information des Marées Terrestres* 123, pp. 9278-9301.

Hartmann, T. and H.-G. Wenzel (1995b): The HW95 tidal potential catalogue. *Geophysical research letters* 22.24, pp. 3553-3556. DOI: 10.1029/95GL03324.

Huess, V. and O. B. Andersen (2001): Seasonal variation in the main tidal constituent from altimetry. *Geophysical research letters* 28.4, pp. 567-570. DOI: 10.1029/2000GL011921.

Iwano, S., Y. Fukuda, T. Sato, Y. Tamura and K. Matsumoto (2005): Long-period tidal factors at Antarctica Syowa Station determined from 10 years of superconducting gravimeter data. *J. Geophys. Res* 110, B.10403. DOI: 10.1029/2004JB003551.

Jahr, T. (2015): Variation der Gezeitenparameter am Geodynamischen Observatorium Moxa aus Beobachtungen mit einem supraleitenden Gravimeter. *Allg. Verm. Nachr. (avn* 122, pp. 163-167.

Kang, S. K., J.-Y. Chung, S.-R. Lee and K.-D. Yum (1995): Seasonal variability of the M2 tide in the seas adjacent to Korea. *Continental Shelf Research* 15.9, pp. 1087-1113. DOI: 10.1016/0278-4343(94)00066-V.

Krásná, H., J. Böhm and H. Schuh: Free core nutation observed with VLBI. *Astronomy and Astrophysics* 555, A29. DOI: 10.1051/0004-6361/201321585

Leeuwenburgh, O., O. Andersen and V. Huess (1999): Seasonal Tide Variation from Tide Gauges and Altimetry. *Phys. Chem. Earth (A)* 24.4, pp. 403-406. DOI:10.1016/S1464-1895(99)00049-6.

Merriam, J. B. (1995): Non-linear tides observed with the superconducting gravimeter. *Geophy. J. Int.* 123, pp. 289-299. DOI:10.1111/j.1365-246X.1995.tb06869.x.

Meurers, B. (2004): Investigation of temporal gravity variations in SG-records. *Journal of Geodynamics* 38, pp. 423-435.

Meures, B., M. van Camp, O. Francis and V. Pálinkás (2016): Temporal variations of tidal parameters in superconducting gravimeter time-series. *Geophys. J. Int.* 205, pp. 284-300. DOI: 10.1093/gji/ggw017.

Müller, M., J. Y. Cherniawsky, M. G. G. Foreman and J.-S. von Storch (2014): Seasonal variation of the M_2 tide. *Ocean Dynamics* 64, pp.159-177. DOI: 10.1007/s10236-013-0679-0.

Munk, W. H. and K. Hasselmann (1964): Super-resolution of Tides. *Studies on Oceanography*, pp. 339-344.

Na, S.-H. and J. Beak (2011): Computation of the Load Love Number and the Load Green's Function for an Elastic and Spherically Symmetric Earth. *Journal of the Korean Physical Society* 58.5, pp. 1195-1205. DOI: 10.2938/jkps.58.1195.

Sato, T., K. Asari, Y. Tamura, H.-P. Plag, H. Digre, Y. Fukuda, J. Hinderer, K. Kaminuma and Y. Hanamo (2001): Continous Gravity Observations at Ny-Ålesund, Svalbard, Norway with a Superconducting Gravimeter CT#039. *Journal of the Geodetic Society of Japan* 47.1, pp. 341-346.

Sato, T., J.-P. Boy, Y. Tamura, K. Matsumoto, K. Asari, H.-P. Plag and O. Francis (2006): Gravity tide and seasonal gravity variation at Ny-Ålesund in Arctic. *Journal of Geodynamics* 41, pp. 234-241. DOI: 10.1016/j.jog.2005.08.016

Schindelegger, M., D. Einšpigel, D. Salstein and J. Böhm (2016): The global S1 Tide in Earth's Nutation. *Surveys in Geophysics* 37, pp. 643-680. DOI: 10.1007/s10712-016-9365-3.

Schroth, E. (2013): Analyse von Gezeitenregistrierungen des supraleitenden Gravimeters SG-056. urn: nbn:de:swb:90-466565. Diplomarbeit. Karlsuhe Institute of Technology (KIT). URL: http://nbn-resolving.org/nbn:de:swb:90-466565.

Schüller, K. (1976): Ein Beitrag zur Auswertung von Erdgezeitenregistrierungen. PhD thesis. Bonn.

Schüller, K. (2015): Theoretical Basis for Earth Tide Analysis with the New ETERNA34-ANA-V4.0 Program. *Bulletin d'Information des Marées Terrestres* 149, pp. 12024-12061. URL: http://orbilu.uni.lu/bitstream/10993/19948/2/bim149.pdf

Tamura, Y., T. Sato, M. Ooe and M. Ishiguro (1991): A procedure for tidal analysis with a Bayesian information criterion. *Geophys. J. Int.* 104, pp. 507-516. DOI: 10.1111/j.1365-246X.1991.tb05697.x.

Wenzel, H.-G. (1996): The nanogal software: Earth tide data processing package ETERNA 3.30. *Bulletin d'Information des Marées Terrestres* 124, pp. 9425-9439. URL: www.eas.slu.edu/GGP/ETERNA34/MANUAL/ETERNA33.HTM

Wenzel, H.-G. (1997a): Analysis of Earth Tide Observations. In: *Tidal Phenomena*. Ed. by H. Wilhelm, W. Zürn and H.-G. Wenzel. Vol. 66. Lecture notes in Earth sciences. Berlin: Springer, pp. 59-75. DOI: 10.1007/BFb0011457.

Wenzel, H.-G. (1997b): Eterna 3.40 Manual. Black Forest Observatory, Universität Karlsruhe. Karlsruhe.

Appendix

Table 5: Definition of wave groups. Name, start frequency f_S and end frequency f_E in cpd.

wave group	f_S in cpd	f_E in cpd
Q1	0.501370	0.911390
O1	0.911391	0.947991
M1	0.947992	0.981854
K1	0.981855	1.023622
J1	1.023623	1.057485
OO1	1.057486	1.470243
2N2	1.470244	1.880264
N2	1.880265	1.914128
M2	1.914129	1.950419
L2	1.950420	1.984282
S2	1.984283	2.451943
M3M6	2.451944	7.000000

Table 6: Senitivites (calibration factor) and time lag in s for Wettzell given in the IGETS data files and a changed version based on information by P. Wolf and H. Wziontek (pers. comm.) and tests which parameters produce no or smaller steps.

	IGETS		changend	
time span	sensitivity	time lag in s	sensitivity	time lag in s
	GWR CD029 (lower sensor)			
05.11.1998-30.09.1999	1.10017	8.000	1.10017	8.000
01.10.1999-20.03.2001	1.10017	5.000	1.10017	5.000
02.04.2001-31.12.2001	1.10017	0.000	1.10017	0.000
01.01.2002-31.12.2003	1.10017	5.000	1.10017	0.000
02.01.2004-16.04.2007	1.10017	40.000	1.10017	40.000
21.04.2007-31.12.2007	1.00000	14.931	1.00000	14.931
01.01.2008-31.12.2008	1.10017	40.000	1.00000	14.931
01.01.2009-06.10.2010	1.00000	14.931	1.00000	14.391
	GWR CD030 (lower sensor)			
26.06.2010-27.02.2015	1.00000	13.400	1.00000	9.000

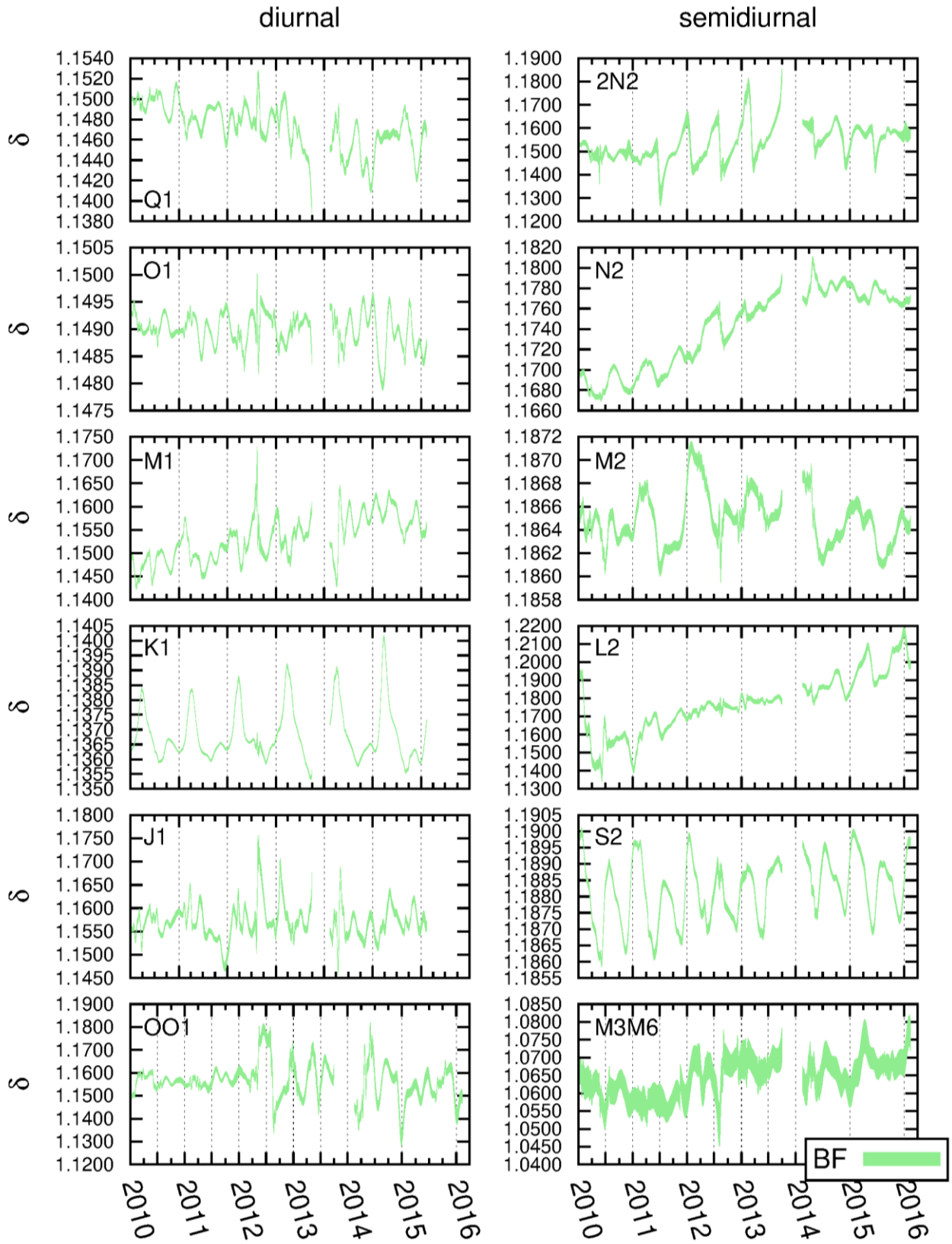

Figure 12: Gravimetric factors for the station BFO.

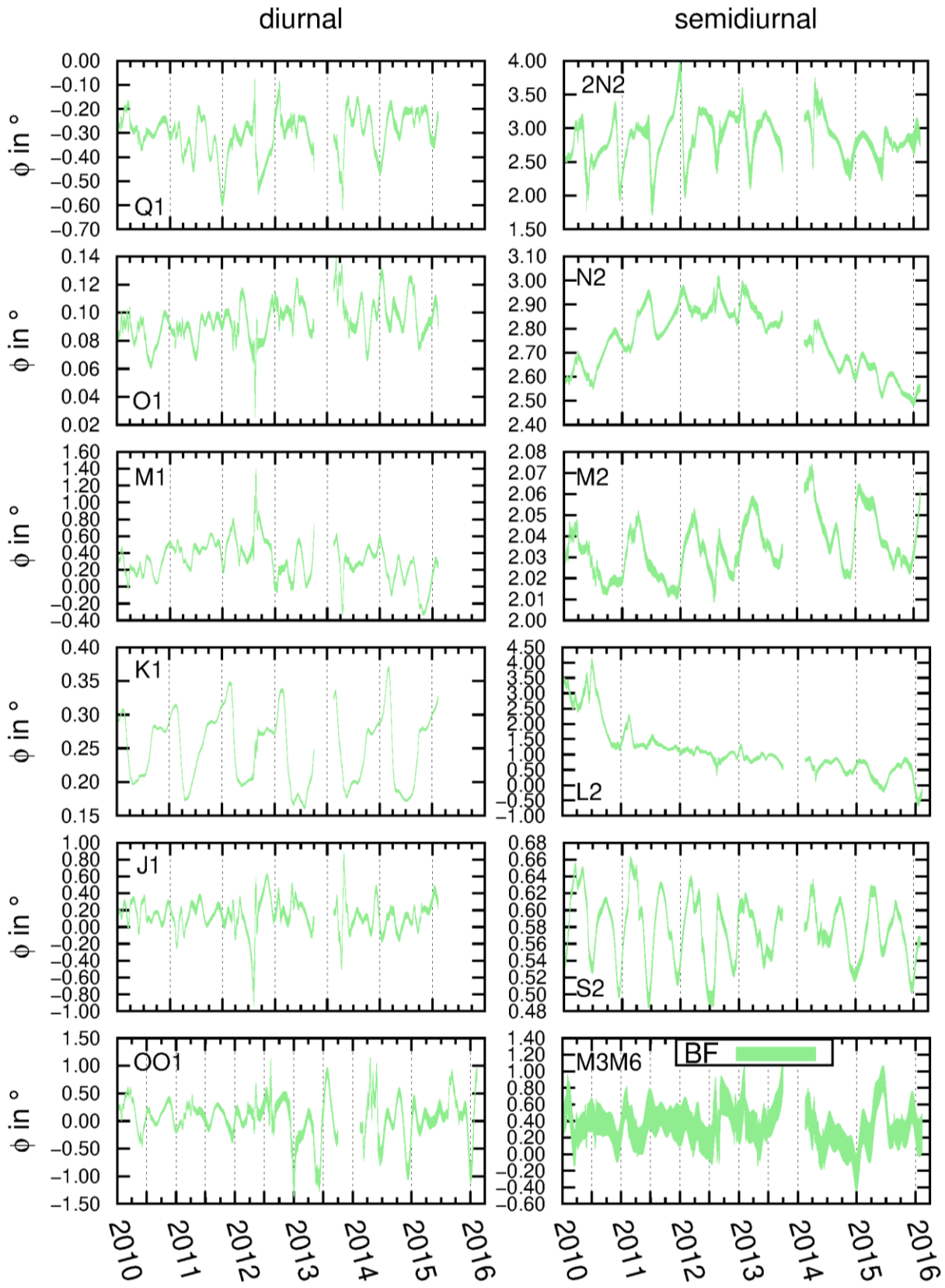

Figure 13: Phase leads for the station BFO.

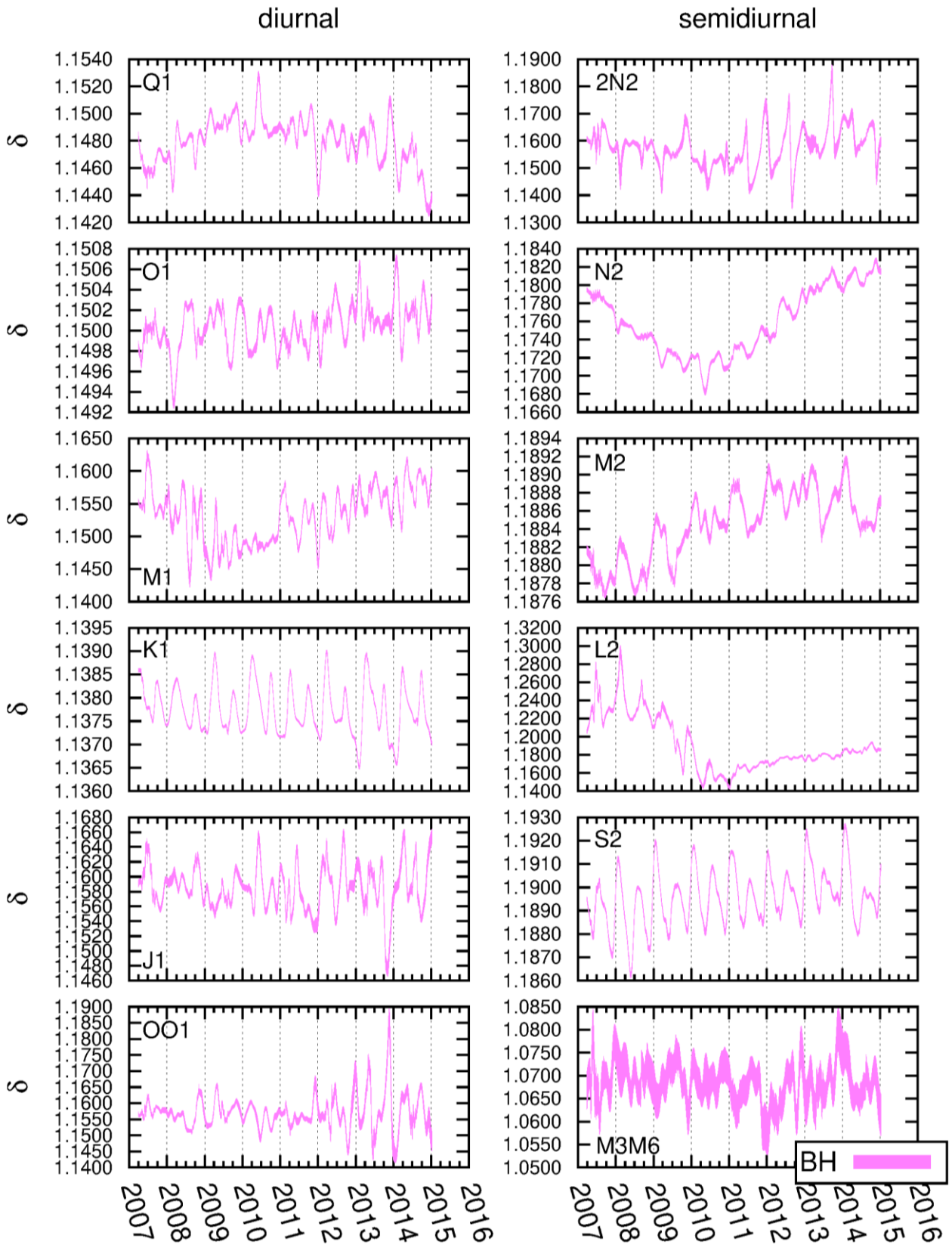

Figure 14: Gravimetric factors for the station Bad Homburg.

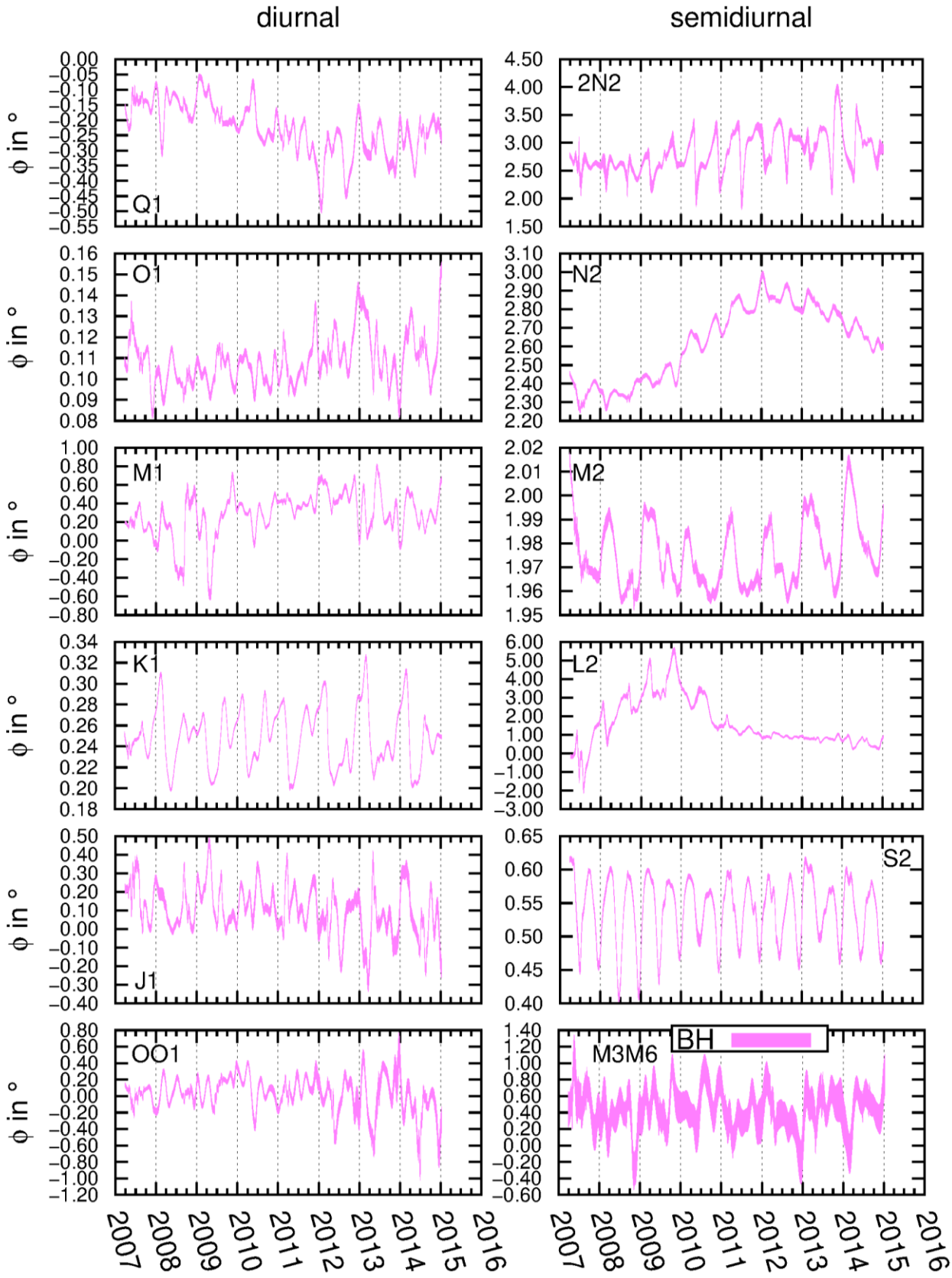

Figure 15: Phase leads for the station Bad Homburg.

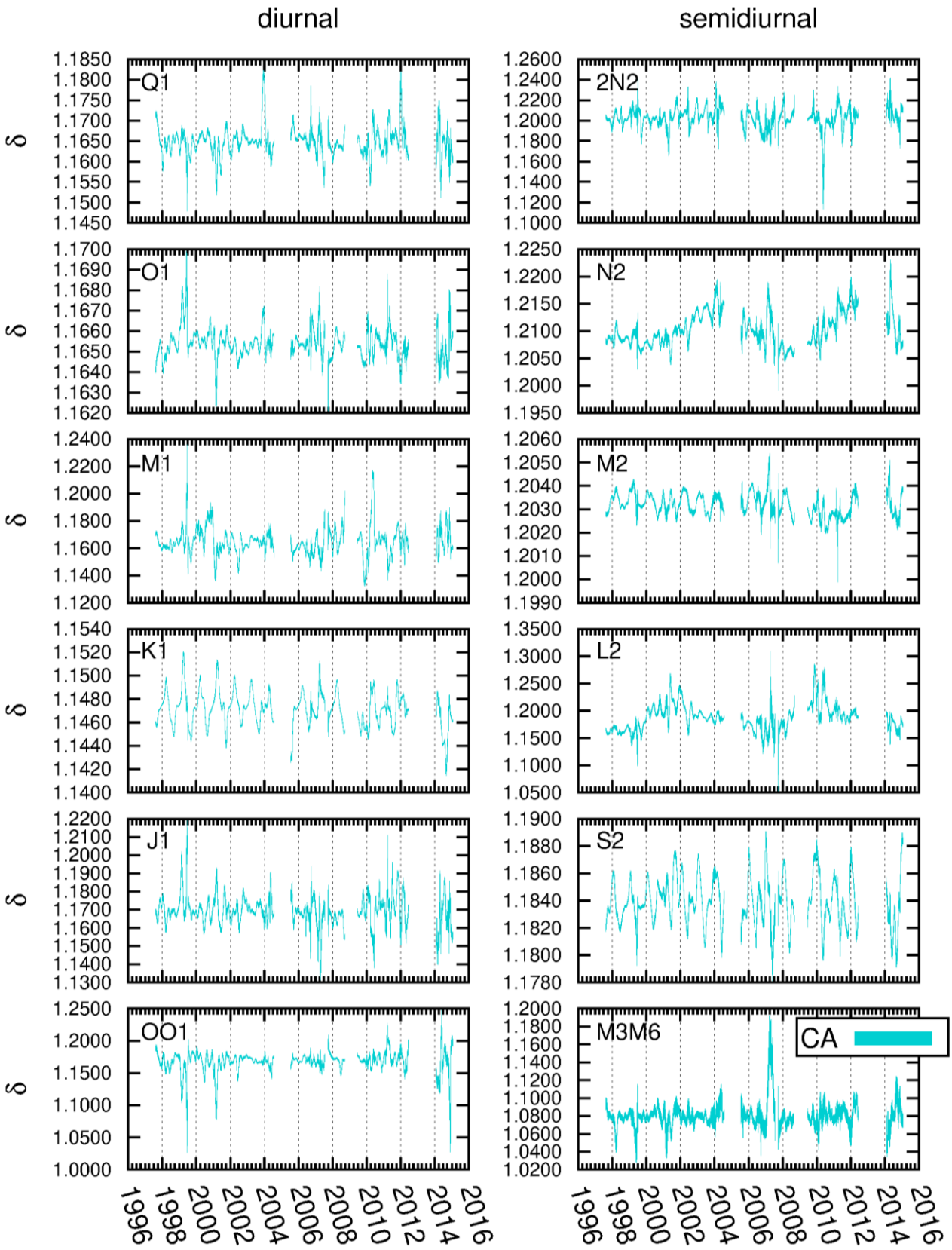

Figure 16: Gravimetric factors for the station Cantley.

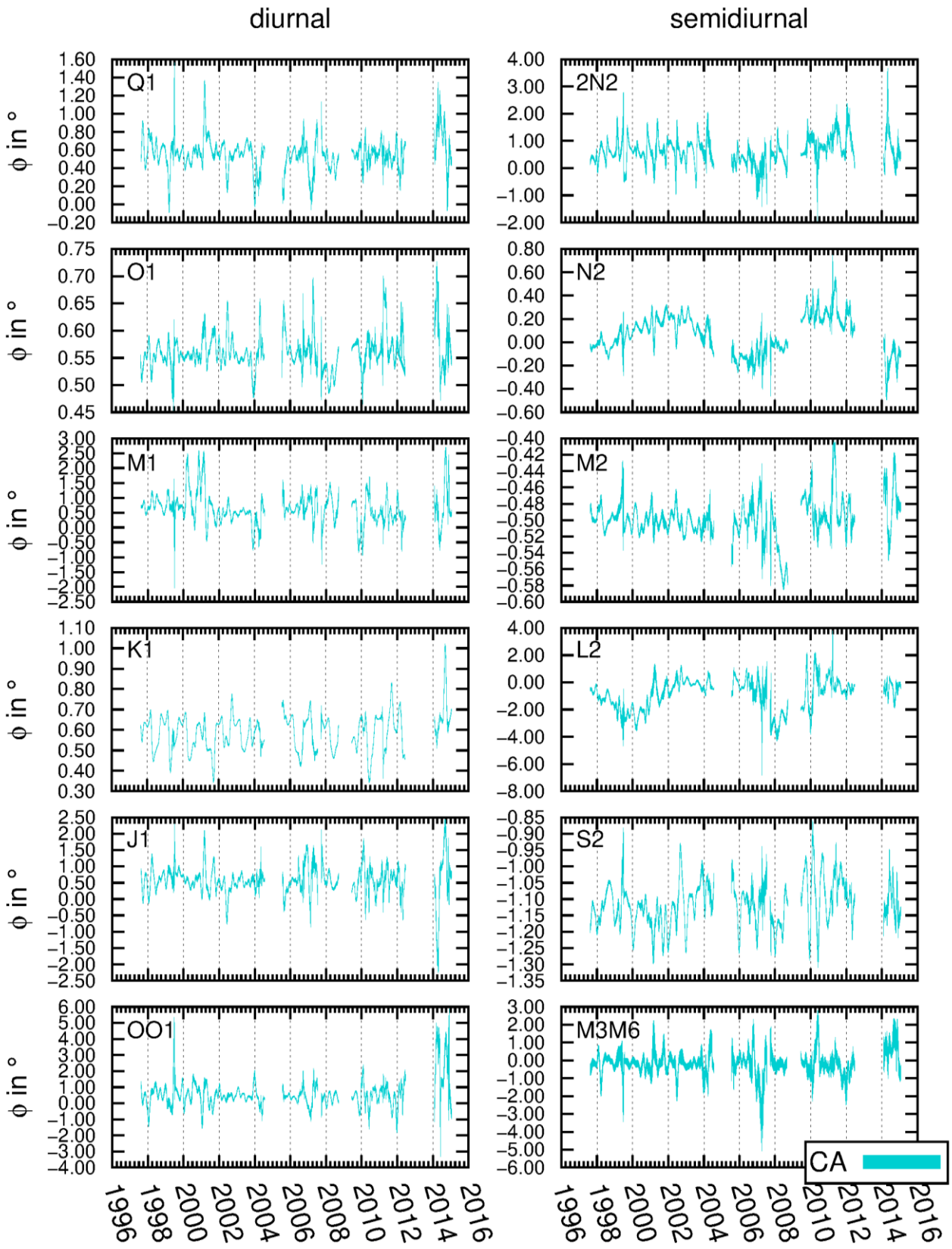

Figure 17: Phase leads for the station Cantley.

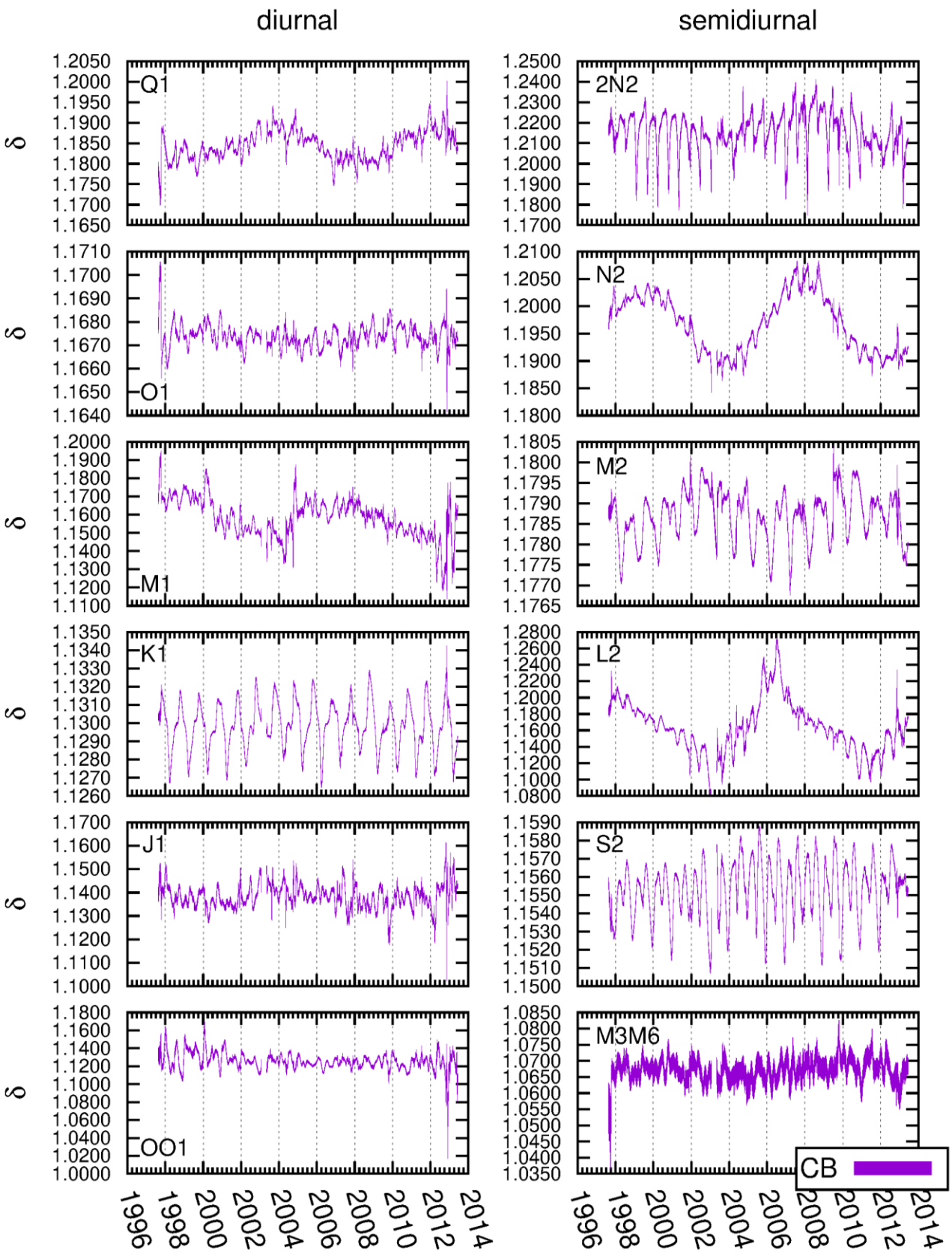

Figure 18: Gravimetric factors for the station Canberra.

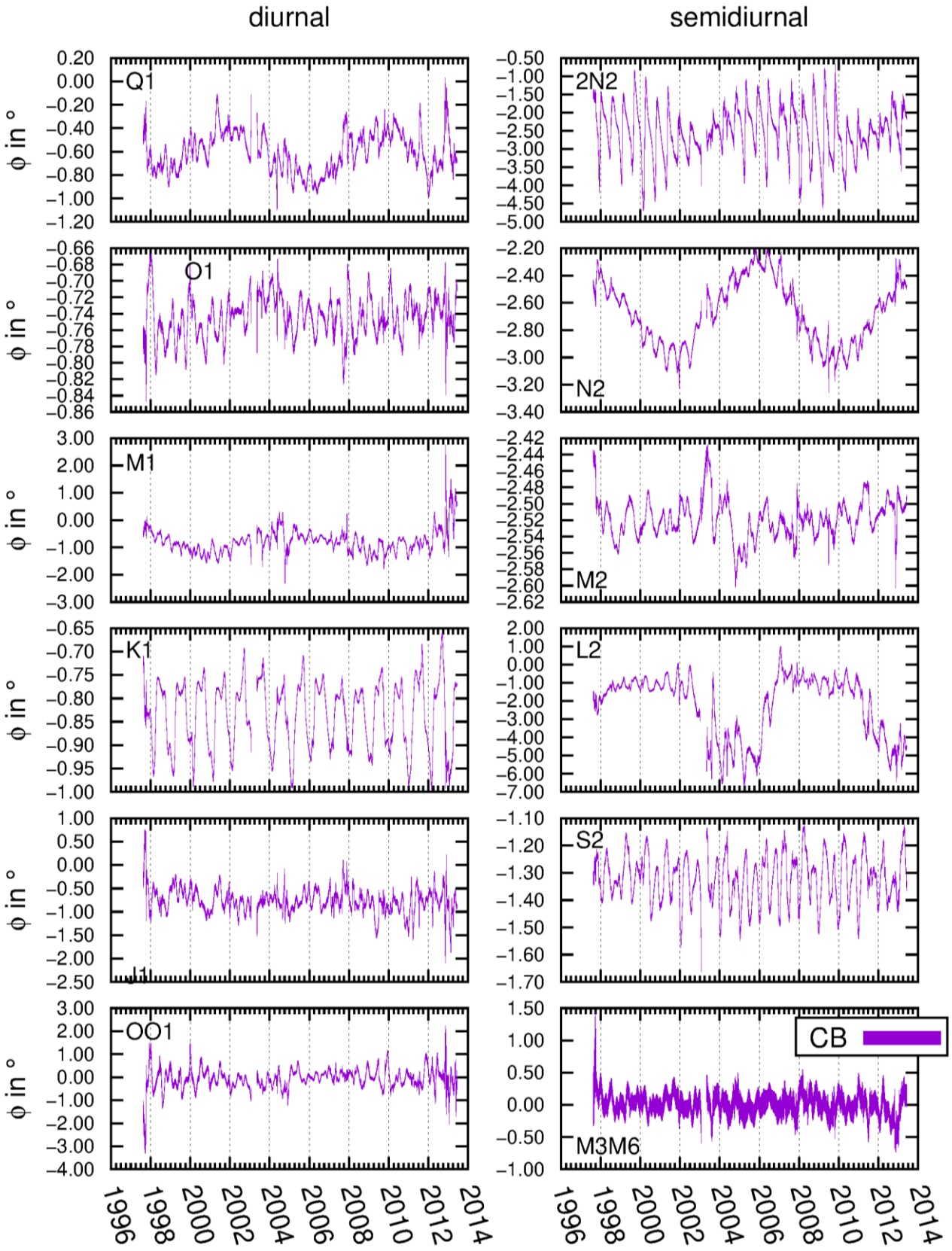

Figure 19: Phase leads for the station Canberra.

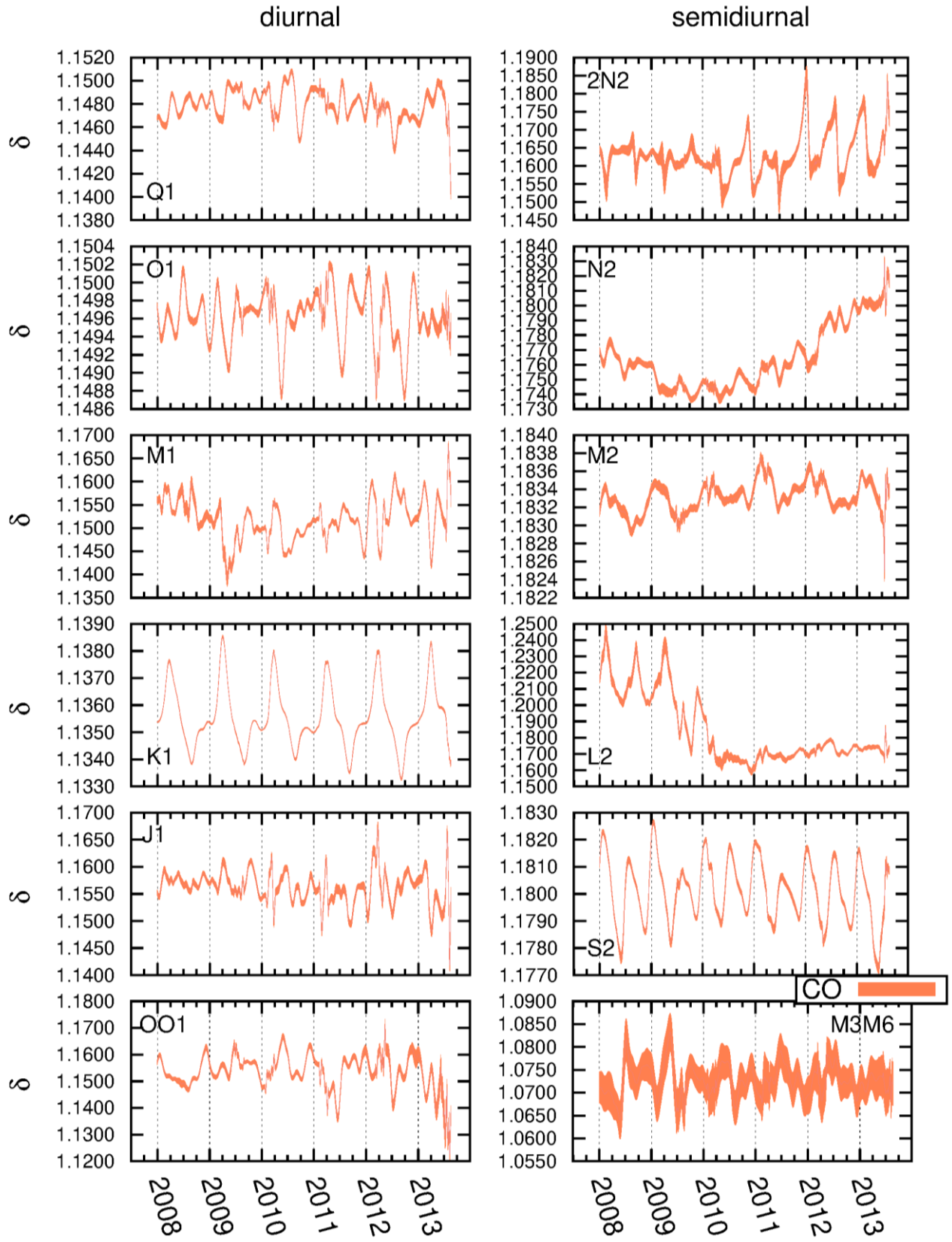

Figure 20: Gravimetric factors for the station Conrad.

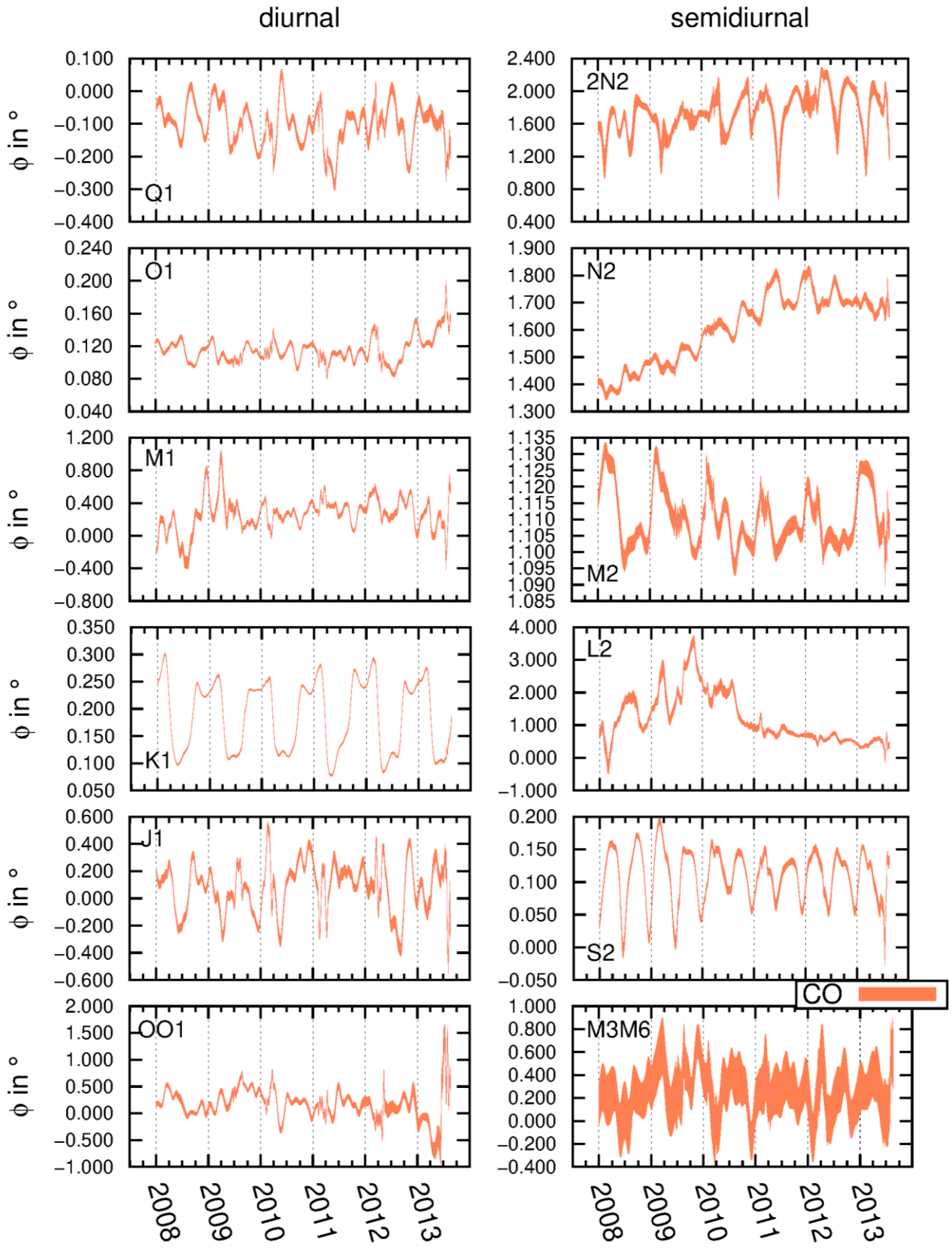

Figure 21: Phase leads for the station Conrad.

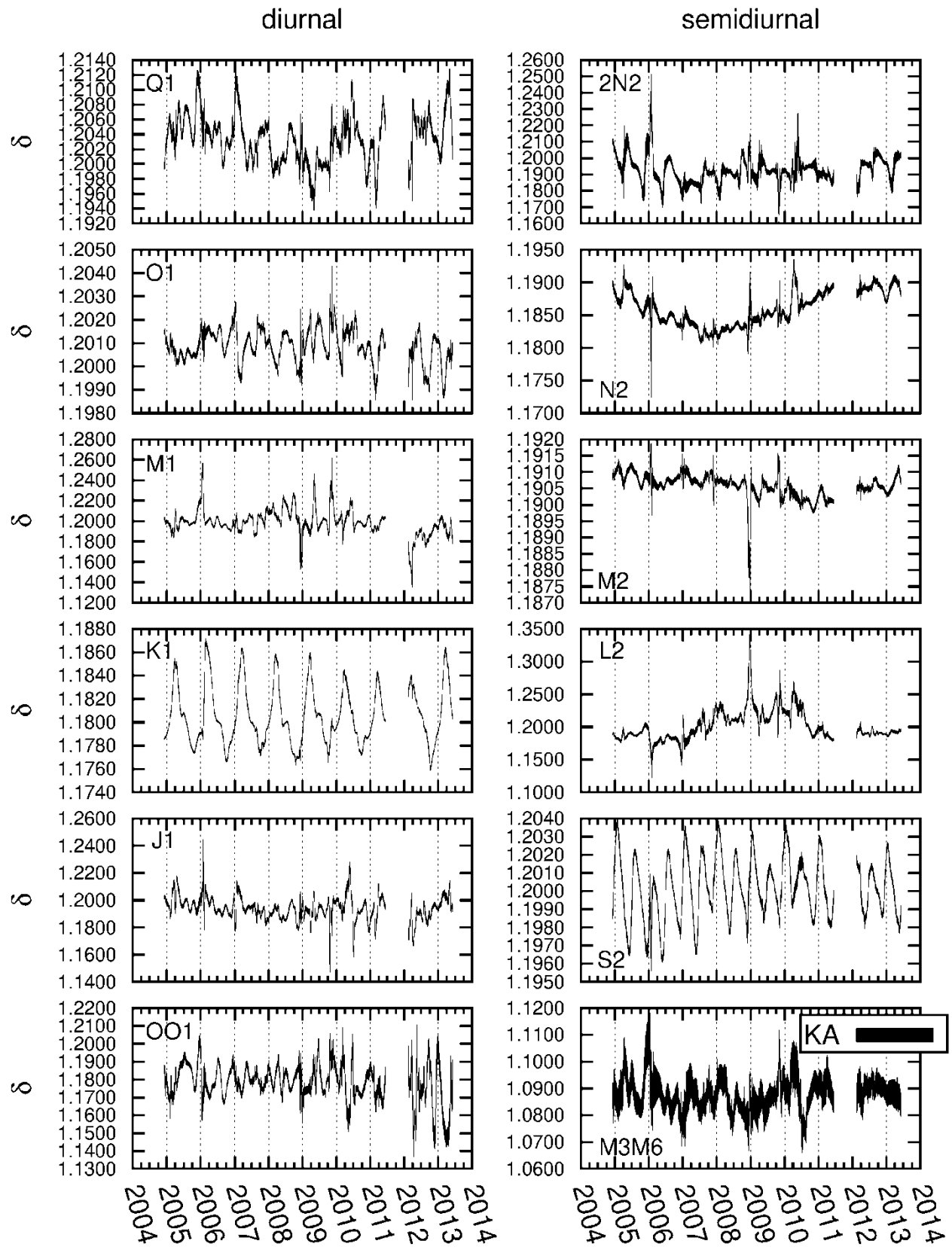

Figure 22: Gravimetric factors for the station Kamioka.

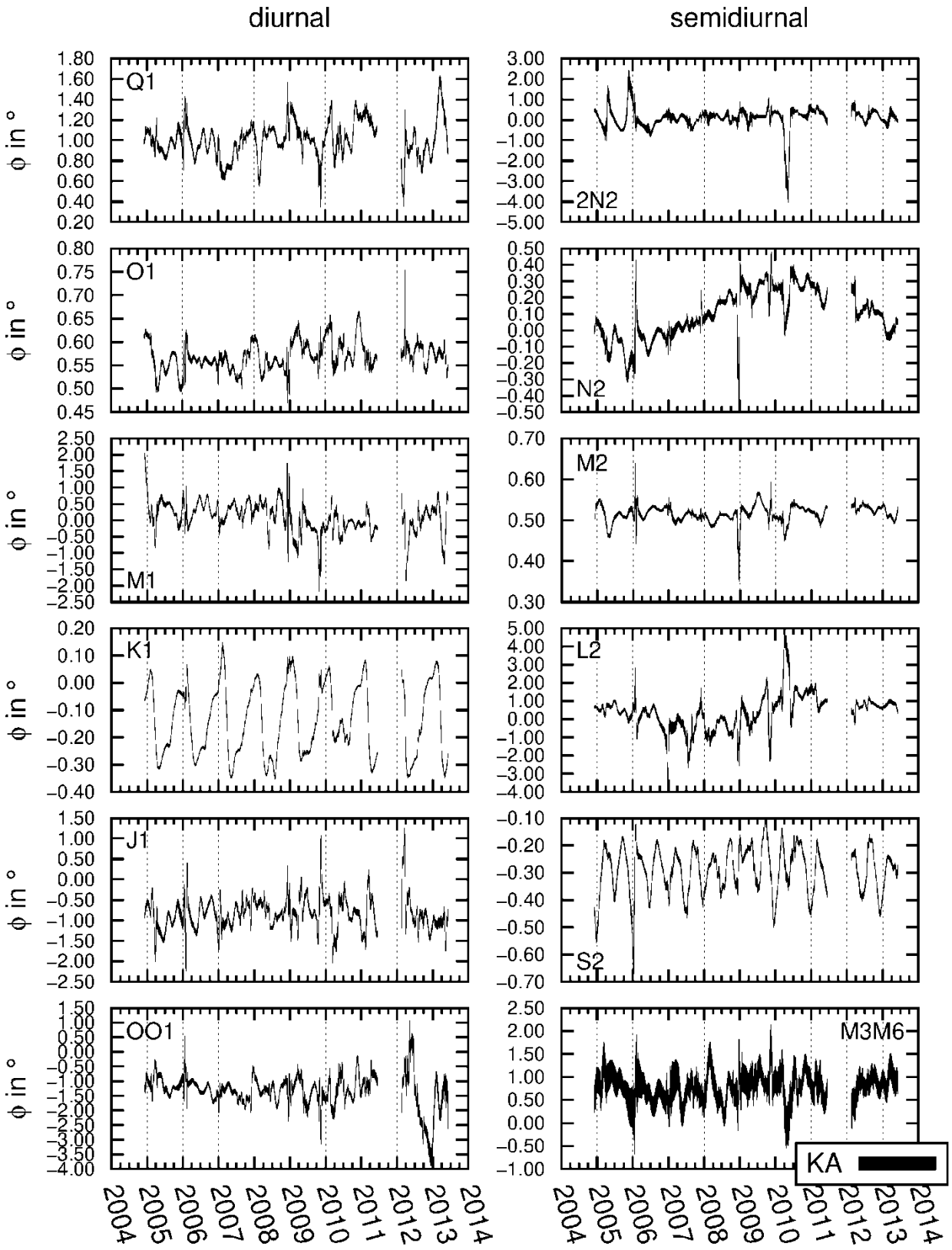

Figure 23: Phase leads for the station Kamioka

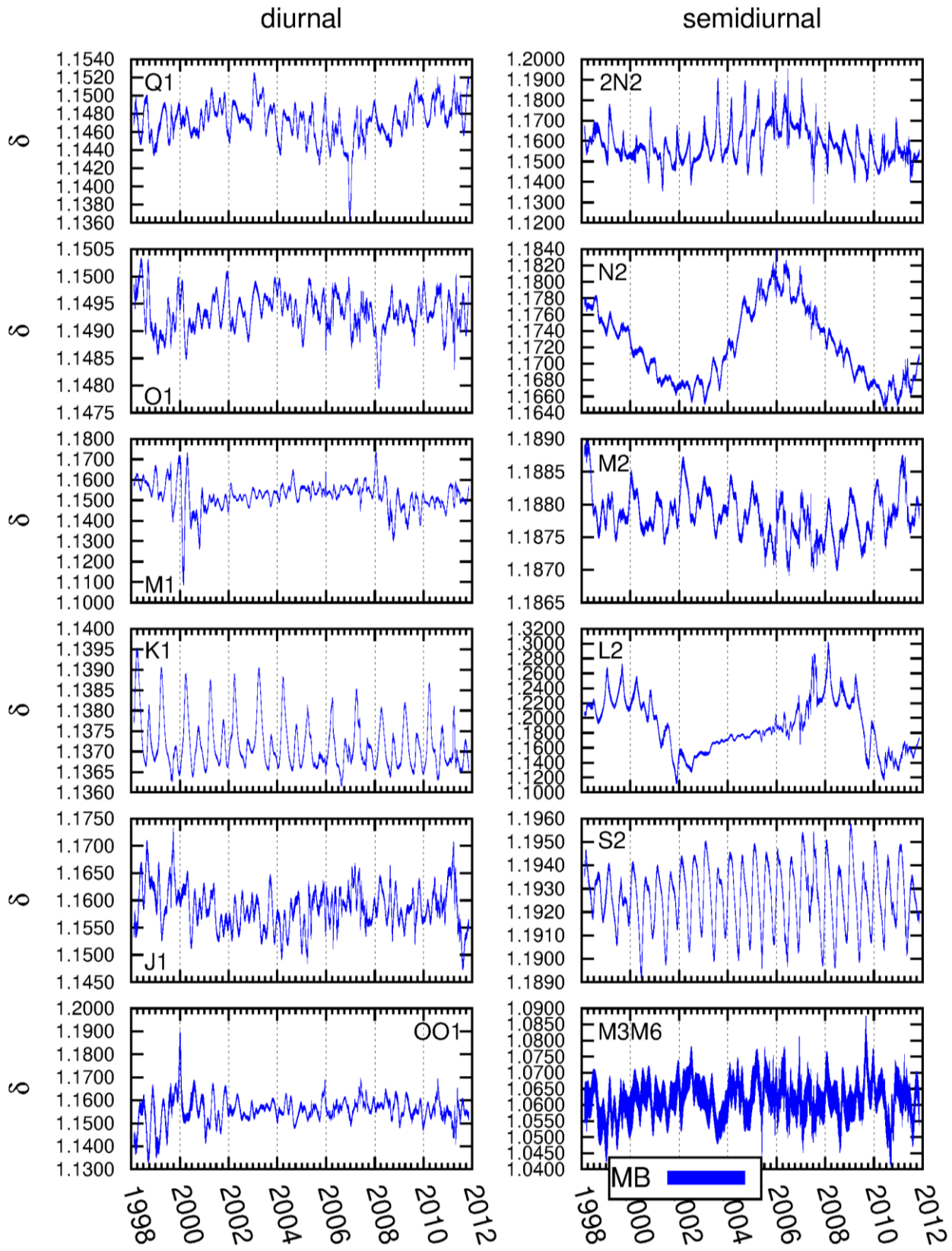

Figure 24: Gravimetric factors for the station Membach.

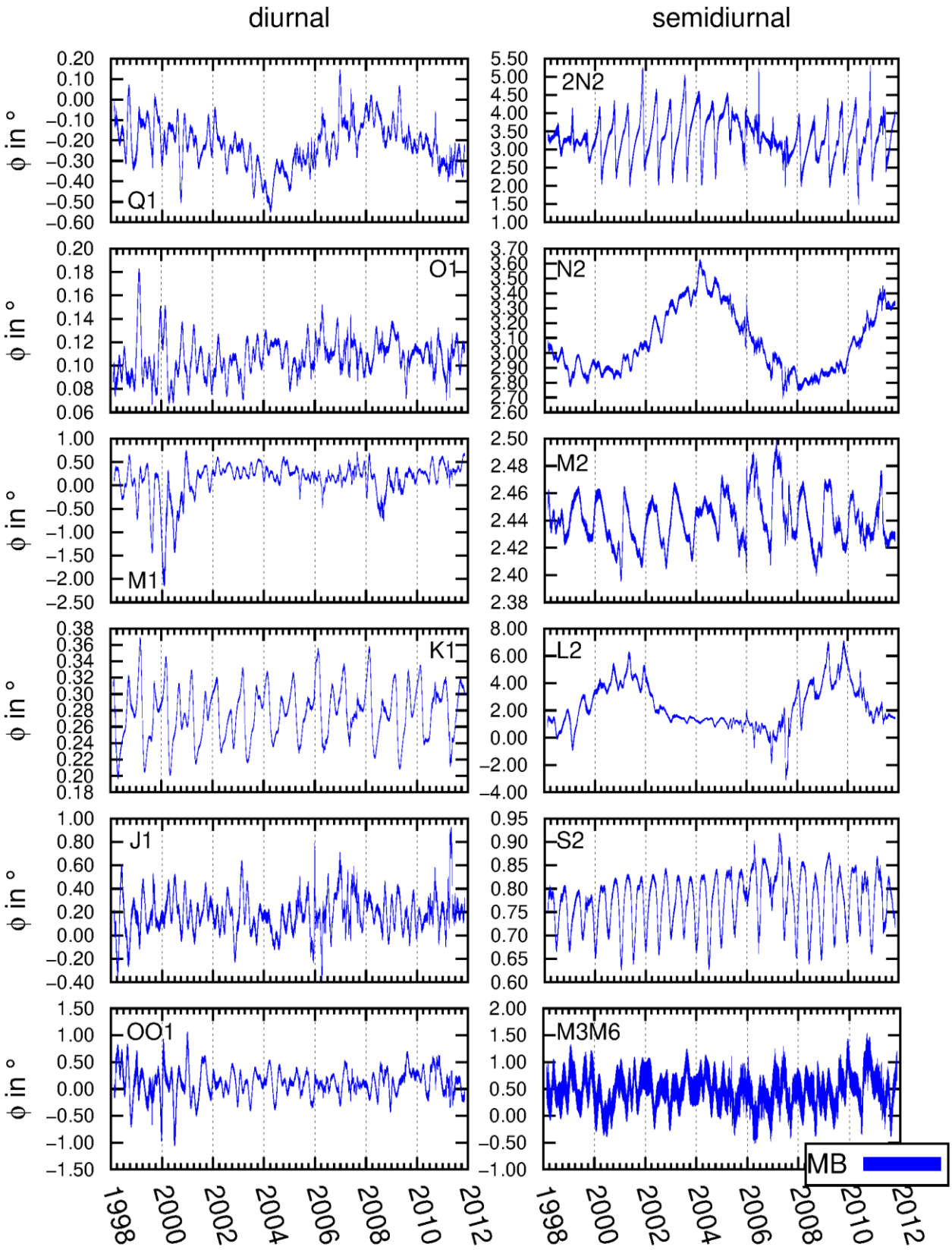

Figure 25: Phase leads for the station Membach.

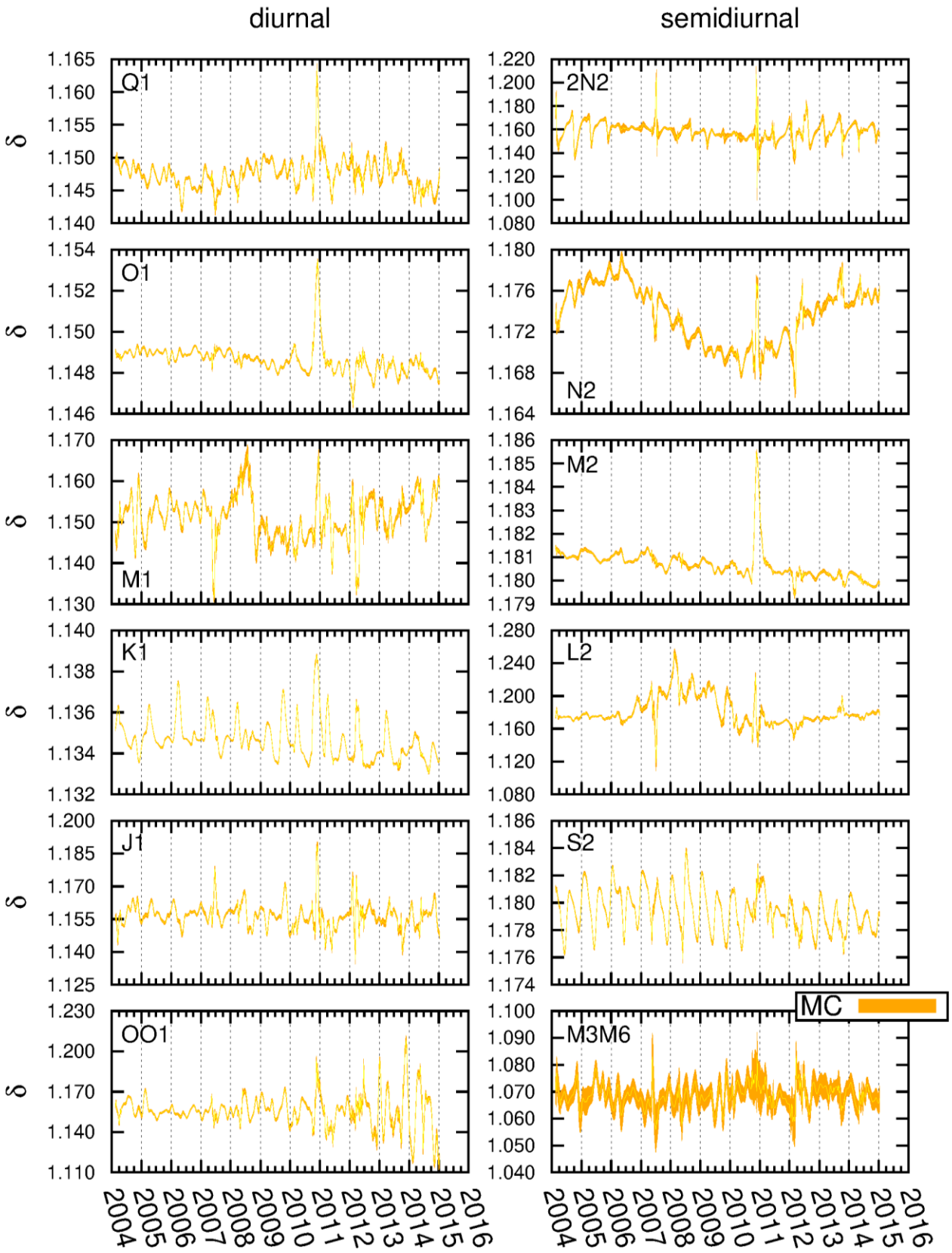

Figure 26: Gravimetric factors for the station Medicina.

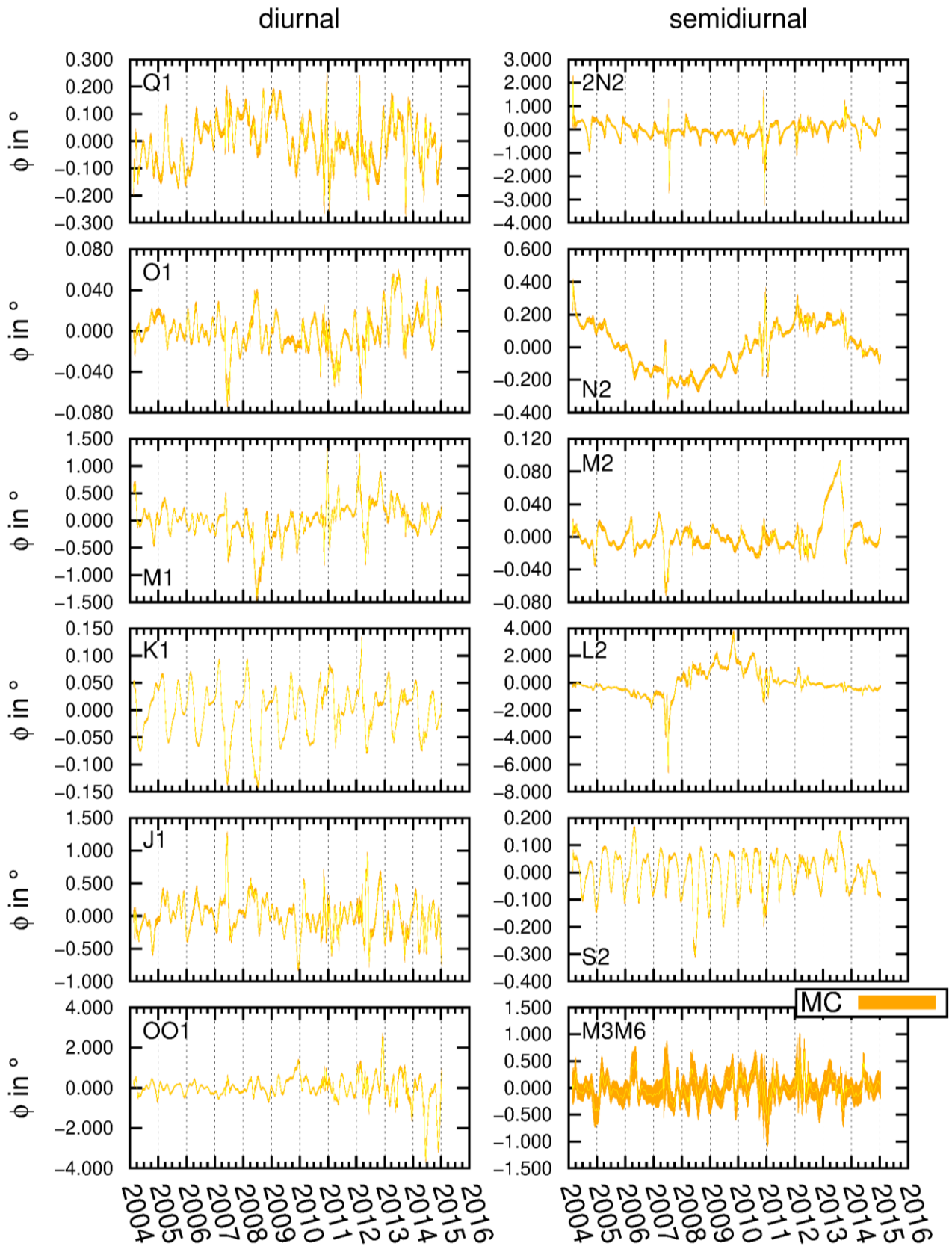

Figure 27: Phase leads for the station Medicina.

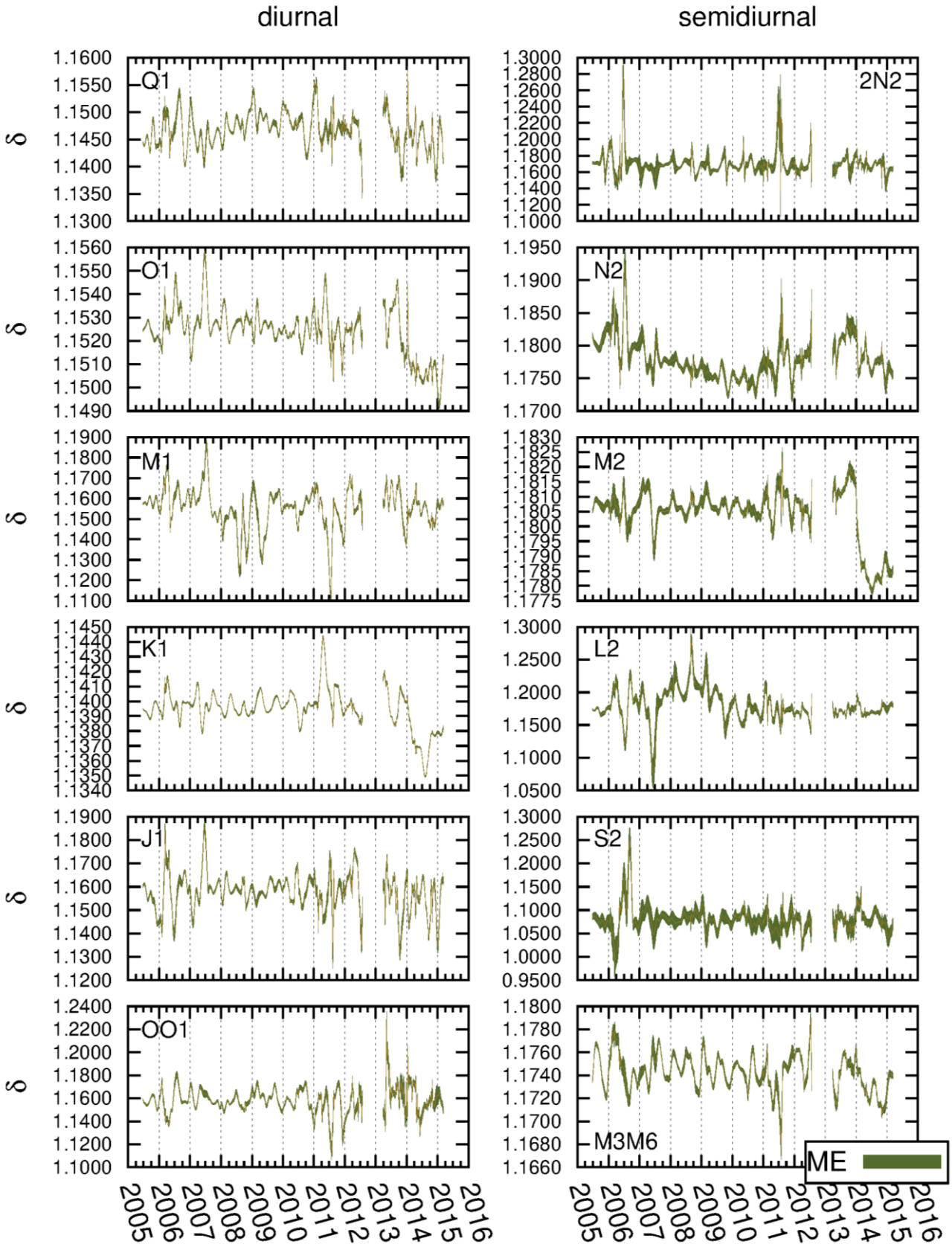

Figure 28: Gravimetric factors for the station Metsähovi.

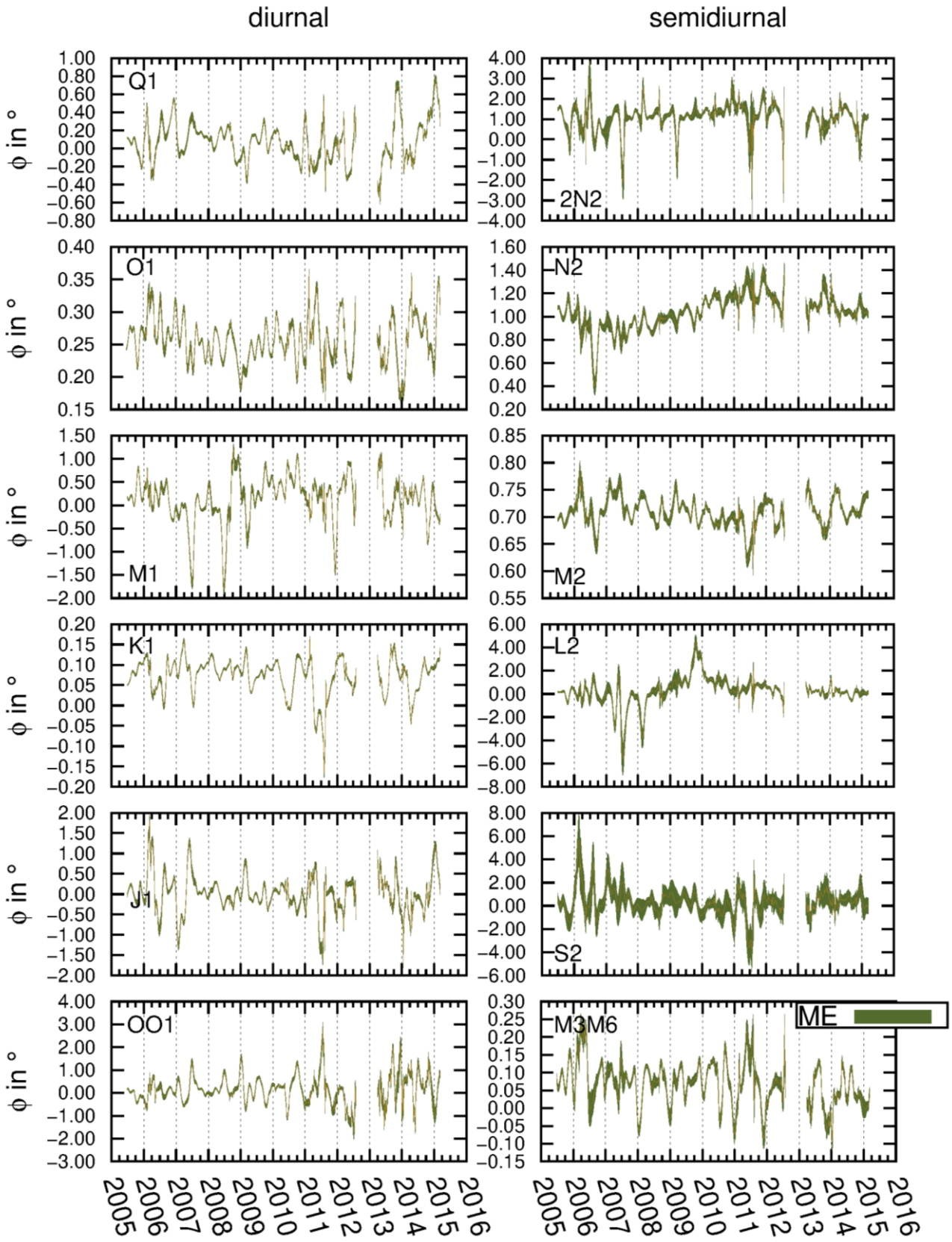

Figure 29: Phase leads for the station Metsähovi.

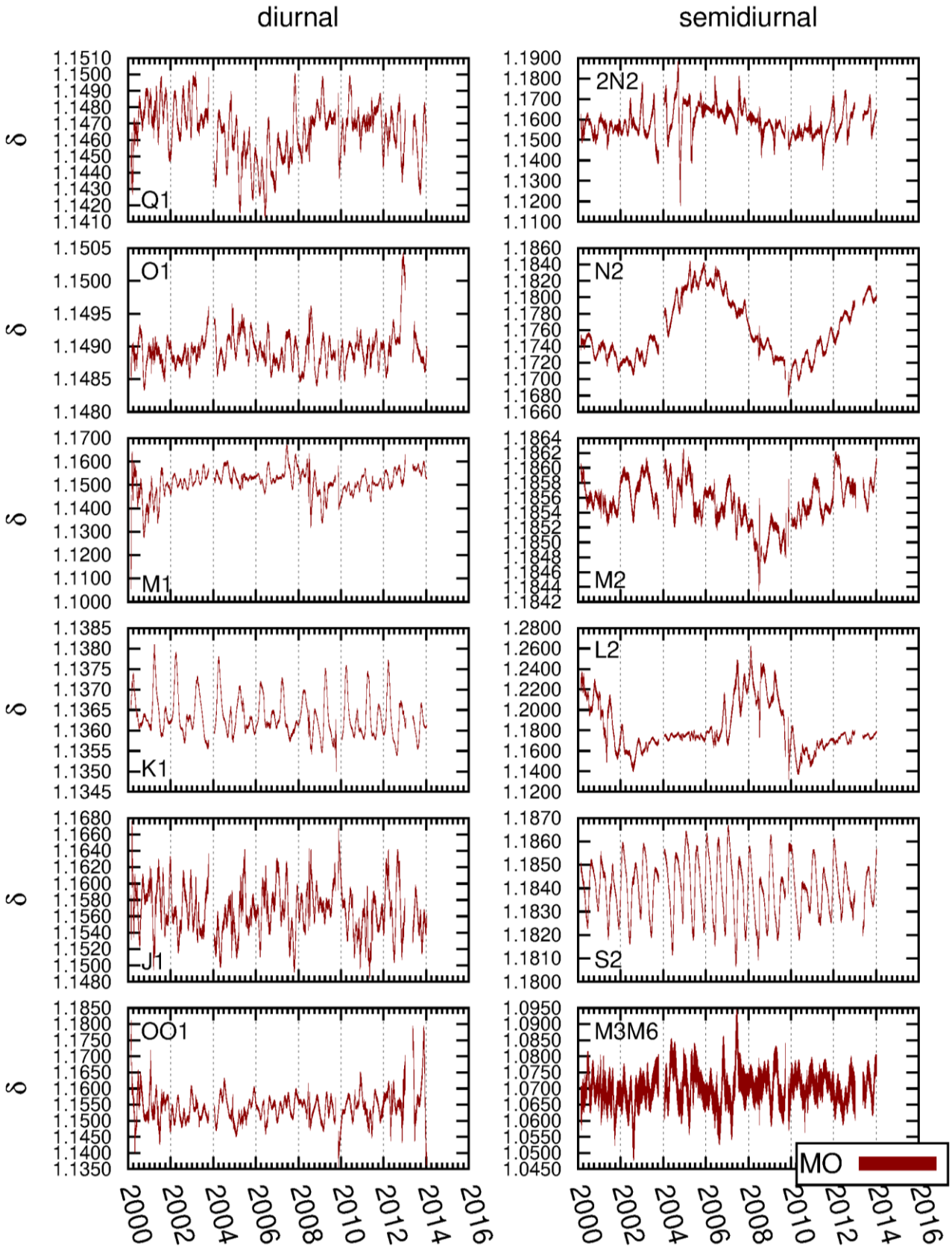

Figure 30: Gravimetric factors for the station Moxa.

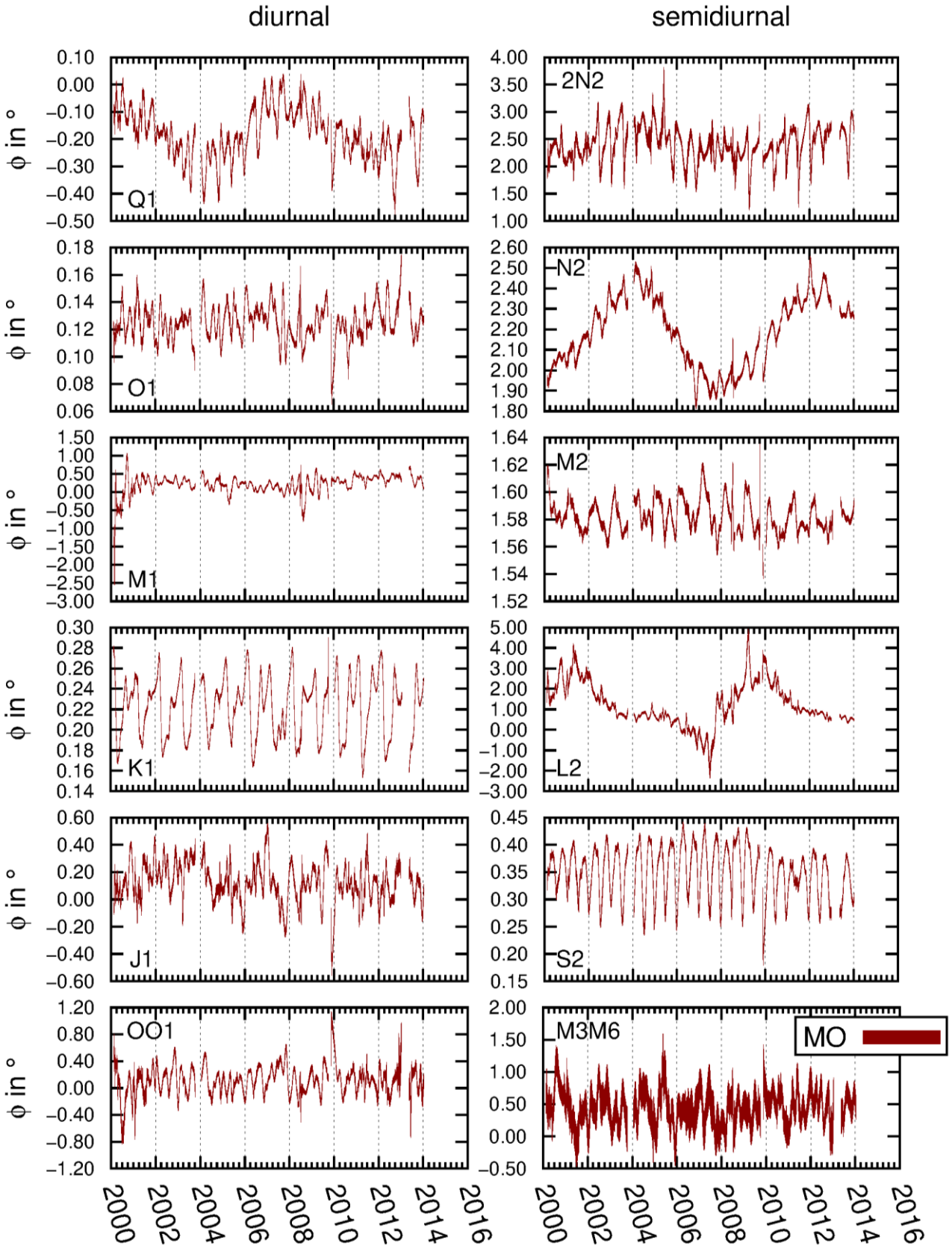

Figure 31: Phase leads for the station Moxa.

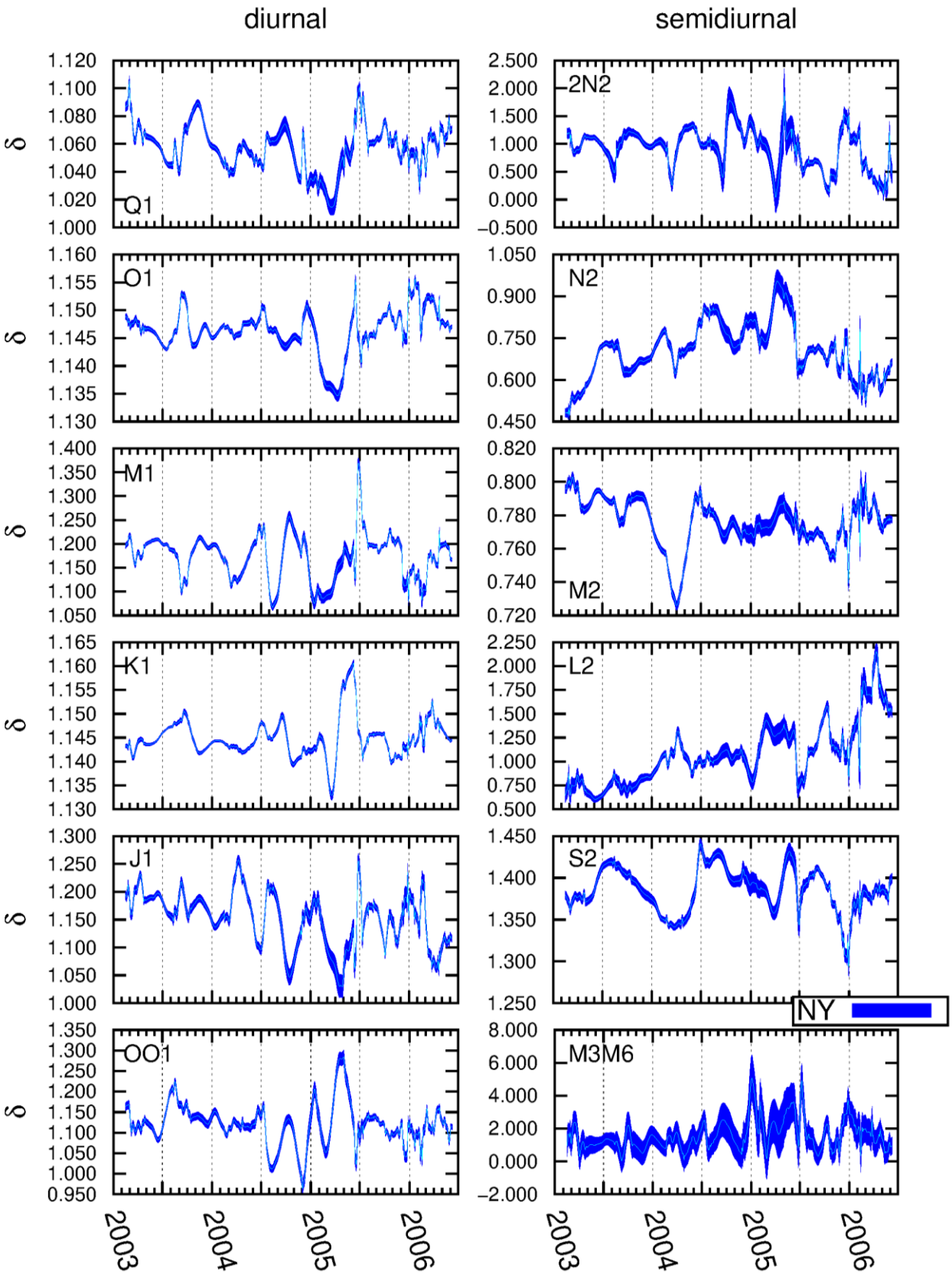

Figure 32: Gravimetric factors for the station Ny-Ålesund.

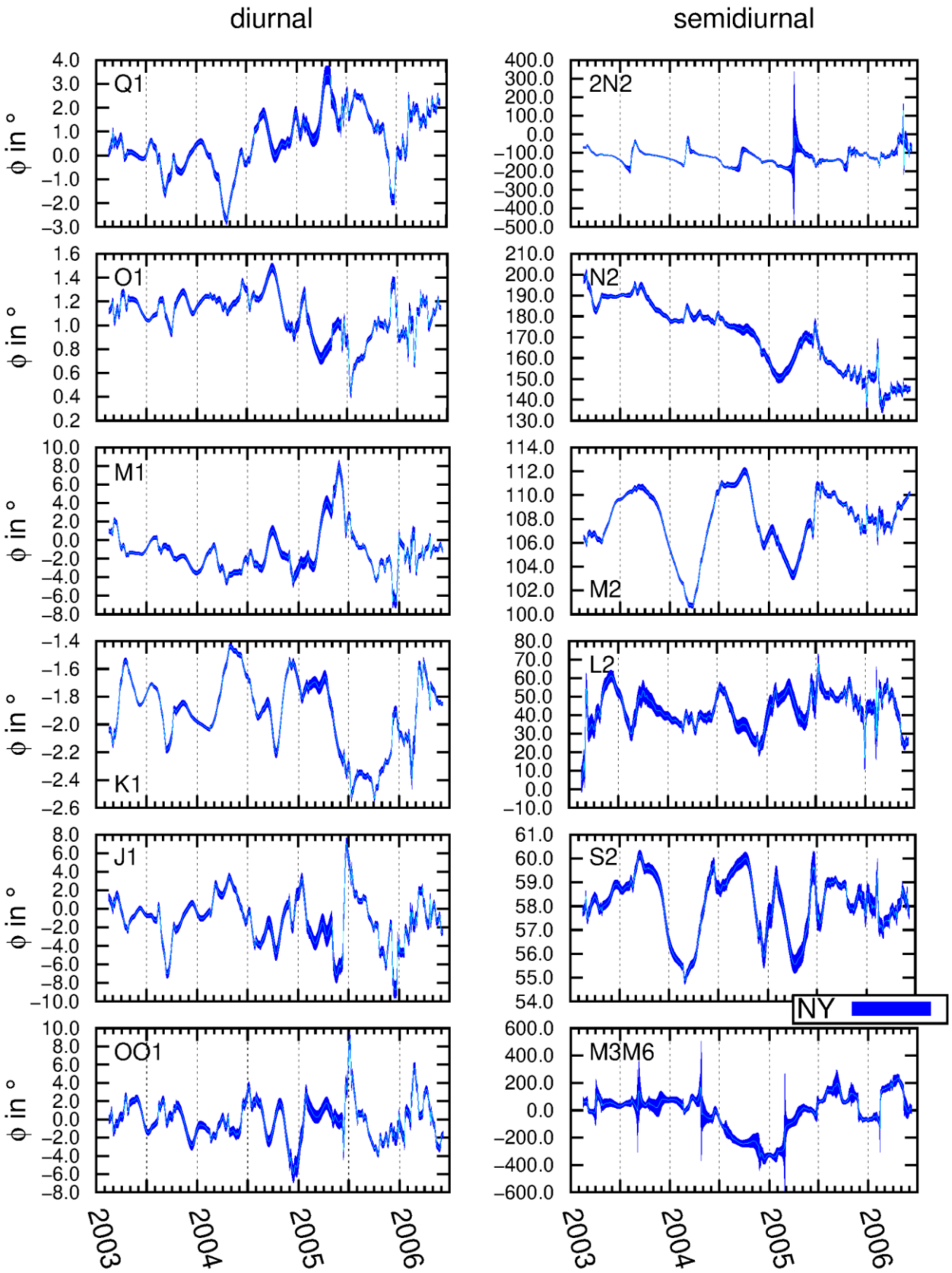

Figure 33: Phase leads for the station Ny-Ålesund.

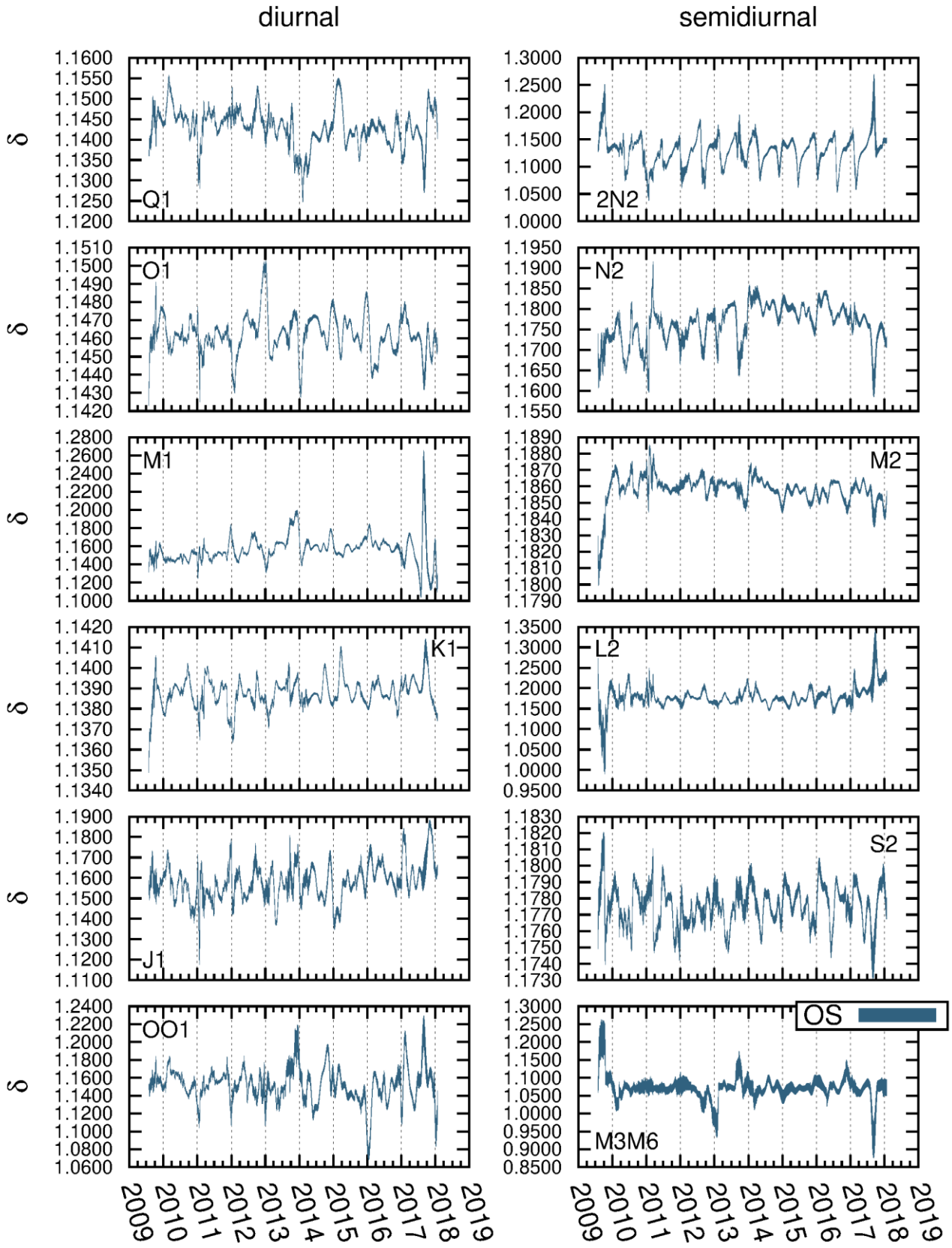

Figure 34: Gravimetric factors for the station Onsala.

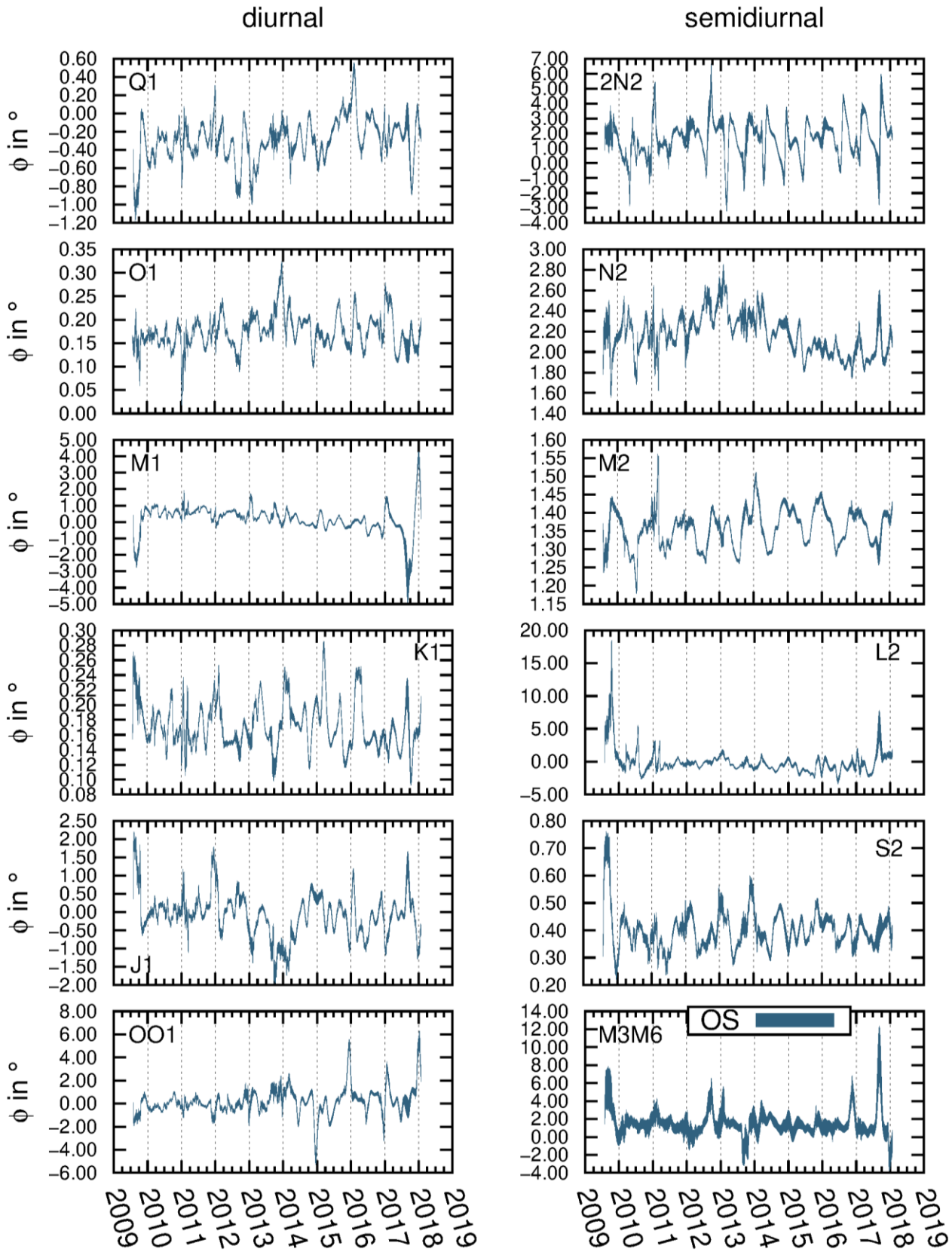

Figure 35: Phase leads for the station Onsala.

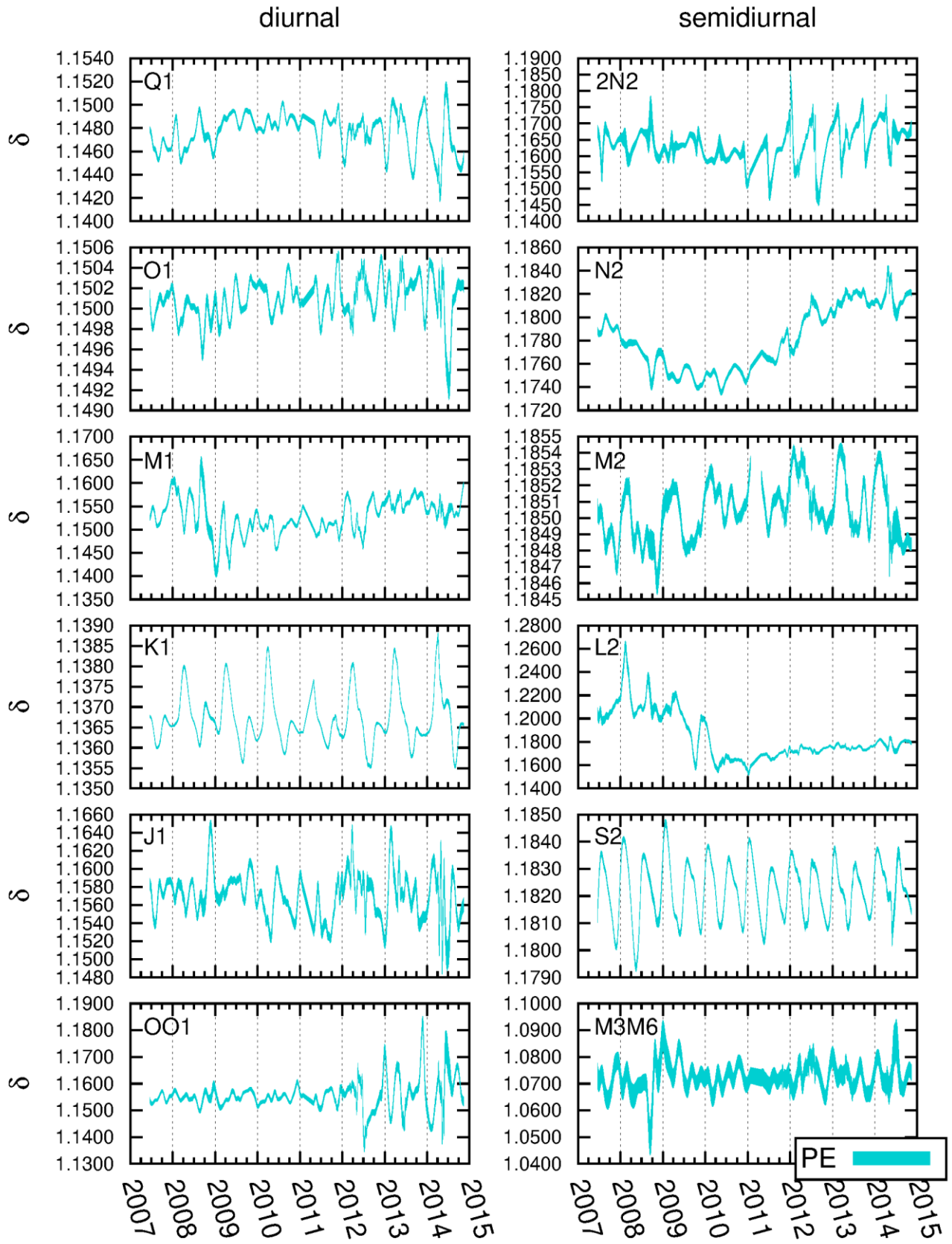

Figure 36: Gravimetric factors for the station Pecny.

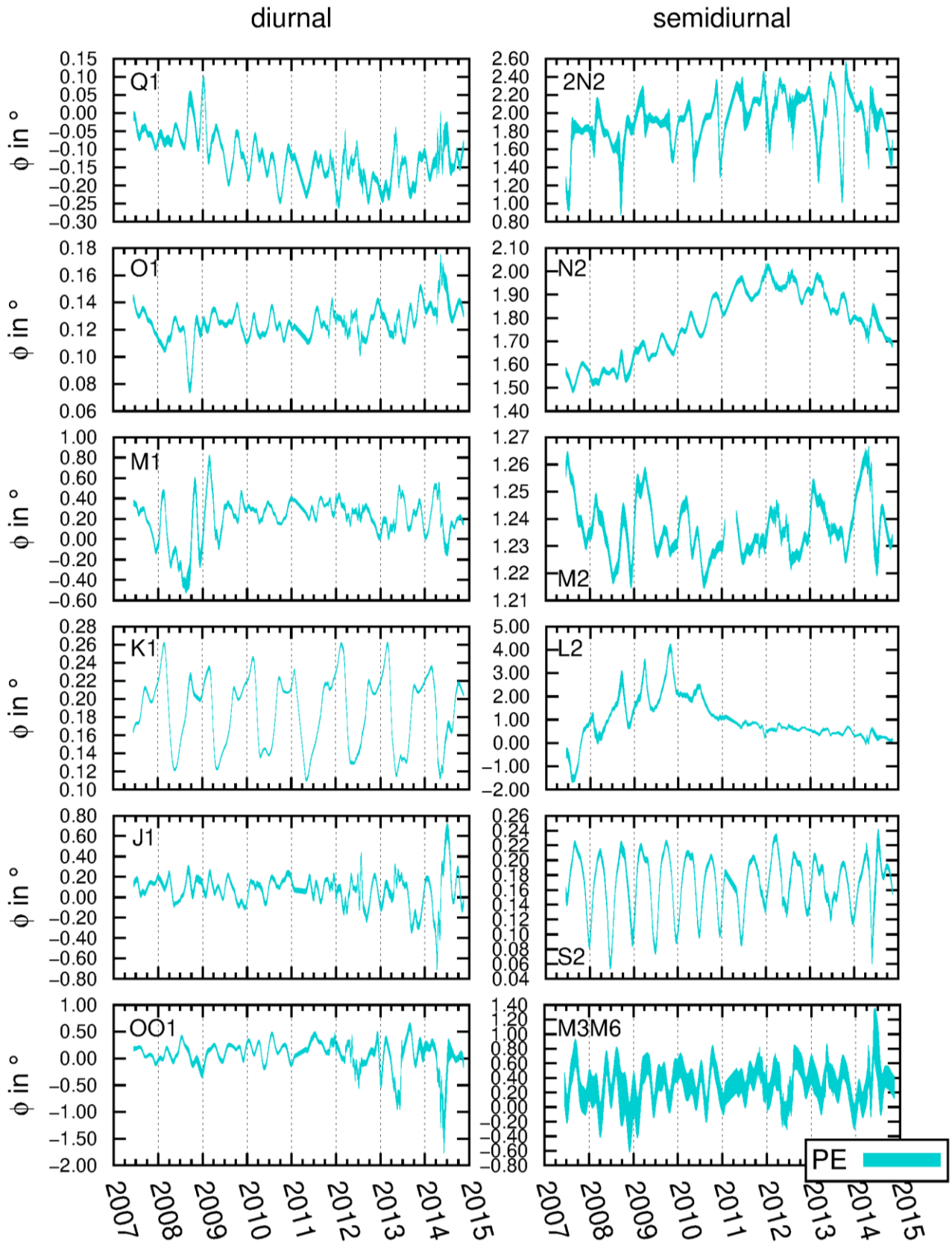

Figure 37: Phase leads for the station Pecny.

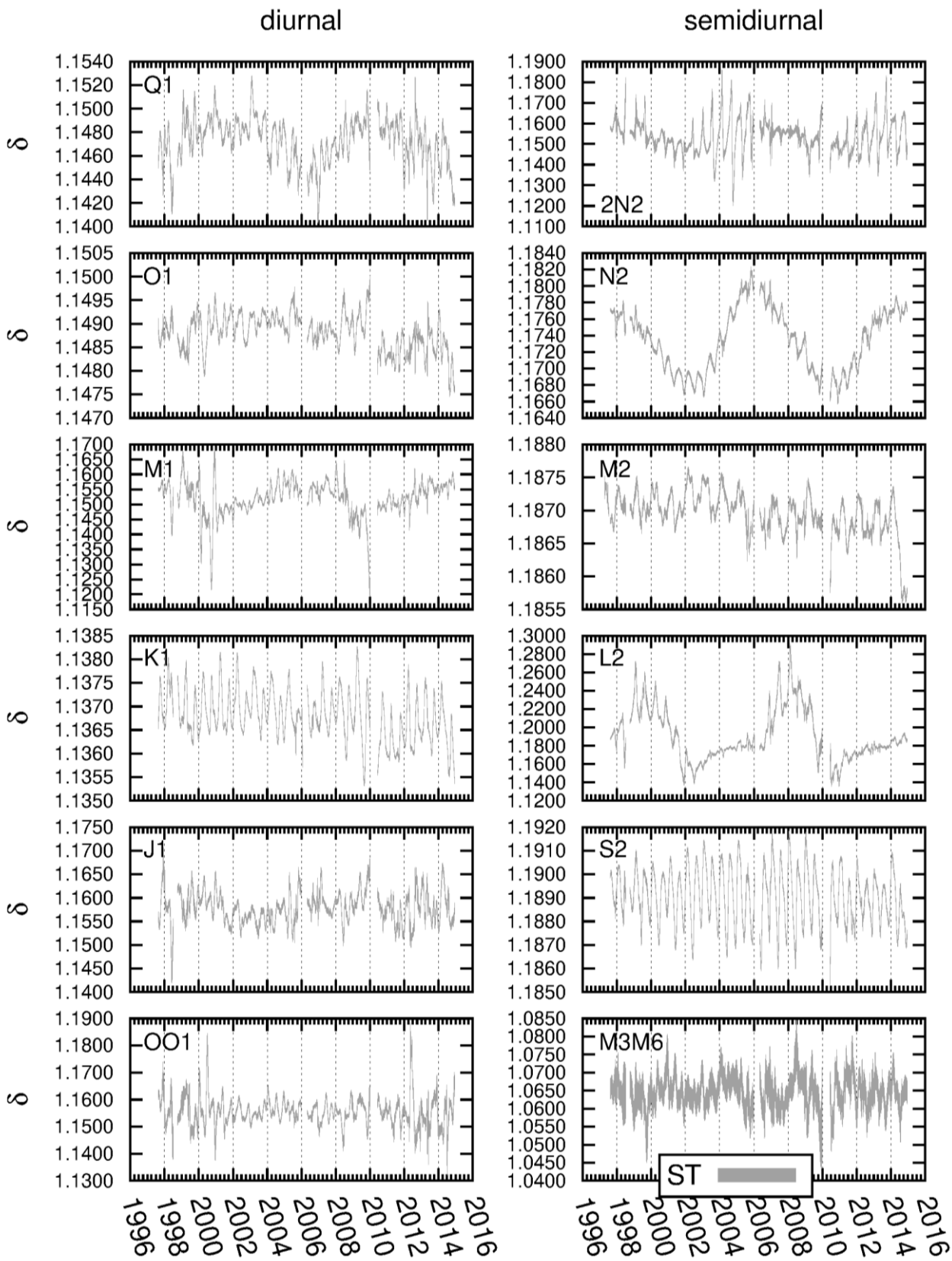

Figure 38: Gravimetric factor for the stations Strasbourg.

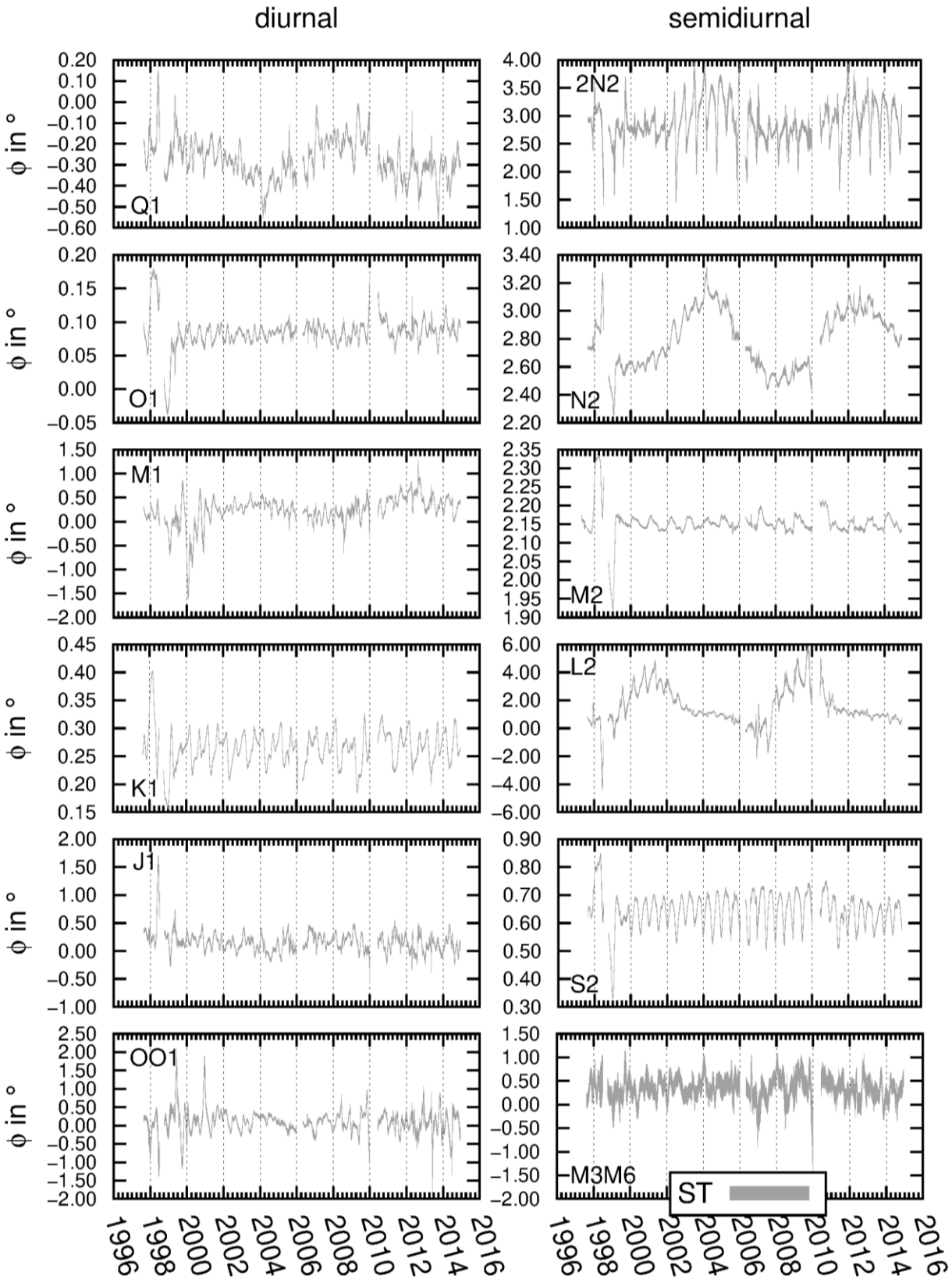

Figure 39: Phase leads for the station Strasbourg.

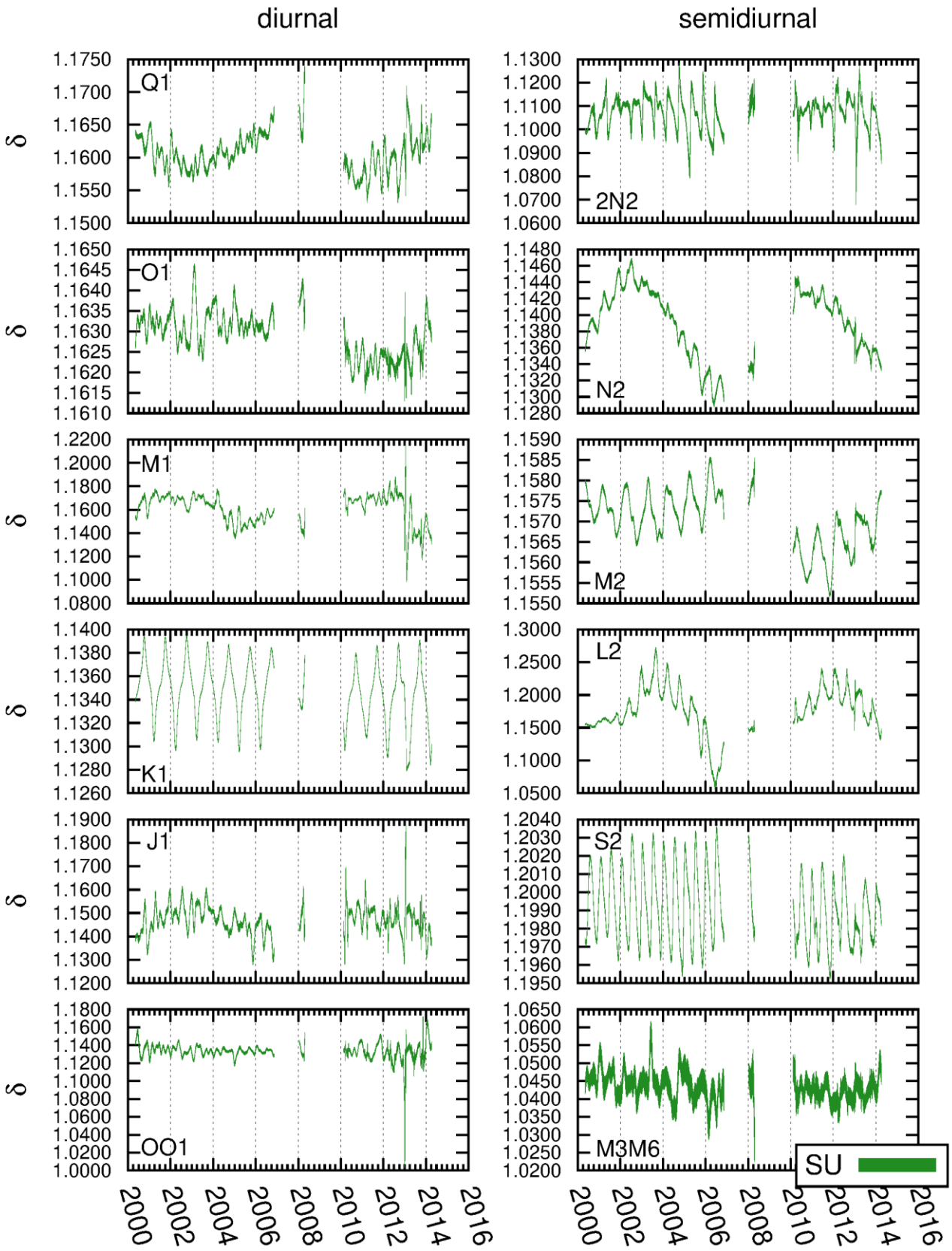

Figure 40: Gravimetric factor for the station Sutherland.

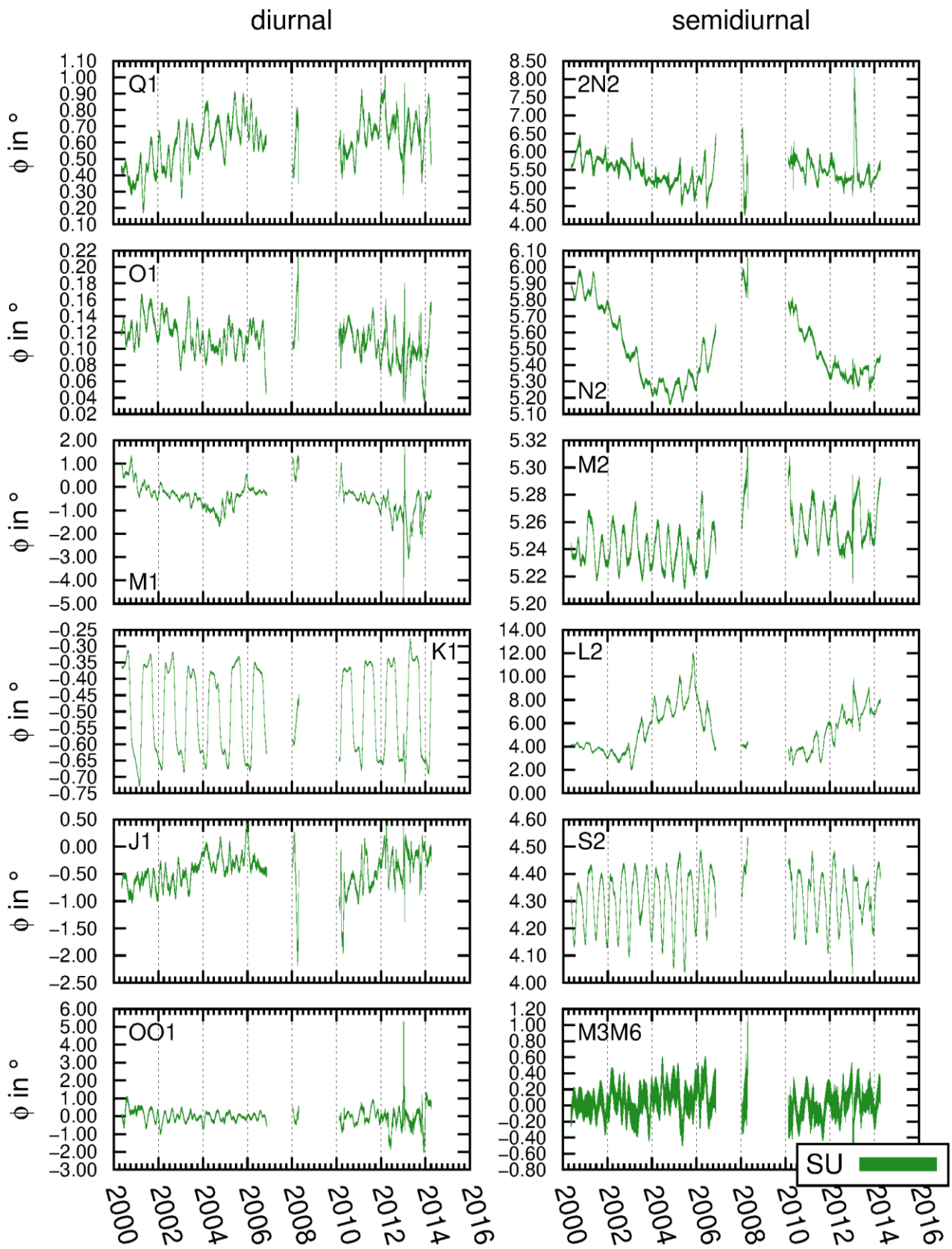

Figure 41: Phase leads for the station Sutherland.

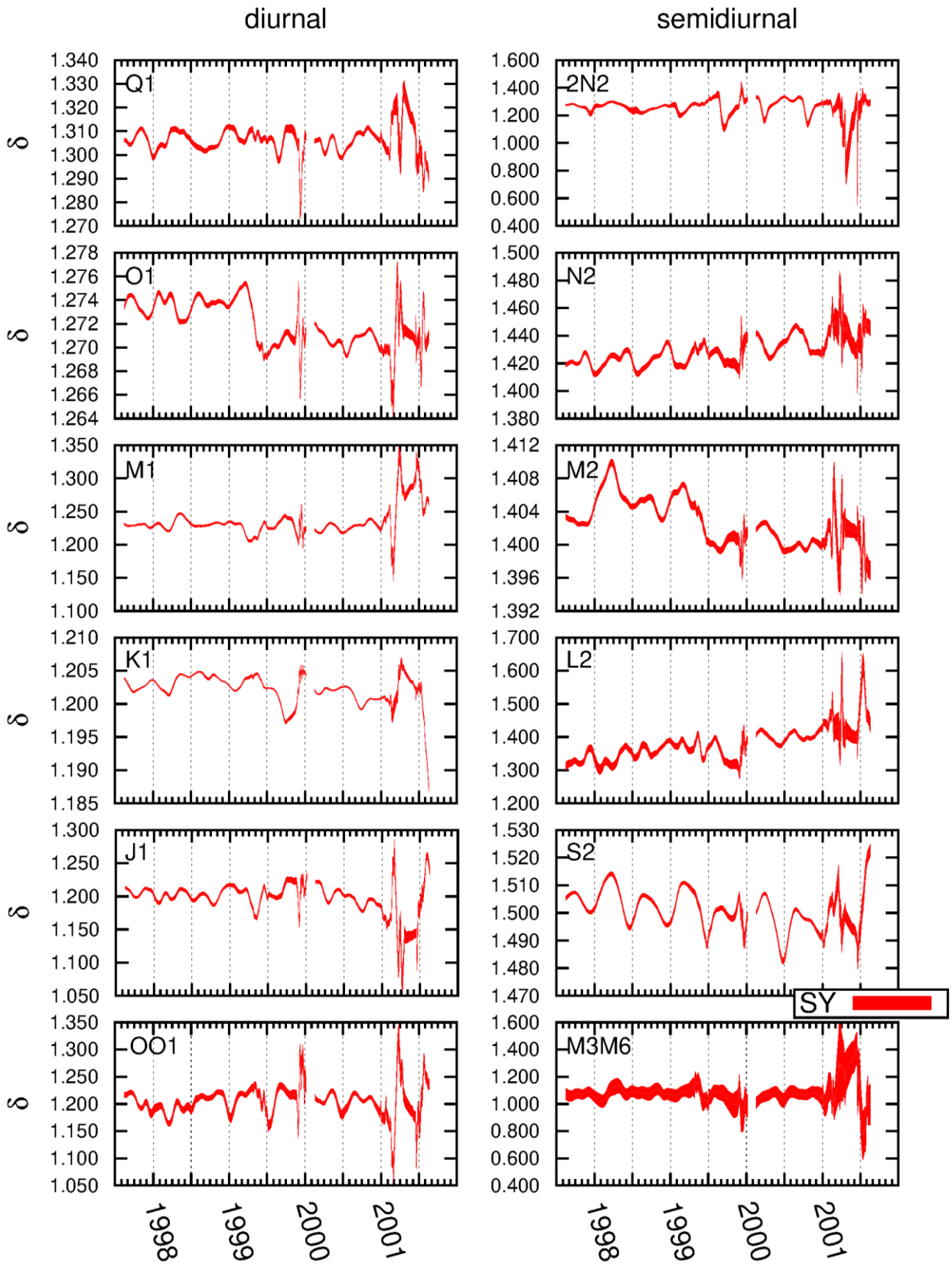

Figure 42: Gravimetric factors for the station Syowa.

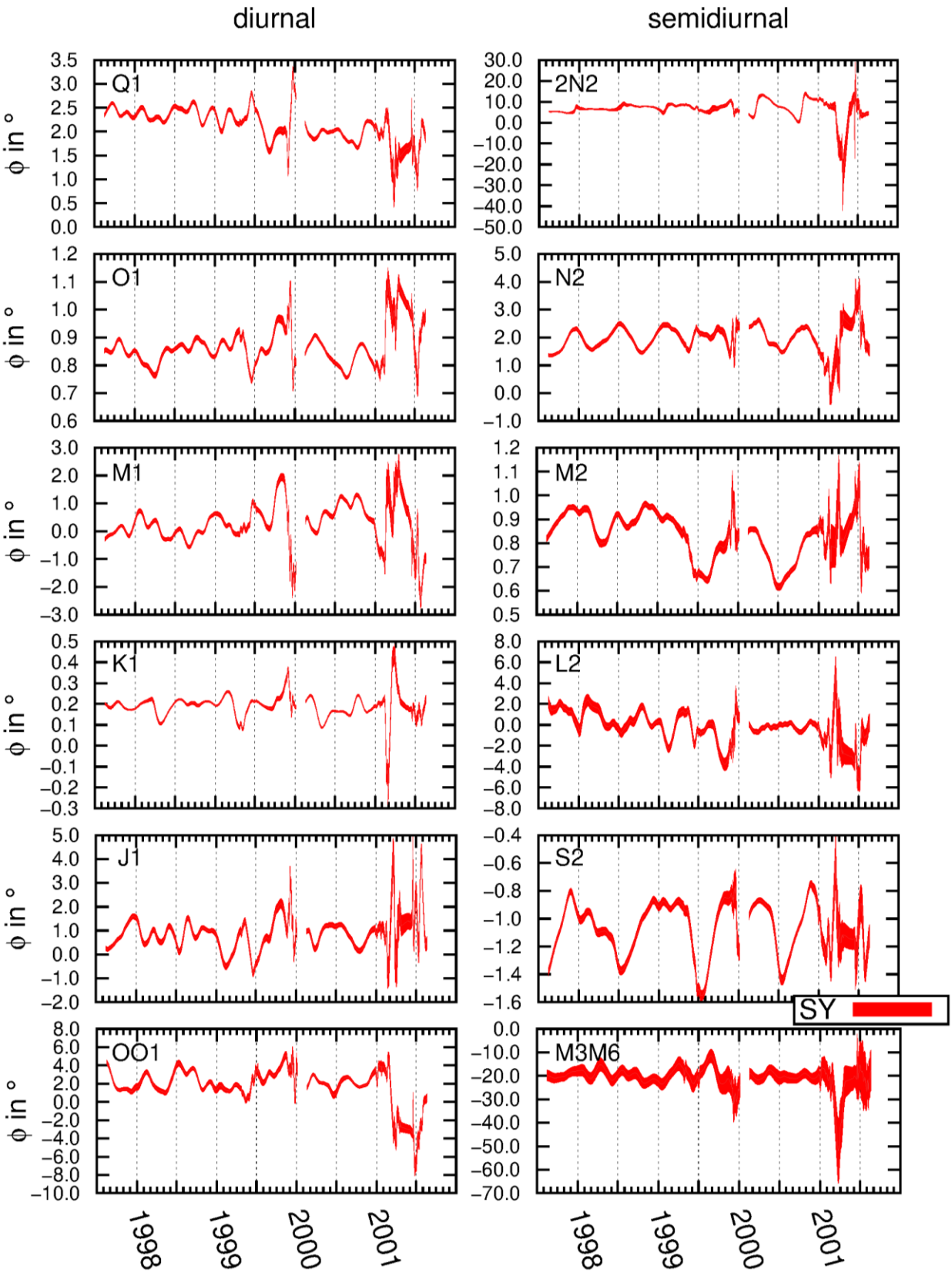

Figure 43: Phase leads for the station Syowa.

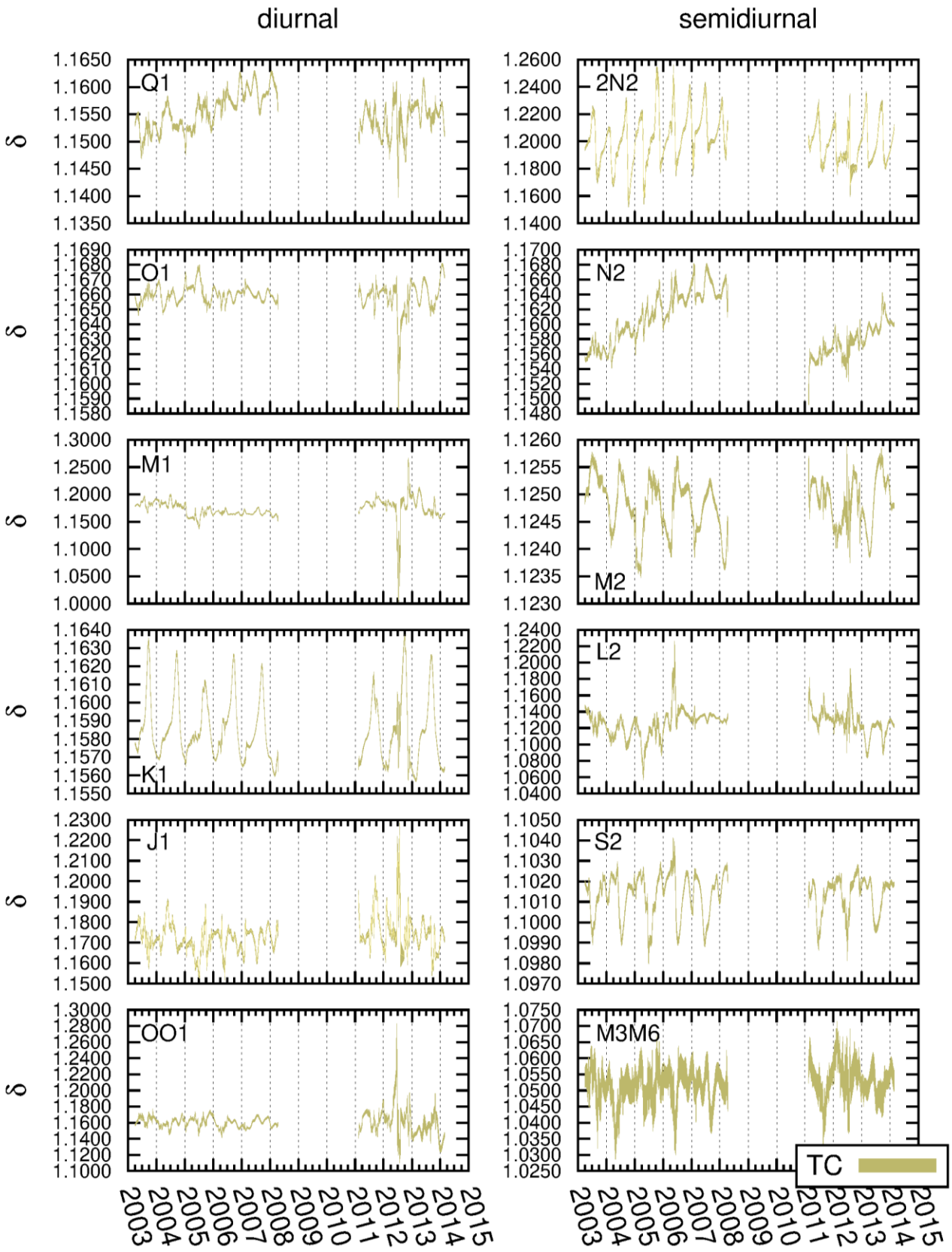

Figure 44: Gravimetric factors for the station TIGO Concepcion.

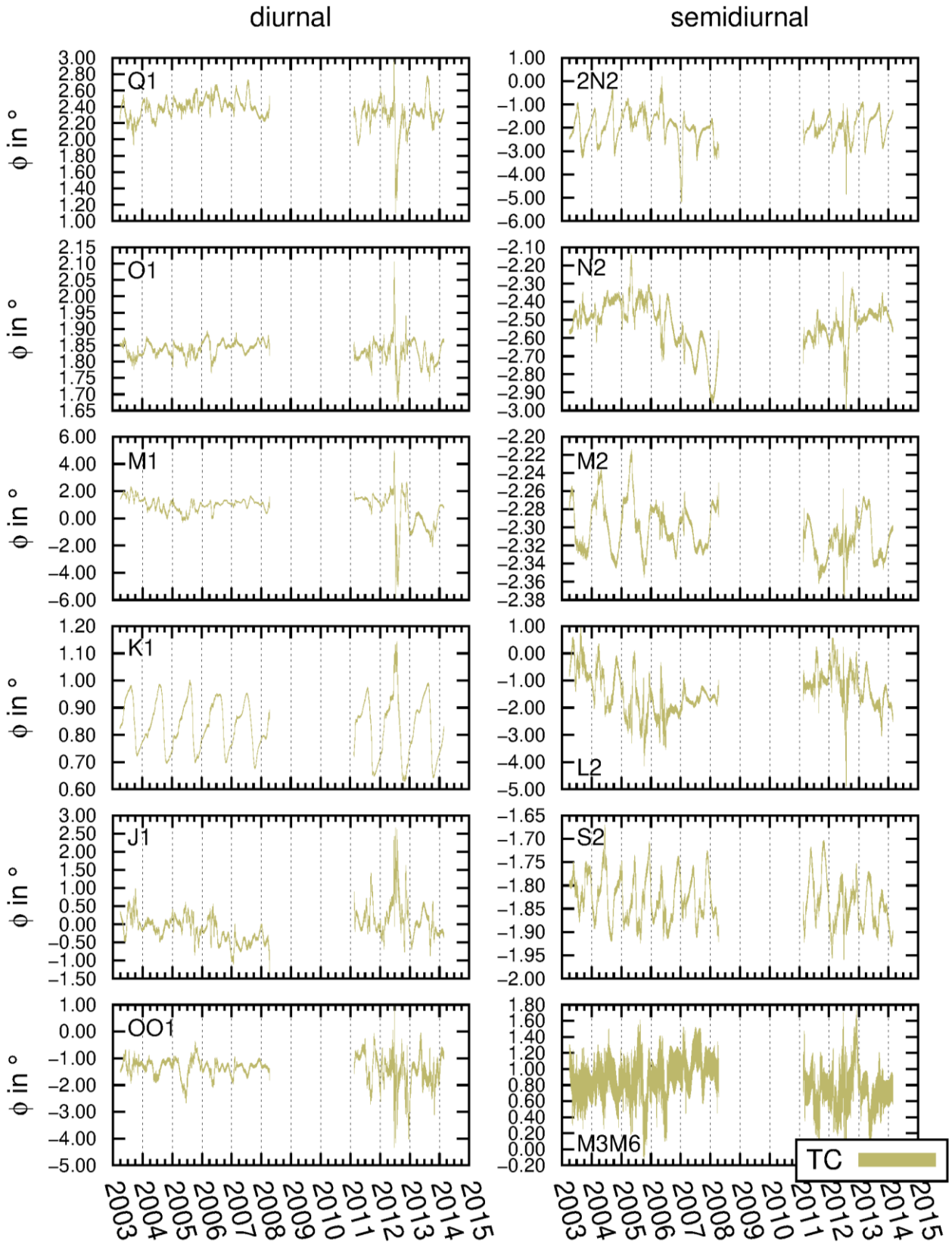

Figure 45: Phase leads for the station TIGO Concepcion.

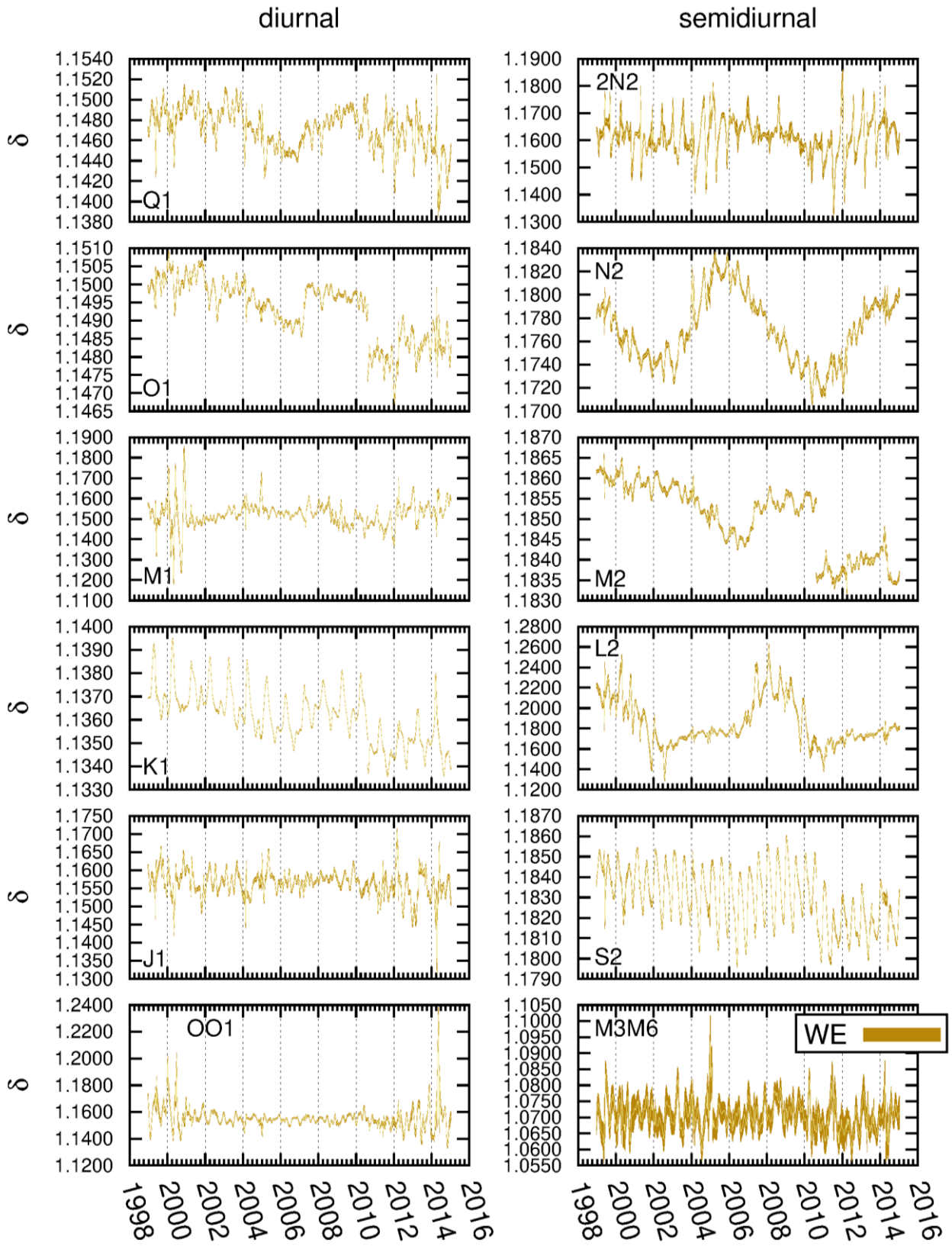

Figure 46: Gravimetric factors for the station Wettzell.

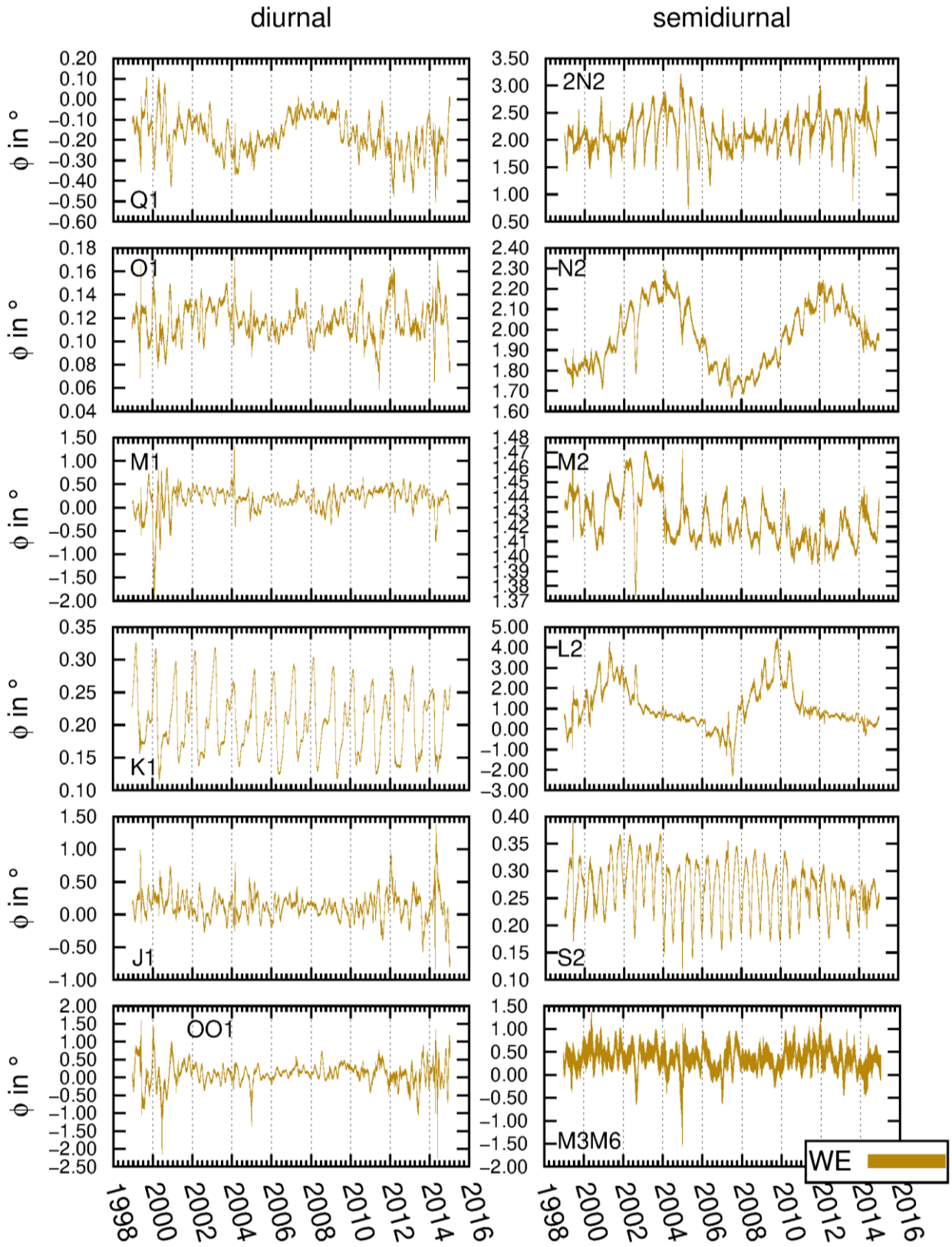

Figure 47: Phase leads for the station Wettzell.

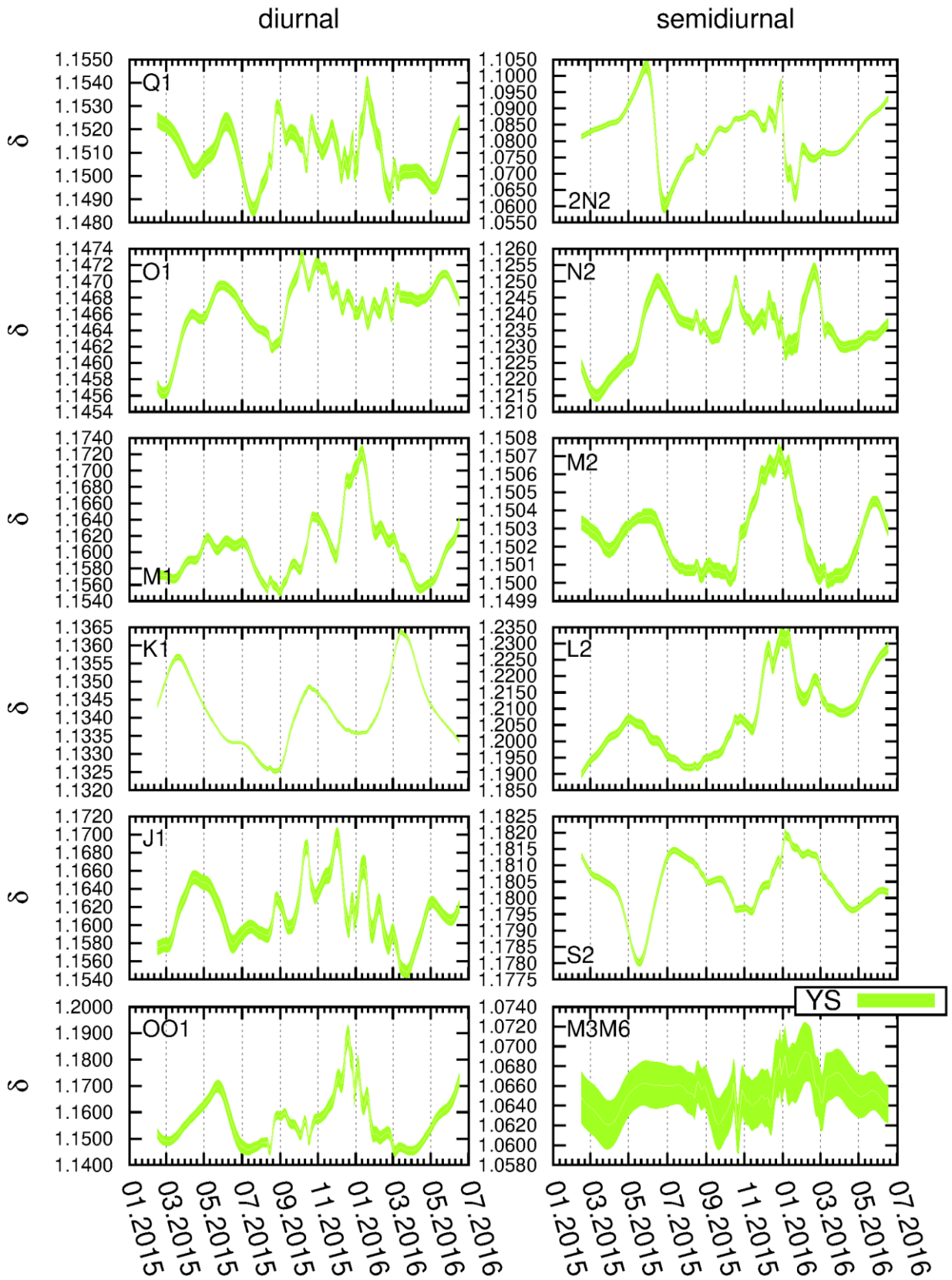

Figure 48: Gravimetric factor for the station Yebes.

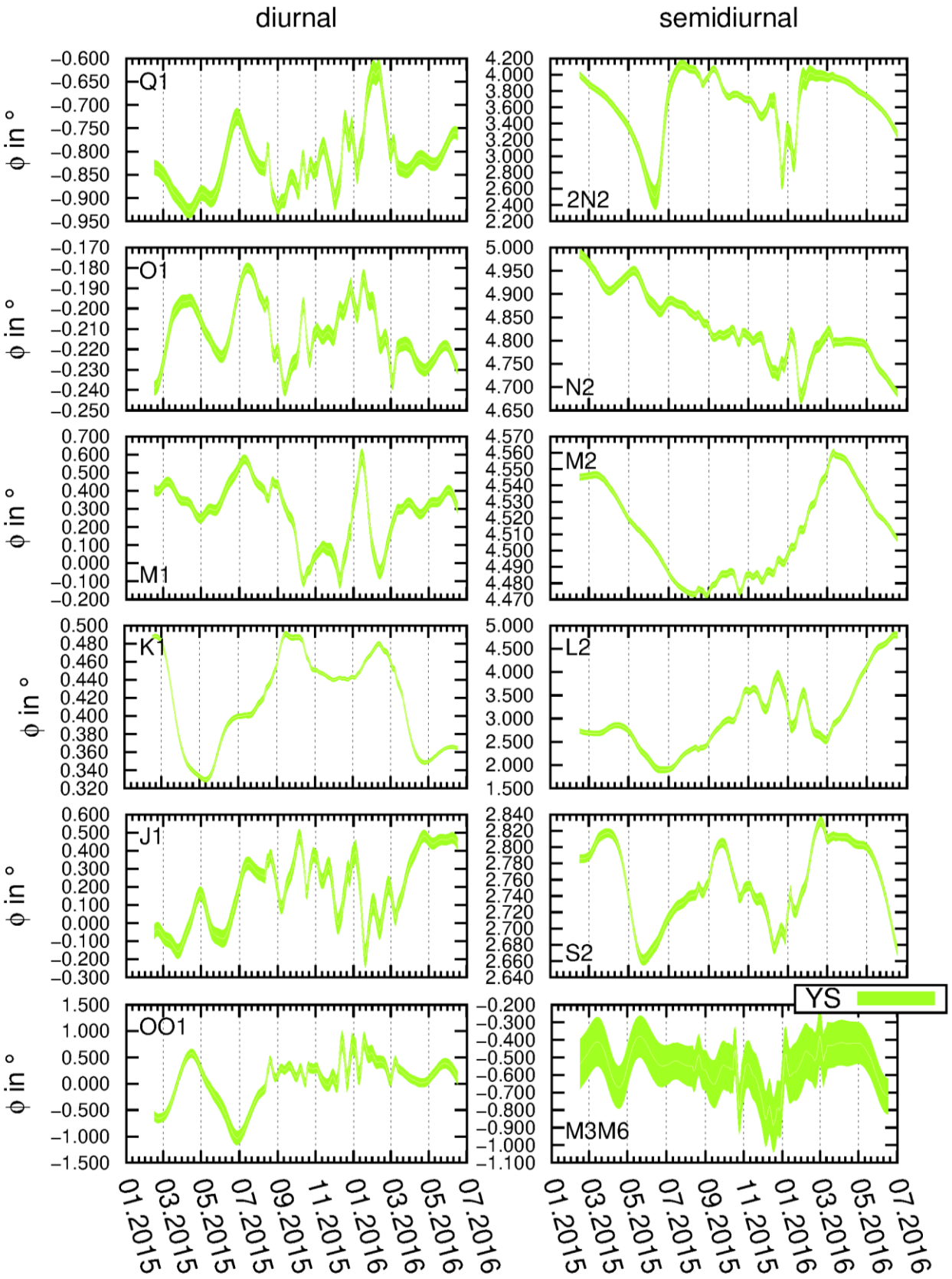

Figure 49: Phase leads for the station Yebes.

KIT Scientific Working Papers
ISSN 2194-1629

www.kit.edu